China-DC/WR

Application of Delft numerical models in the Lower Yellow River

Final Research Report of Cluster 3
Yellow River Project 2002

June 2002

Hohai University (HU)
North China Institute of Water Conservancy and Hydroelectric Power (NCIWCHP)
China Institute of Water Resources and Hydropower Research (IWHR)
Nanjing Hydraulic Research Institute
Yellow River Conservation Commission (YRCC)
Changjiang (Yangzi) Water Resources Commission (CRWC)

Delft Cluster
Nijmegen University

China-DC/WR

Application of Delft numerical models in the Lower Yellow River

Final Research Report of Cluster 3
Yellow River Project 2002

June 2002

Hohai University (HU)
North China Institute of Water Conservancy and Hydroelectric Power (NCIWCHP)
China Institute of Water Resources and Hydropower Research (IWHR)
Nanjing Hydraulic Research Institute
Yellow River Conservation Commission (YRCC)
Changjiang (Yangzi) Water Resources Commission (CRWC)

Delft Cluster
Nijmegen University

Application of Delft numerical models in the Lower Yellow River

Final Research Report of Cluster 3

The second period of the Yellow River Group Project, a subproject of the China-DC WRE project

June 2002

Application of Delft numerical models in the Lower Yellow River

Researchers: **Mrs Liu Hailing (YRCC)**
Mr. Liang Guoting (YRCC)
Mr. Wu Shiqiang (NHRI)
Mr. Ji Zuwen (IWHR)

Supervisors: **Prof. Dr. Huib de Vriend (TUD)**
Dr. Zheng Bing Wang (TUD)
Dr. Paul J.Visser (TUD)
Dr.H.Winterwerp(WLD)
Dr. ir C.J.Sloff (WLD)

Faculty of Civil Engineering and Geosciences

Delft University of Technology

May 2002

Application of Delft numerical models in the Lower Yellow River

Content

Chapter 3 2D Case study for lower Yellow River

Chapter 4 1D case study on dredging and recovery in lower Yellow River

Chapter 5 Summary and Conclusions

Application of Delft numerical models in lower Yellow River

Chapter 1 Introduction and Background

1.1 Project Background

The Yellow River is a dream for serious hydraulic engineers who love challenge. The downstream of the Yellow River is famous as suspended river in the world. Historically, bank breached twice in three years and route changed every 100 years, the river is the "sorrow of China".

China has a long history of harnessing the Yellow River. There were significant successes to tame the river in some periods during the past five thousand years, especially since new China was founded. The Yellow River, with its very fine loess particles and very high sediment concentration, is a difficult river to be tamed. With a length of 5464km, it is the second longest river in China and the sixth one in the world. However, its mean annual runoff at 40.2 billion m^3 (statistic information from 1919~1975 in Xiaolangdi hydrology station) can not reach 1/20 of Yangtse River's, its mean annual sediment transportation of 1.4 billion tons is 30 times of Yangtse River's. The lower reach of the Yellow River with the length of 800km has no tributary entering into it. In fact, the river is on the high ridge of the land, serving as the watershed divide between the Hai River Basin to the north and Huai River Basin to the south. For a significant portion of this lower reach, the river bed is higher than the adjacent floodplain, as shown in Fig.1.1, known as suspension river in China. Because of sediment deposition, the floodplain inside river banks is 4~6 meters higher than the adjacent floodplain outside, topical reach even higher more than 10 meters. The river width diminishes from upstream to down-stream.

What makes the Yellow River different from other rivers is the fine sediment it carries. During floods, the sediment bed is moving rheologically over a large extent, and it is difficult to define in the usual hydraulic sense where the bed is. The river bed changes

its route continuously with changing discharge and sediment of flow. Modeling of such a river is more difficult than modeling most other rivers.

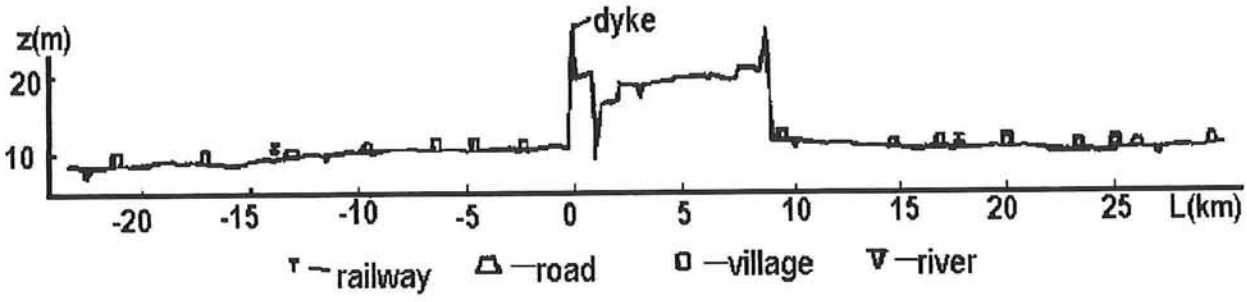

Fig 1.1 Sketch of suspended lower Yellow River

After Xiaolangdi Reservoir was taken into operation in 2000, the natural water and sediment process changed greatly, large amount of sediment deposited in the reservoir during its initial operation, the river morphology changed correspondingly. According to the situation at present, four concrete targets to tame Yellow River are shown for the Yellow River Conservancy Commission (YRCC). They are "*dyke not breach, river not dry, pollution not over standards, river bed not raise*". To reach the aim, YRCC plan to construct *three forms of Yellow Rivers*, which are the prototype Yellow River, the digital Yellow River and the physical model of Yellow River. The first one is final river to tame, develop and manage the river. The second one is Yellow River in digital form of which the mathematical model is one of the most important part of it that can be adapted to directly forecast the flooding caused by different cause. The third one is a physical model system including loess plateau model, estuary model, reservoir model and river model. The last two model forms had been built which simulated Xiaolangdi reservoir and its downstream reach with 350km long, the wandering reach. It is necessary to corporate with foreign countries and learn their advanced technology to manage the Yellow River. It is urgent to train graduates have the ability to communicate with foreigners. YRCC and other research institutes/universities have sent many excellent youths to be trained abroad, to learn the advanced technology and experiences in management of river basin.

Netherlands is a famous country not only because of its beautiful landscape but also because of its history to live with water, especially nowadays to integrate water

management practice. China is similar with Netherlands in many aspects. Two countries have cooperated with in many fields, such as education, dredging, water management etc. As a part of education project between two countries, the group consisted of 12 graduates from different hydraulic research institutes in China has studied in Delft University for 3 months from March to June 2002. The group was divided into 3 clusters in different topics, this report was written by Cluster 3 which mainly learn mathematical model and flood management practice.

1.2 Objectives and Scope of the Study

With development of numerical technology, the digital Yellow River has become an important task for YRCC. The mathematical model is the main part of it. Although a lot of sediment models for Yellow River were developed in China through a few generations, werful model software lacked to be widely applied in the Yellow River up to now. It is very helpful to learn some advanced model methods and experiences from the Netherlands. Delft numerical models, which are famous in the world, have been used widely in many countries and regions. A well pre and post processor is present.

Because of heavy deposition and water shortage, the Yellow River faces the risk of flooding and no-flow since the middle of 1980s. The problem could be solved only by integrated water management. However, Dutch has a long history fighting the flood and gets a lot of experiences in water management, especially river ecosystem recovered after 1993 and 1995's flooding. It is now accepted that there is more to ensuring safety than continually making the dikes higher. It is helpful to learn the flood management practice in Netherlands. Based on the purvious points, the objectives of this study should primarily include following aspects:

1. Modeling methods of numerical model, focusing on a case study for lower Yellow River by use of the series numerical model developed by Delft Hydraulics, including flood forecasting and dredging.
2. Flood management practices in Netherlands, including flood defense measures, flood forecasting and warning system, compensate policy etc.
3. Improvement of English communicating ability

It is a convenient way to study numerical methods by use of Delft3D model to calculate wandering reach. Running Delft3D model to simulate a flood process occurred in 1996 and comparing the calculated results with the measured data, we can easily know the advantage and disadvantage of the model. This is a base for a further cooperation too.

In order to control flood hazard, dredging has become an important method. But, some problems, such as the recovery rate of dredged channel, have to be solved before the large scale of application. These problems will be studied by Sobek(Delft 1D model) running combined with experimental data and the part field data analysis.

1.3 Structure of this report

This report summarizes the obtained results for two case studies by use of Delft3D model and SOBEK model and the flood management practices in the Netherlands through reading collected references and visiting some flood control projects and RIZA. So the report is structured as follows:

Chapter 1 described the background and objectives of this study.

Chapter 2 explains the outline and practices of flood management in the Netherlands that we learned through reading relative references, attending lectures and visiting some projects.

Chapter 3 gives the results of case study on lower Yellow River by use of Delft3D model, involving the description of studied condition and Delft3D-FLOW/MOR models.

Chapter 4 provides the results of case study on dredging .

Chapter 5 provides the main conclusions and recommendations for further improvement.

Chapter 2 Flood Management Practices in Netherlands

2.1 Introduction

The Netherlands are commonly known as the low Countries. Two-third of it is situated as much as six meters below storm-surge level.

Water is both friend and foe in the Netherlands: the inhabitants have struggled against it down through the centuries and have overcome it by turning water into dry land. Among the benefits water has yielded its access for shipping that has been responsible for the blossoming trade for which the Netherlands are well known, while freshwater rivers together with adequate rainfall have ensured a successful agricultural industry on land of fertile sea clay.

The Netherlands is situated on the delta of three of Europe's main rivers: the Rhine, the Meuse and the Scheldt. As a result of this, the country has been able to develop into an important, densely populated transport nation. On the other hand, large parts of the Netherlands lie below mean sea level and water levels which may occur on the rivers Rhine and Meuse. High water levels due to storm surges on the North Sea or due to high discharges of the rivers form a serious threat for the low lying part of the Netherlands. Construction, management and maintenance of flood defences are essential conditions for the population and further development of the country. Without flood defenses much of the Netherlands would be regularly flooded.

The Rhine is 1320 km long. It rises as a small glacial brook on Mount Sankt Gotthardt in the Swiss Alps. Gathering the water of many tributaries, it drains through France, Germany and the Netherlands into the North Sea. The Rhine's basin covers an area of 185,000 square kilometers, some 25,000 square kilometers of it in the Netherlands. The Dutch part of the Rhine starts from the Dutch-Germany border near Lobith and ends at the North Sea at Hoek van Holland. At Lobith, an average of 2,300 cubic meters of water flows down the river every second. The highest discharge ever measured was 12,000 m^3/s (in 1926, resulting in a dike failure near the city of Nijmegen). Lowest flow of the river Rhine ever measured: 623 m^3/s in 1947 (in 1929 - with ice cover 575 m^3/s).

For the river Rhine, snowmelt is an important source of water, implying a rather constant discharge, on top of which rain-fed tributaries contribute to variability in discharge.

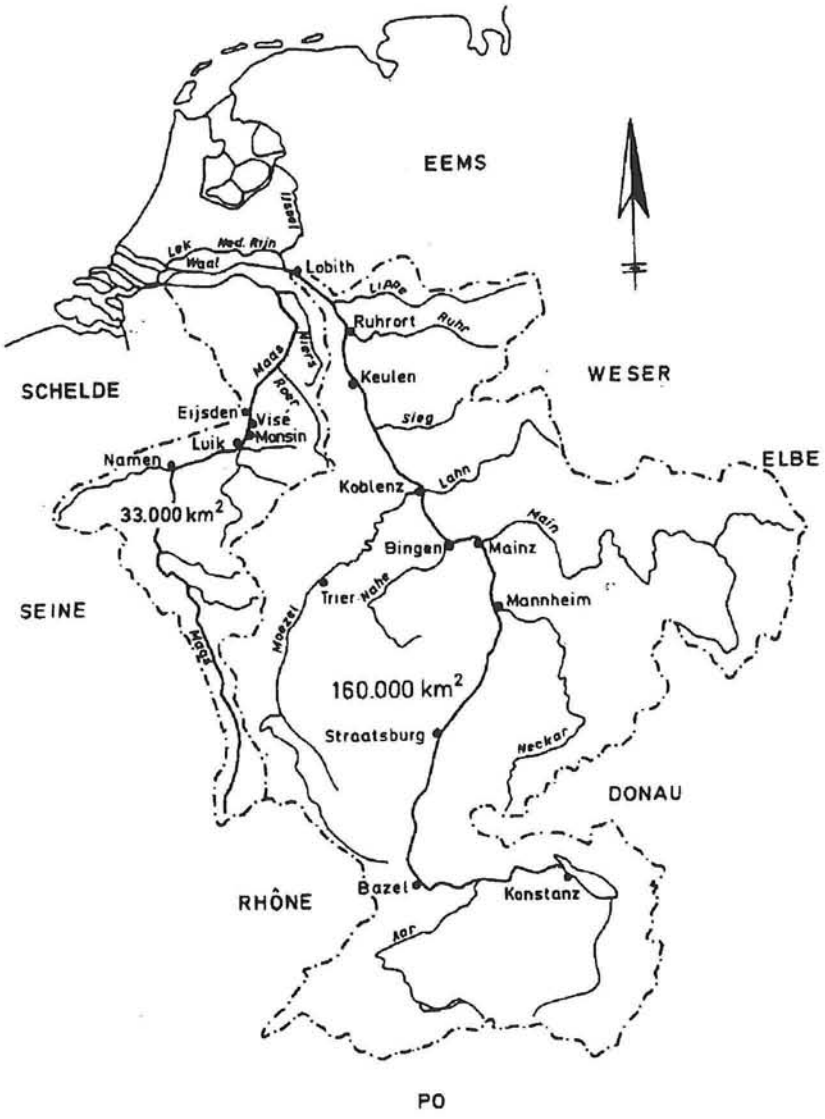

Figure 2.1 The catchment area of the rivers Rhine and Meuse

The Meuse is a river with a length of 874 km from the source in France to Hollands Diep (Dutch Deep). Its cathchment has an area of about 33,000 km^2 (fig 2.1). After passing through France, Luxembourg and Belgium, the river enters the Netherlands at Eijsden, to the south of Maastricht. The Meuse's course through the Netherlands, measured up to the mouth of the Haringvliet, is approximately 250 km. The Hollands

Diep and the adjoining Haringvliet are artificial lakes separated from the sea by means of a dam. At the beginning of the Hollands Diep the Meuse flows together with the Nieuwe Merwede (New Merede), an important Rhine branch. Because of the confluence, and the Haringvliet are rated as belonging to the Meuse basin, too, its catchment area is enlarged by 3000 km^2 and the river is almost 60 km longer. So the Meuse is 935 km long. The main tributaries of the Meuse are Chiers, Viroin, Semois, Lesse, Sambre, Ourthe, Roer, Niers and Dieze. The river Meuse is exclusively rain-fed, and has a more variable discharge. The mean discharge of the river Meuse near the village of *Borgharen*, where the river enters the Netherlands, is about 1500 m^3/s. The extreme discharges of the Meuse river vary between 1300% and 0% of the average (230 m^3/second), while the extreme discharges of the river Rhine range from 600% to 0.3% of the mean discharge. Thus the difference between mean level and high level is much higher in case of the river Meuse.

In this chapter, the Dutch history of flooding and flood protection system will be first introduced. The flood management practices in the Netherlands will be reviewed,including flooding management system, flood forecasting and warning, disaster management and so on. Then the flood prevention measures on the lower Yellow River is introduced and compared with the practices in Netherlands.

2.2 History of flooding

There were at least 140 floods with casualties between AD 1200 and 1953 in the Netherlands. One of the most serious floods happened in February 1953. A weather depression - combined with an exceptionally high spring tide - caused a storm surge on the North Sea, pushing water levels to record heights. Dikes in the southwestern part of the country failed in several places. The direct result of the disaster was 1835 victims with more than 72,000 having to be evacuated and economic damage of NLG 1.5 billion (1956 price index). The indirect economic damage is estimated as a multiple of this. Flooding in Central Holland was barely avoided. The concentration of economic activities in this part of the country would have meant much, much greater damage.

The parliament then decided that this kind of disaster was intolerable and should be prevented in the future. The disaster led the Minister of Transport, Public Works and Water Management immediately to install the Delta Committee to investigate the

hydrotechnical problems in the disaster area as well as other parts of the Dutch tidal area. As the result of the Delta Committee, the Delta Plan was adopted by law and implemented. In the past decades many dikes and dunes have been strengthened, estuaries have been closed off from the sea by dams and storm surge barriers were built in the Eastern Schedt and New Waterway.

In the end of 1993, a flood from the Meuse, the second largest river in the Netherlands, occurred in France, Belgium and the Netherlands. The flood and inundation in the Netherlands resulted in an estimated total material loss of about 250 million Dutch Guilders and about 8000 people were evacuated. The perception of the emotional damage was described as "very great"(MTPW,1994)

In January 1995, a serious flood occurred in Germany, France, Belgium and the Netherlands. The flood which occurred in the Dutch part of the river basin of the Rhine and the Meuse was the most serious one since the flood in 1953. Dikes had to be inspected every hour due to water load and soaking of soil. Rescue teams were standing by to strengthen dikes with protective covering and sand-bags to maintain the hydraulic and geo-mechanical stability if possible dike deterioration/failure was identified. The estimated direct and indirect damages were 200 million and 1.0 to 1.5 billion Guilders, respectively, and 250,000 people and millions of livestock were evacuated. The inhabitants thought that they deserved to be better protected from floods. The prime minister called for another "Delta Plan" to improve the river dikes.

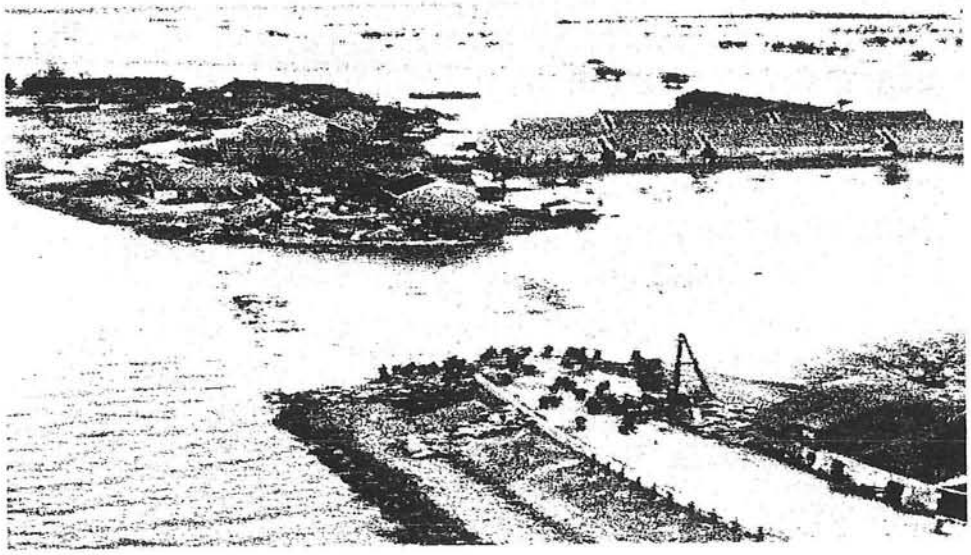

Fig. 2.2 Zeeland, The Netherlands, 1953

Table 2.1 A comparison between the Rhine and the Meuse

Characteristics	The Rhine		The Meuse	
	Catchment	Dutch Part	Catchment	Dutch Part
Catchment area in km^2	185,000	25,000	33,000	11,740
Length in km	>1000	167	874	200
Max. Known discharge (m^3/s)	12280 at Lobith		3000 at Borgharen	
Mean discharge (m^3/s)	2200 at Lobith		230 at Borgharen	
Source: Cazemier,1988;Berger, 1992				

2.3 The flood defence system

About half of the Netherlands lies below the mean sea level and has to be protected by dikes and natural dunes from flooding by sea and rivers. When a part of delta areas, lagoons, flood plains, or any level area which was originally subject to a high water level, either seasonally or permanently and due to surface or ground water, is separated from the surrounding hydrological regime, it becomes a polder. In this way its water level can be controlled independently of the surrounding regime.

As far as is known, the construction of flood protection works started approximately in the third century before Christ when people in the northern part of the Netherlands built artificial mounds to live on. In the first century, under the influence of the technical capabilities of the Romans, people began to construct small dams along the rivers. Later dams were also constructed to connect several mounds. These dams could resist the regular floods and protect the lands, to some extent, against flooding, but they were certainly too low to safeguard the land under extreme conditions. Large activities in dike construction during the seventh and eight century made it reasonable to expect that in the eighth century the first polders were constructed. During the following centuries the protection against flood was improved phase by phase.

The Dutch flood defence system consists of dunes, sea dikes, storm surge barriers, sluices and river dikes. If one of the elements fails, the polder will be flooded and inundated. The main fault tree is presented in Fig.2.3

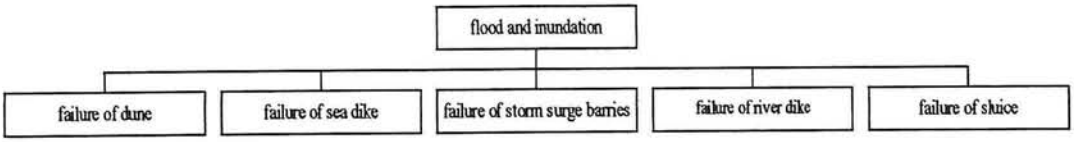

Fig 2.3 The main fault tree of the Dutch flood defence system

The influence of the sea would be felt principally in the west. The influence of the waters of the major rivers is of more limited geographic effect. Along the coast, protection against flooding is principally provided by dunes. Where the dunes are absent or too narrow or where sea arms have been closed off, flood defences in the form of sea dikes or storm surge barriers have been constructed. Along the full length of the Rhine and along parts of the river Meuse protection against flooding is provided by dikes. In fact, the low lying part is divided into more than 50 smaller areas, called dike ring areas or polders, which individually are protected by a system of flood defences(see Fig.2.4). A polder is protected from flooding by enclosing dike sections and some hydraulic structures such as a sluice. There are currently approximately 3440 km of dikes, of which about 570 km pass through villages and towns. In total, 13 km of dike reach is characterized by cultural-historical buildings of high value at both sides (Peerbolte, et al 1991). Dikes play a crucial role in flood protection in this country and have formed a unique dike landscape.The protection offered by flood defences is not absolute. There are no known upper limits to the possible impact of rain and wind. Under extreme weather conditions flood defences may collapse and the low-lying hinterland may be flooded. Even under less extreme conditions the behaviour of flood defencs is also not fully predictable such that there is always an albeit limited chance of flooding.

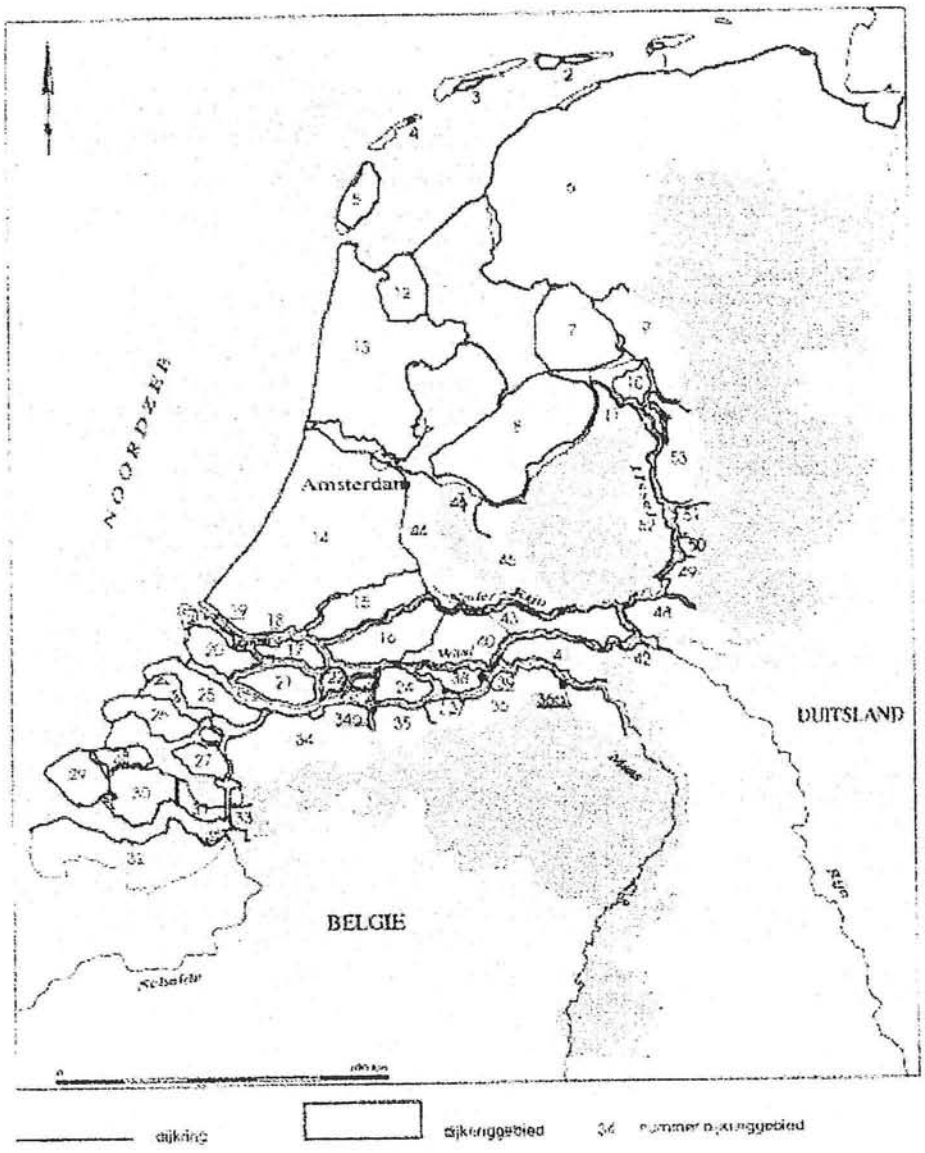

Figure 2.4 Sketch of polders in the Netherlands

Since the flood in 1953, storm surge barriers were built in the Eastern Scheldt and New Waterway, dunes were improved, and dike improvements (heightening and strengthening) have been implemented. Construction of sea dikes and storm surge barriers requires substantial investments, but meets less societal resistance than river dike improvements. Since the 1970's, protest grew against the harmful effect on the landscape and natural and cultural assets on and along river dikes. It was felt that the dike improvement measures were too strongly dominated by limited technical engineering approaches based on traditional design criteria lacking attention for the

social and environmental impacts and alternatives. This protest represents the changing societal appreciations of social and environmental assets.

2.4 Design of flood defences

The design of flood defences in The Netherlands is dominated by the hydraulic loads, which may occur. In the old days this hydraulic load was determined in a very simple manner. To the highest known water level a safety margin was added. This safety margin ranged from 0.5 to 1.0 metres. In the years directly before and after the Second World War it was Wemelsfelder, who introduced the concept of frequency exceedance curves for water levels along the coast. He drew attention to the fact that the logarithm of the mean number of high tides per year exceeding a certain level resembled a straight line. The Delta Commission integrated this concept in the design procedure of flood defences. Based on a econometric optimization the required safety of a flood defence was expressed as a water level, which had to be withstood. No failure is allowed under the prescribed design conditions. This seems to be a very optimistic demand, because failure of a dike section is always possible. In practice the probability of failure is kept sufficiently low by introducing additional criteria. These deterministic criteria like the steepness of inner and outer slopes of dikes are applied in the practice of dike design. Furthermore there is a minimum margin between crest height and design water level of 0,5 m. And the volume of overtopping water is limited to values ranging from 0,1 to 10 l/m/s. With regard to the crest height the design procedure is as follows. The required crest height follows from the design water level and a margin for wave run-up or overtopping. The design water level is calculated with a hydraulic model using the design discharge. The margin is determined is such a way, that the frequency of exceeding the tolerated overtopping discharges is kept within the prescribed values ranging from 1/10,000 to 1/1,250 per year. The safety level is a prescribed frequency of exceedance of a water level. Each individual dike section has to withstand this water level and the associated hydraulic loads. No failure is allowed if the design water level occurs. This prescribed probability of exceedance is uniform along each dike ring area. The criterion varies however between the various dike ring areas, depending on the relative economical importance of each dike ring area. In this way four classes of dike ring areas can be distinguished in terms of water level exceedance frequencies: dike ring areas with a criterion of 1/1250, 1/2000, 1/4000 and 1/10000 per year

For calculating the required margin not only the design water level is considered. Also combinations of lower water levels with more extreme wind speeds are taken into account. The minimum crest height is 0.5 metres above the design water level, even if there is practically no wind load.

For river dikes the required margin may reach up to 2.0 metres (at locations with long fetches). However in most cases the minimum margin of 0.5 metres or little more is sufficient. This means that the required crest height is almost directly determined by the design water level.

For sea dikes the required margin ranges from 2.5 metres (facing east) to 6.0 metres (facing northwest). So, for sea dikes the design water level doesn't play the crucial role as it does for river dikes. The combined hydraulic load caused by water level and waves has to be taken into account. Both extreme value statistics and correlation between water level and waves are relevant.

2.5 Institutional structure

The Netherlands is a decentralized unitary state with three levels of government, i.e. central government, twelve provinces and over 600 municipalities. An elaborate system of co-governance between local and central layers of public administration has developed, with the provincial level traditionally being relatively weak. Each municipality has an elected municipal council, a mayor and an executive Board of Mayor and Aldermen. The Board of Mayor and Aldermen, which often consists of full-time professional administrators, plays a leading role, while the Council generally limits itself to legislative oversight and control of the Board's policies. The Aldermen are elected from the Council, while the mayor is appointed by the central government. Historically, mayors were supposed to act as the eyes and ears of the central authorities, and to enforce central rule if necessary. Nowadays, mayors have become almost purely local officials who will not shy away from tough negotiations with their superiors at the Ministry of the Interior in The Hague to defend local interests. Municipalities have both autonomous and co-management tasks. The most important tasks delegated to or implemented by the local government are the maintenance of public order and fire protection, the upkeep of roads, and several tasks related to public transportation, economic policy, primary education, culture, social welfare and health care. In water

management, an important role is played by so-called polder board districts. Founded in the Middle Ages, these are regional, self-governing administrative bodies of elected representatives and a permanent staff tasked with the management of water ways and water levels on their territory.

At the national level, Rijkswaterstaat, a division of the ministry of Transport, and its provincial branch offices are in charge of the construction and maintenance major water infrastructures including sea and river dikes.

2.6 Flood forecasting and warning system

The expected discharges of the rivers Rhine and Meuse are monitored by the National Institute for Inland Water Management and Waste Water Treatment (*RIZA*), an operational department of the ministry of V&W, in co-operation with the responsible agencies from the other riparian countries. Hence, *RIZA*'s effectiveness is premised on optimal communication arrangements with those agencies.

When a flood is expected, a flood warning system goes into operation. RIZA first calculates the anticipated water levels at Lobith and Borgharen (the places where the Rhine and the Meuses, respectively, enter the Netherlands) so as to predict the advance of flood waves. In this way, about half a day's notice for the Meuses and a few days' notice for the Rhine (2-3 days). Using the forecast data for Lobith and Borgharen, the Regional Directorates calculate water levels along the river branches. The earlier imminent problems are detected, the more damage can be prevented by setting up dike watches, closing culverts, taking ferries out of service and, where necessary, evacuating people and livestock. Water level information and flood warnings are posted on the Dutch Teletext.

Water levels on the Rhine are considered to be high if they are more than 14.00 meters above Dutch Ordnance Datum at Lobith and a further rise of at least one meter is anticipated. On the Meuses, flood is defined as any discharge greater than 1,500 m^3/s. To produce such a discharge, at least thirty to forty millimeters of rain per day must fall on the river basin for several days. RIZA issues flood warnings for the Meuse if the

level at Borgharen reaches 44.00 meters above Dutch Ordnance Datum and is expected to rise further.

For the Rhine, flood can be predicted much further in advance than for the Meuses, whose water level responds more quickly to rainfall in the river basin. The size of the Rhine's basin means that rainfall often takes two days or more reach Lobith.

Warning at an early stage enables people to take necessary precautions and preparations to limit the effects of a flooding as far as possible. In the Netherlands, the minister of Transport Conmmincion and Public Works has the final responsibility for the dissemination of information about water levels and the warning of the responsible authorities in case of alarming high water levels.

When the figures come in from the neighbor countries, calculations and estimates are passed on by RIZA to the various regional departments of the State Water Management Authority (*Rijkswaterstaat*). Subsequently, the regional departments produce estimates for each municipality along the river, including the maximum water level and peak-level times. In case high water is expected, *Rijkswaterstaat* informs regional fire brigades and a selection of municipalities. *Rijkswaterstaat*'s predictions for the river Meuse are valid for a maximum period of 12 hours, those for the Rhine have a validity of 48 hours. The entire warning and dissemination process is co-ordinated at *Rijkswaterstaat*'s headquarters in The Hague.

A few days before the Meuse flooding in 1993, the Department Limburg of *Rijkswaterstaat* sent out an early warning signal, withdrew it two days later and had to send out a new warning signal shortly after. Communication with the Belgian authorities passed off with difficulty. A further complication were the 12-hour forecasts of *Rijkswaterstaat*. According to *Rijkswaterstaat*'s specialists longer-term forecasts would lead to unacceptable margins of error. In addition, municipal authorities perceived *Rijkswaterstaat*'s forecasts as inconsistent. Soon after the first floods, *Rijkswaterstaat* issued another early warning signal, but this turned out to be a false alarm.

Two years later, towards the end of January 1995, *Rijkswaterstaat* made again an alarming prognosis about the water level of the Meuse. It seemed the water would reach

a level exceeding the one of 1993. Whereas in 1993 forecasting and response authorities did not initiate action until extreme high water levels were reached, in 1995 they did not wait for that to happen but took a more pro-active attitude (Rosenthal *et al.*, 1997). Also in contrast to 1993, *Rijkswaterstaat* was prepared to issue "unofficial" predictions that contained a much wider time horizon than the official maximum of 12 hours.

With regard to the near-flooding situation in the Rhine basin in 1995, the water boards in the region and the Department Oost-Nederland of *Rijkswaterstaat* had initially different opinions about the seriousness of the situation. The water boards were of the opinion that the prognosis of *Rijkswaterstaat* was too optimistic, which was later admitted by the latter. At a later stage there were problems in communication between *Rijkswaterstaat* and the authorities responsible for disaster management. The authorities asked for more long-range forecasts and specific policy-oriented advice, but *Rijkswaterstaat* held on to its own standards and procedures.

In reaction to the miscommunication and lack of longer-term forecasts in 1993 and 1995, the Rhine Action Plan on Flood Defence aims to improve the system of flood forecasting (ICPR, 1998). In the short term this should be realised by international co-operation. Targets in the longer term include the prolonging of the forecasting period by 50% by the year 2000, and by 100% by the year 2005 (reference year 1995).

2.7 Disaster management (planning and response)

In the Netherlands disaster planning, management and response is outlined in the Disaster Act (*Rampenwet*) of 1985. This Act defines a disaster as an event that endangers the life and health of a large number of people, or causes severe harm to material interests, and requires coordinated efforts from various fields of expertise. This conceptualization of disaster reflects the prevailing principles of disaster management in the Netherlands. A very general notion of the social and economic disruption of the community is combined with an explicit demand for governmental activity and for coordination between governmental agencies. According to this act, a disaster - hydrological disasters being just one type of disaster- is an event that puts life at risk for a large number of people, or affects material interests severely, and requires mitigation activities of various nature. .

The Dutch disaster management structure is characterized by different levels of government being involved, i.e. central, provincial and local level. At the local level, the mayor is the head of the disaster response organization. At the provincial and central level the responsible persons are respectively the Royal Commissioner (head of province) and the Minister of Interior Affairs. Other actors that play a role in disaster response are the fire brigade, the army, the police, the first aid assistance (*EHBO*), the hospital transport services (*GGD*), and the Red Cross. Evacuation decisions are in principle in the hands of the mayor, but the Minister of Interior Affairs may take over the competence to evacuate, if deemed necessary.

Generally, local emergency management coordination centres and operational centres are established. In addition to these centres, the so-called 'action centres' become active. Here teams composed of members from specific divisions perform tasks in fields including public relations, civil services, public works, environmental services (see figure 2.5).

The question may be raised how regulations concerning the authority of water boards relate to regulations in the Disaster Act (*Rampenwet*). In the first place, it is important to realise that the act is only applicable when an event falls under the legal definition of a disaster. In case a disaster occurs, the water boards keep their regular authority, but they have to accept that other authorities, such as mayors, the Royal Commissioner, and the Minister of Interior Affairs, have additional powers.

The Disaster Act (*Rampenwet*) requires municipal authorities to develop contingency plans. These plans should address each hazard that exists in the municipality (e.g. flooding, and explosions), and must include the organisational structure, the emergency management activities and a list of all agencies and/or authorities that should be involved in emergency activities. Local fire chiefs have the primary operational responsibility in the activities on site.

To inform the water boards on disaster management, the union of water boards (*Unie van Waterschappen*) has established a paper outlining the necessary elements of dike security plans. The union has also stressed the importance of disaster management, and gives the advice to municipalities to discuss their disaster management plans with the water boards involved.

The phenomenon of a disaster subculture often plays an important role in taking action or not by authorities and citizens, but it is not easy to predict what the influence is of having experience with disasters. A disaster subculture is defined as a complex interconnecting set of meanings, norms, values, organisational arrangements and technological appurtenances which have emerged in response to repeated disaster threat and impact.

The flooding in the province of *Limburg* in 1993 caused in general only minor changes in the disaster response organisation. However, the region of *Nijmegen* was the big exception. In 1994, this region initiated the drafting of a model-contingency plan "Flooding and Dike Failure" for the province of *Gelderland.* Subsequently, the plan needed to be elaborated into concrete measures for each specific region within the province. The region of *Nijmegen* was the first to accomplish this task, just in time before the flooding of 1995.

The contingency plan of *Nijmegen* played an important role in the response to the flooding disaster in 1995. It may even be stated that without the plan an evacuation of citizens would not have taken place, because nobody would have known how to react. In the previous period, there was almost no communication between water boards, authorities and social groups. The mayor of *Nijmegen*, strongly influenced by the responsible water board *Polderdistrict Groot Maas en Waal*, was the first to decide that evacuation of citizens was necessary. Several mayors of other municipalities followed his decision.

In the preparedness phase of emergency management local authorities are often the key actors, following the essentially decentralized approach envisaged in the Act. When the situation becomes more serious and/or transcends the boundaries of one municipality, provincial or even national authorities (especially the Ministry of the Interior) may decide to coordinate or otherwise intervene. More specifically, when mayors do not

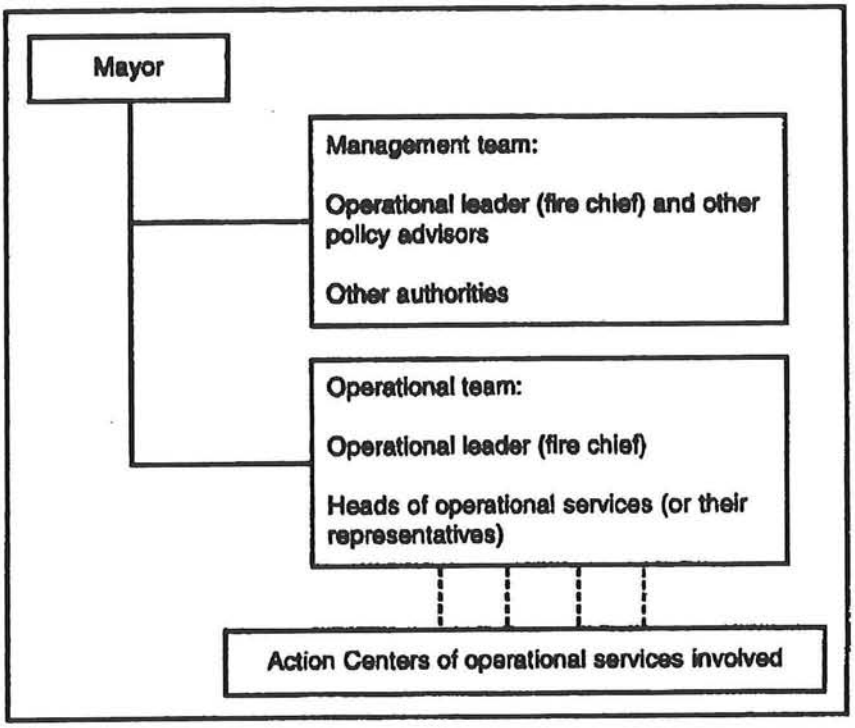

Figure 2.5 The organization of emergency management at the local level (ref.[3])

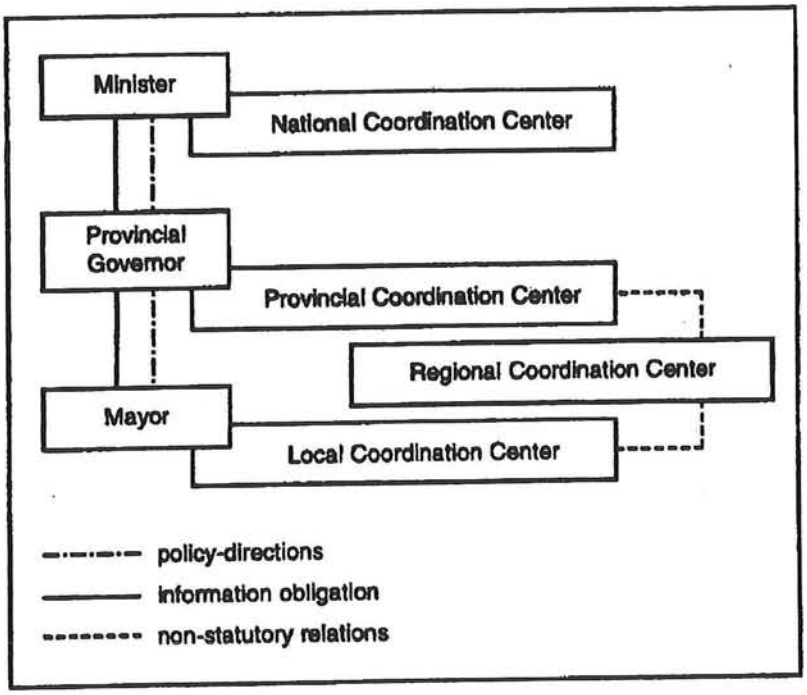

Figure 2.6 Intergovernmental relations during major disasters (ref.[3])

cooperate regionally or when their approach runs counter supramunicipal interests, the provincial governor may give indications for administrative action. A similar rule applies between provincial governors and the minister of the Interior when a disaster transcends the boundaries of one province (see figure 2.6).

2.8 Damage compensation

Shortly after evacuees returned to their properties, public attention shifted towards the assessment of damage and the question of damage compensation. This issue attracted much public attention since compensation for flood damages is not covered by private insurance companies in the Netherlands. Victims of the floods turned to the government and its National Disaster Fund to claim reimbursement.

The financial compensation of losses as a result of natural disasters has not been subject to formal regulations in the Netherlands prior to the 1995 floods. The Disaster Act covers only costs of emergency aid by municipalities. The discussion about the insurability of natural risks started after the 1953 floods in the southwestern part of the Netherlands. During this flood, 1,835 people died and more than 200,000 numbers of cattle drowned. The flood damage rose to 152 million guilders to buildings, 280 million guilders to farmland and 300 million guilders for the repairment of dikes. The considerable damage was only partially compensated for by insurance companies after the 1953 floods.

In the Netherlands, only very recently legal arrangements were made to provide damage compensation in case of floods, earthquakes and other disasters or accidents. The Act on Compensation of Financial Losses due to Disasters and Serious Accidents (*Wet tegemoetkoming schade bij rampen*) entered into force in June 1998. However, since 1799 (Napoleon) the national government has supported, on an *ad-hoc* basis, individuals and firms that suffered from damage due to floods (actual damage from water or damage because of the business interruption at evacuation of areas at risk). Support was distributed by the Disaster Fund (*RampenFonds*), which was established by charity organisations together with the government. Not all damage was covered, in the 1993 case (Meuse flooding) deductibles were established (this started after the large flooding in 1809). After the floods of 1995, the government paid 165 million Euro to

compensate for the financial damage. The households subject to evacuation received a compensation of 225 Euro each.

In a strict legal sense, there was no law that made the government liable for damages caused by natural disasters. Hence, compensation of damage in Netherlands is dependent upon the liberal attitude of governmental agencies (e.g. National Disaster Fund). Ultimately, the 1993 and 1995 damage compensation depended upon generosity, not on any consistent policy or legal liability. Generosity was enforced by political pressure, however. The government was perceived-by many to have neglected the maintenance of the river dikes. Being generous to flood victims was therefore not only the decent but also the politically opportune thing to do.

2.9 Flood control in Lower Yellow River

The Yellow River is known all over the world for its high sediment concentration. The high sediment concentration complicates the problem of achieving flood protection on the lower reaches of the Yellow River. Damage by the Yellow River, formerly called the Sorrow of China, was mainly in the form of breaching and overflowing of dikes along the lower reaches, essentially due to too much sediment. Sediment carried by the river should be handled satisfactorily through an overall evaluation of the factors involved and various branches of national economy concerned, while dealing with the problem of flood protection.

Flood protection on the lower reaches of the Yellow River has always been the first task of river management. The design discharge is 22000m^3/s at Huayuankou and 10000m^3/s at Lijin hydrological station. Flood control has long history in the Yellow River. After lots of failures and experiences, the strategy applied at present is 'pond in upstream, discharge downstream and division along the banks'. That is to store the water in the reservoirs upstream and reduce the flood pressure downstream, to increase the cross section of main channel for flood transport to the sea quickly and descend the water level in the river, also, to operate flood detention areas to divide water along the river.

A series of reservoirs have been built in upstream of main Yellow River and its tributaries, such as Long Yang, Liujiaxia, Qikou, Sanmenxia, Xiaolangdi, Luhun

reservoir etc. These reservoirs will co-operate with each other to reduce peak discharge during flood period. Beijindi and Dongping Lake as flood detention areas were located in the Shandong reach at the left and right side of dykes respectively. They will be used in critical condition for flood diversion. Xiaolangdi Multipurpose Dam Project is located at the exit of last gorge of the middle reach of Yellow River, 130 km downstream of Sanmenxia, 128 km upstream of Huayuankou. The main objectives of the project are: flood control, ice jam control, sediment control, irrigation, water supply, as well as hydroelectric power generation. The total storage capacity of the reservoir is 12.65 billion m^3 or live storage. Of the Yellow River drainage basin, 694,000km^2 or 92.3 percent is located upstream of Xiaolangdi Dam Site. Thus, Xiaolangdi is located in the key position for flood and sediment control of the lower Yellow River. Xiaolangdi Reservoir will effectively mitigate catastrophic floods, the control level will be increased from the present less than 100-year return period up to 10,000 years. By cooperation of Xiaolangdi, Sanmenxia, Lunhun and Guxian reservoirs, peak discharge at Huayuankou 42100m^3/s will reduce to 22600m^3/s. The Beijindi flood detention area would not be used if designed flood discharge is 22 000m^3/s in Huayuankou hydrology station. Meanwhile, the usage frequency of Dongpinghu Lake flood detention area is reduced greatly. Also, Xiaolangdi reservoir will reduce the severe deposition of the river bed of the lower reach. Depositing sediment in dead storage space of the reservoir can reduce about 10 billion tons sediment into river, deposition of the river will reduces 7.6 billion tons, that almost equal to deposition of 20 years in lower Yellow River.

However, the situation of flood defense is still serious. The first problem is that the possibility of enormous flood still exists. From Xiaolangdi to Huayuankou, two tributaries flow into Yellow River, the once every 100 years flood peak discharge can reach 15700m^3/s in Huayuankou station after co-operated of Sanmenxia, Xiaolangdi and two reservoirs in tributaries. Leading time of such kind of flood is very short, it threaten the safety of the dyke seriously.

The second one is sediment problem that could not be solved in a long period, suspended river formed historically will last for long time. The flood protection circumstance is so severely because of sediment deposition and continuous river bed raising. The floodplain in the river is higher 4~6m than outside, some reach even higher more than 10m. The fundamental method is to practice integrated measure of flood control, to conserve water and soil in loess plateau and reduce sediment into river

thereby. However, the practice will only have a striking effect after a few generations' hard work. The sediment reduction would be obviously to deter sediment in the reservoir in the middle reach but only in a limited period. So the serious flood protection situation have been kept for a long time.

The third one is floodplain and Dongping Lake flood detention area need to strengthen flood protection system further. Since the middle of 1980's, the water entering into lower Yellow River had reduced greatly and no-flow in the river often happened. After united operation of Longyang and Liujiaxia reservoirs in 1986,the flow process entering the lower Yellow River was changed. The 60% of water in flood months was reduced to 45%, percentage of water in unflood months was gone up. This change has advantageous for water run off in the lower reach but disadvantageous for sediment transport. Because of water shortage, main channel of the lower river was deposited severely, the situation of 'suspended twice river' was even more dangerous. Average deposition every year was 0.25 billion ton between 1986 and 1997, deposition in main channel reached to 71%. As the cross section of main channel became small, full bank discharge 6000m^3/s was reduced to 3000m^3/s. Water level could be very high and water covered floodplain in small flood period. In August 1996, when peak discharge was 7600m^3/s, which was a moderate discharge at Huayuankou hydrological station, the water level was higher 0.91m than it in 1958 when the discharge was 22300m^3/s. Water level was reached a previously unrecorded rate in most hydrological station of the lower reach. The floodplain flooding could not cause big loss in 1950's and 1960's because of undeveloped economy and less people. However, nowadays about 1.79 million are living in the floodplain where 250,000 hm^2 farmlands are cultivated. The flooding frequency of floodplain and corresponding consequences are increased greatly than before. The floods in 1990's, moderate discharge had inundated large extent of floodplain. In August 1996, total submerged farmland was 230,000hm^2, 11,6000 rooms was collapsed and 1.07 millions people suffered. Inside Beijindi flood detention area, population has hit to 1.57 billion and farmland 160 thousands hm^2 and most part of Zhongyuan oil filed. Population is 358 thousands and farmlands 31.8 thousands hm^2 in Dongping Lake detention area. If Beijindi and Dongping Lake flood detention areas were used for water division, consequences would have been tremendous and many problems left. It is urgent to complete evacuating system. Although full bank discharge will increase and frequency of flooding floodplain will lower, the floods still threaten

lives. Dongping Lake detention area is the key project to assure Shandong reach downstream Aishan hydrological station.

Therefore, the integrated flood management system is required to be built in Lower Yellow River. Some strategies, including structural and non-structural measures, are needed to be improved/strengthen in future.

There are many similar properties between Lower Yellow River basin and the Netherlands. Hence, some flood management practices in the Netherlands can be applied in Lower Yellow River. However, it is too short time to learn about detail experience of flood management in the Netherlands. Therefore, comparison with both basin is a little bit difficult to be carried out. However, the outline of flood management experiences in the Netherlands is clear to us.

2.10 Summary

It is emphasized that the limited scope of the country experience with flood management in the Netherlands is drawn in pervious sections. In many respects, the study is rather superficial due to the limited time. However, many advanced technical measures and strategies are successful applied in flood prevention in the Netherlands. It is worth to summarize this experience and apply it on the flood management of lower Yellow River and other rivers of China taking account of the specific conditions.

Chapter 3 2D Case study for lower Yellow River

3.1 Description of the studied reach

The studied reach, from Huanyuankou to Jiahetan, is the most complex part of the lower Yellow River. Mountains or hills control upstream Huayuankou, the river is suspended and restricted by dikes downstream. Because it is almost in the beginning of lower Yellow River, the dyke failure would have impact to the whole nation. So it is very important for flood defense. This reach is about 100km long. It is the ancient route of the Yellow River, downstream the Jjiahetan, the route is the original Daqing river's which was occupied by Yellow River in 1855. Average width between dykes is about 15km, river slope 15‰. Width of main channel is 3~5km. There are million peoples live in floodplain.

This is the reach extremely wandering. According to the records, main channel could move horizontally a few kilometers within a day. Because the dyke was formed from local embankment and constructed by loose sand, it is easy to be breached by leakage and sand flow; it is more dangerous if main flow shifts near the dyke. On the other hand, people need relative steady floodplain for living and farming. River training is one of the most important tasks in wandering reach. Many regulation projects have been built since 1970's and river shift distance reduces greatly. All of the designed regulation projects have been constructed except one position in this reach at present. However, the river regime changes randomly and is impacted by complex factors, the main flow does not follow the way designed. Fig 3.1, Fig3.2 and Fig3.3 show the main flow routes in recent years. It is obviously main channel still shifts horizontally to a large extent. One of the reasons is that the real discharge was quite different with designed (design discharge for regulation projects is 5000m^3/s in lower Yellow River) due to shortage of water. The radius of flow curve has become small as the discharge reduced. Xiaolangdi Reservoir began to operate in 2000, the wandering reach would be scoured without doubt. It is good to lower water level, but the regulation projects would face the problems of basement stone lost and river regime change. During the initial operation of Sanmenxia Reservoir, heavy scour happened and large area of floodplain was lost in

this reach. Such kind of situation is not allowed to happen after Xiaolangdi operation. The scoured sediment should be transported to the sea and could not cause deposition downstream. The morphology variation of lower Yellow River will impact the operating scheme of Xialangdi Reservoir. It is a challenge to predict the river regime in wandering reach of the Yellow River. The result will be extremely useful for the project management to prevent disaster.

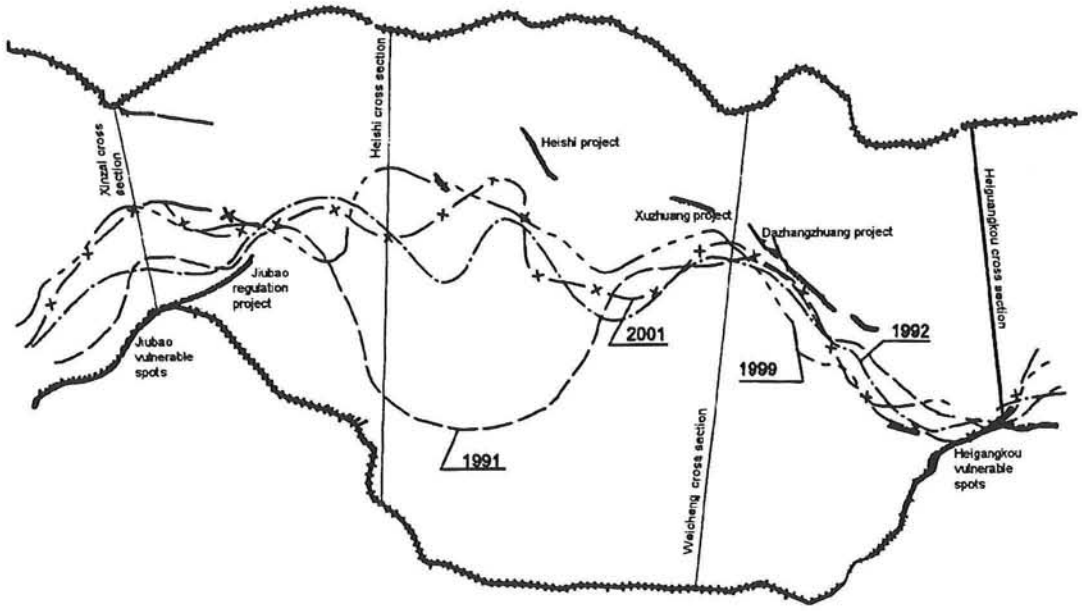

Fig3.1 Main flow streamline from Jiubao to Heigangkou

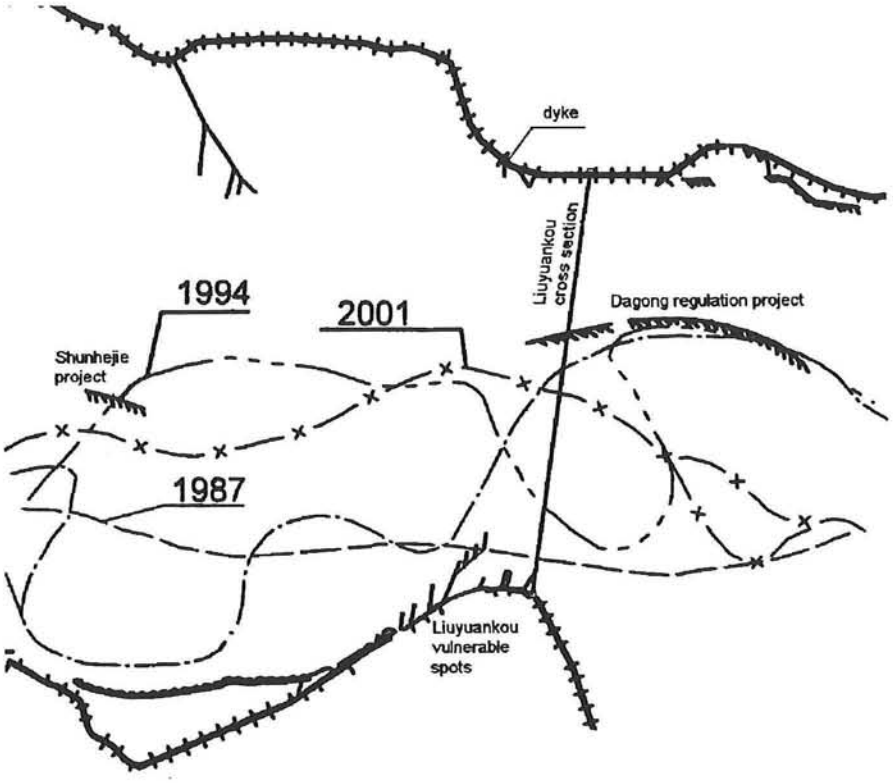

Fig3.2 Main flow streamline in Liuyuankou reach

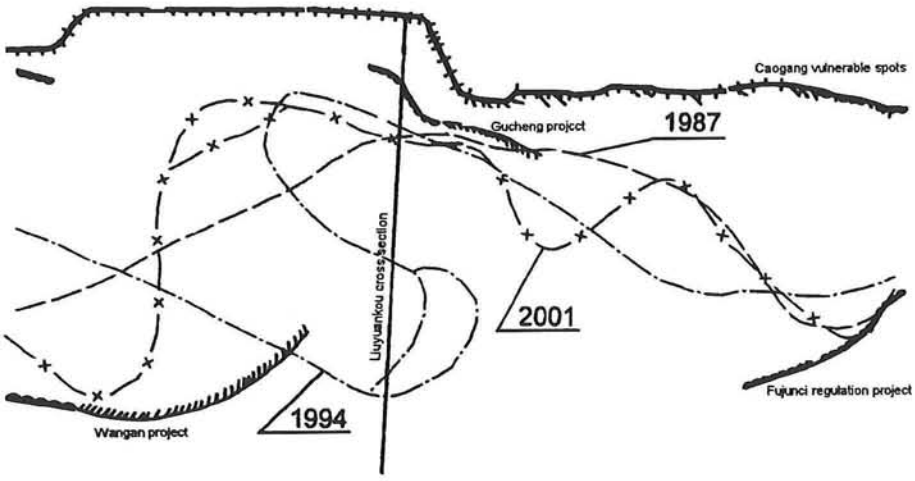

Fig 3.3 Main flow streamline from Wangan to Fujunsi

3.2 Available data

3.2.1 Basic information

Verified computation is very important for numerical models. Reasonable results depend on the reliable basic data, especially for 2D mathematical models. As the river with the most complex boundaries in the world, detail information of flood is very difficult to be obtained in the Yellow River though the measurement of the flow characteristics is conducted during flooding. In general, morphology changes are measured twice every year in the fixed cross-section locations, one is in June before flood season, and the other is in September after flood season. The available information collected is presented below.

3.2.2 Geographic Map

Available geographic map is the base of this case study, ranging from Huayuankou to Jiahetan with about 100 km and involving bank locations, river training projects, channels, roads, levees, village locations etc. This map scale is 1/50000. A part of the map is shown in Fig.3.4.

3.2.3 Description of the 1996 flood

The flood started on the 14th July, 1996, lasting more than one month with maximum discharge of 7860m^3/s at Huayuankou hydrological station. The flood included two peaks and the first one is main discharge peak. Sediment concentration in flow had reached maximum value with 200 kg/m^3 prior to peak flood discharge. Most of sediment deposited in main channel of the river. The processes of hydraulic characteristics at different stations are shown in Figures 3.5, 3.6, 3.7 and 3.8

There are three main peak discharge during this flood, the maximum peak of water level and discharge at Huayuankou section occured in Aug 6, 1996 and Aug 5, 1996, respectively, a few time difference. The values of these features are 94.73m and 7860 m^3/s. In the period of this flood, some floodplain are overflow and the main channel is changed through sediment desposit and erosion, specially after the maximum peak discharge occurred, see Figures 3.9 and 3.10.

Fig. 3.4 Sketch of lower Yellow River map

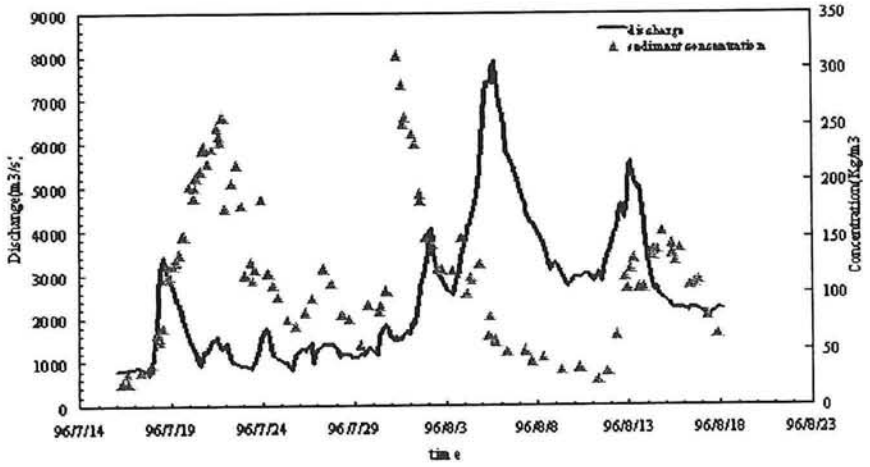

Fig. 3.5 Process of discharge & sediment concentration at Huayuankou station

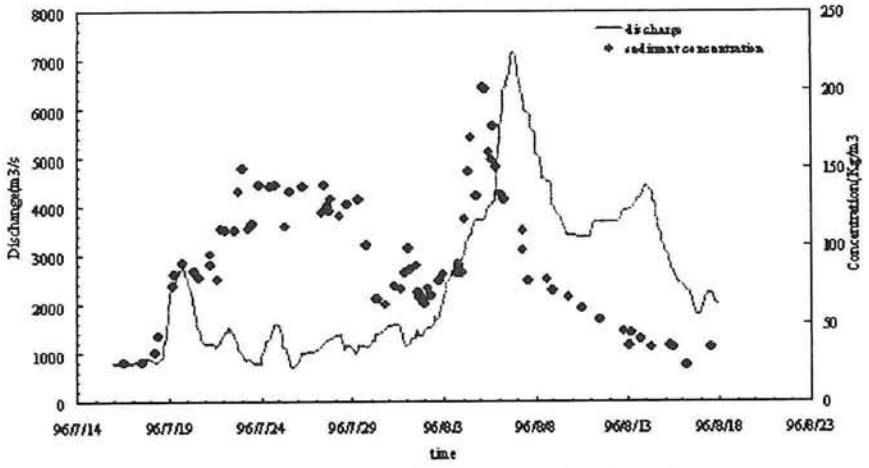

Fig. 3.6 Process of discharge & sediment concentration at Jiahetan station

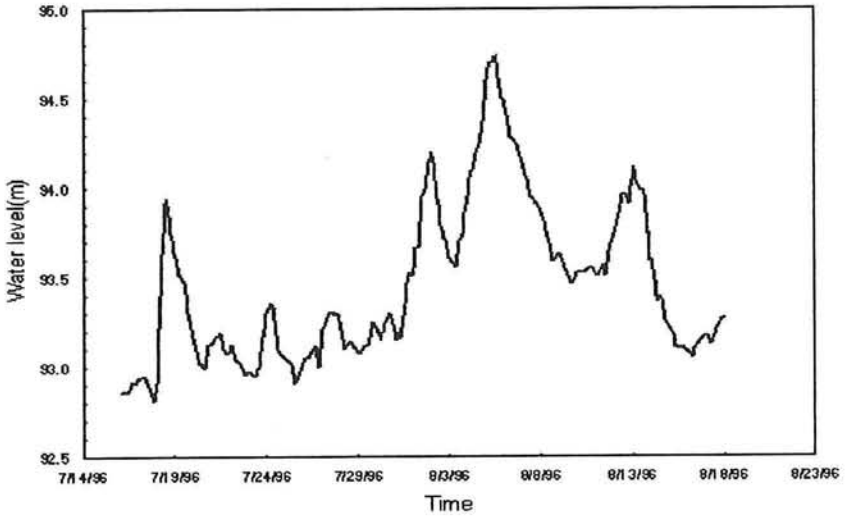

Fig. 3.7 Process of water level in the 96' flood at Huayuankou station

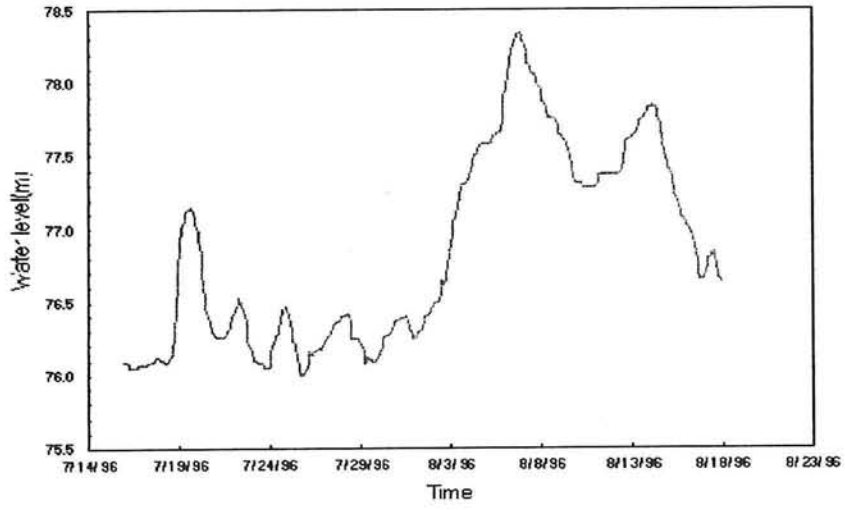

Fig. 3.8 Process of water level in the 96' flood at Jiahetan station

3.2.4 The data of cross sections

There are 11 cross sections in the studied reach from Huayuankou to Jiahetan. Comparison of morphological changes prior to and after flood season at Huayuankou and Weicheng are conducted in Fig.3.9 and Fig.3.10. Amount and distribution of deposition and erosion along the reach is shown in Table 3.1.

Table 3.1 Amount and distribution of deposition and erosion (Unit: 10^8 m^3)

Reach		Distance(km)	Whole Section
Huayuankou	Babao		0.0515
Babao	Laitongzhai		0.0513
Laitongzhai	XinZhai		0.2568
Xinzhai	Heishi		0.1436
Heishi	Weicheng		0.2797
Weicheng	Heigangkou		0.1850
Heigangkou	Liuyuankou		0.0629
Liuyuankou	Gucheng		0.2543
Gucheng	Caogang		0.1890
Caogang	Jiahetan		0.1324
Total			1.6500

On the basis of Table 3.1, if the average width of main channel and floodplain is 1749m and 3023m respectively, the deposited thickness is 0.37m and 0.35m correspondingly; The riverbeds for main channel and floodplain were simultaneously raised 0.36m through flood season in 1996.

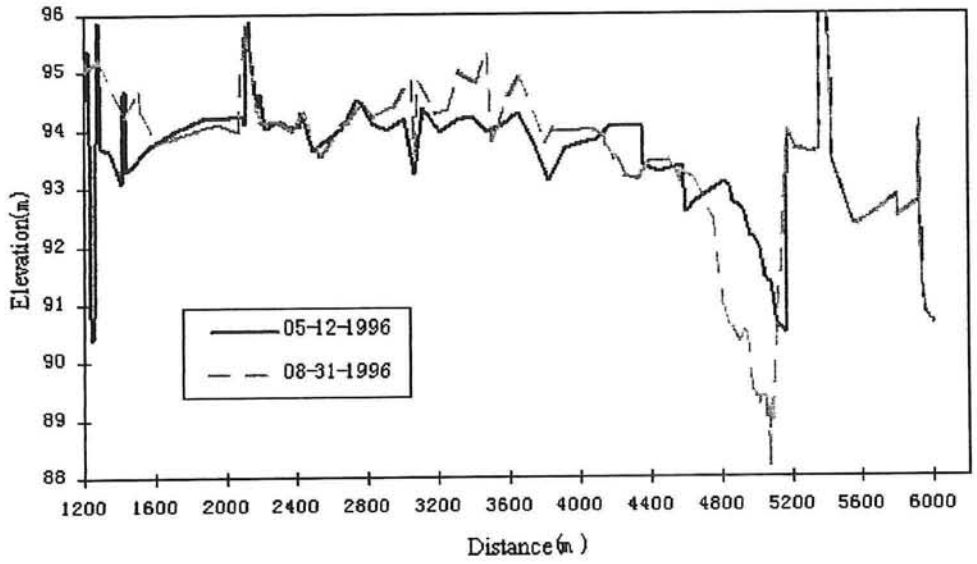

Fig.3.9 Morphological changes at Huayuankou section

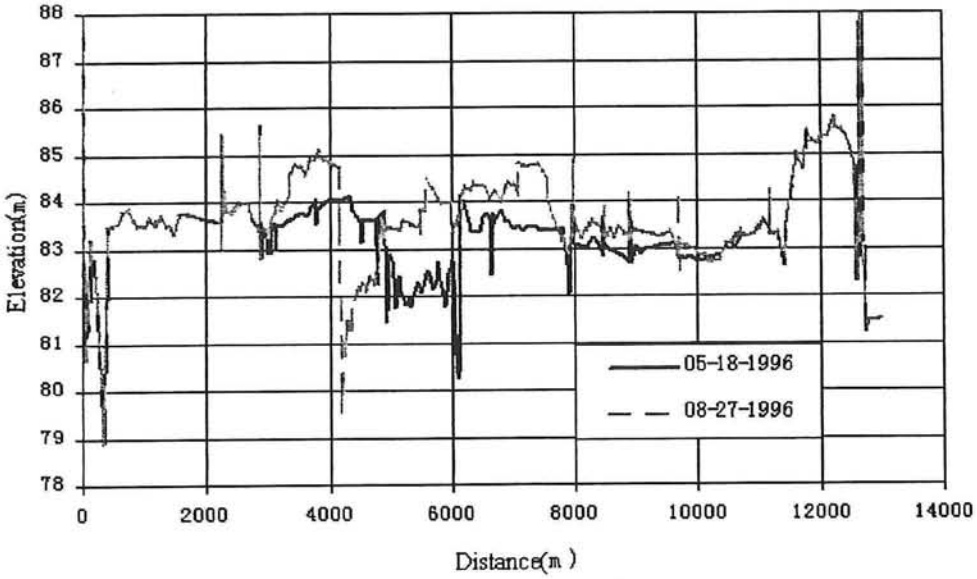

Fig.3.10 Morphlogical changes at Weicheng section

3.2.5 Grain size of Sediment

Data on grain size of sediment are scarce. The median diameters of bed material D_{50} and suspended material d_{50} are about 0.07~0.09mm and 0.01~0.035mm respectively.

3.3 Introduction to Delft3D-FLOW

3.3.1 General background

Delft3D is the integrated flow and transport modeling system of WL Delft Hydraulics for the aquatic environment. It has been designed for experts and non-experts alike. The Delft3D package is composed of several modules, grouped around a mutual interface, while being capable to interact with one another. The flow module of this system, viz. Delft3D-FLOW, provides the hydrodynamic basis for other modules such as water quality, waves and morphology. The hydrodynamic module Delft3D-FLOW simulates two-dimensional (2D,depth-averaged) or three-dimensional (3D) unsteady flow and transport phenomena resulting from tidal and meteorological forcing on a curvilinear, boundary fitted grid, including the effect of density differences due to a non-uniform temperature and salinity distribution (density-driven flow). The flow model can be used to predict the flow in shallow seas, coastal areas, estuaries, lagoons, rivers and lakes. It aims to model flow phenomena of which the horizontal length and time scales are

significantly larger than the vertical scales.

Delft3D-FLOW have the following standard features:

- Tidal forcing.
- The effect of the Earth's rotation (Coriolis force).
- Density driven flows (pressure gradients terms in the momentum equations).
- Advection-diffusion solver included to compute density gradients with an optional facility to treat very sharp gradients in the vertical.
- Space and time varying wind and atmospheric pressure.
- Advanced turbulence models to account for the vertical turbulent viscosity and diffusivity based on the eddy viscosity concept. Four options are provided: k-, k-L, algebraic and constant model.
- Time varying sources and sinks (e.g. river discharges).
- Simulation of the thermal discharge, effluent discharge and the intake of cooling water at any location and any depth.
- Drogue tracks.
- Robust simulation of drying and flooding of inter-tidal flats.

Also it can be coupled to other modules. The hydrodynamic conditions (velocities, water elevations, density, salinity, vertical eddy viscosity and eddy vertical diffusivity) calculated in the Delft3D-FLOW module are used as input to the other modules of Delft3D, which are WAQ, SED, ECO, PART, WAVE, MOR modules. Delft3D Model includes the following utilities: Delft-RGFGRID for generating curvilinear grids, Delft-QUICKIN for preparing and manipulating grid oriented data, Delft-TRIANA for performing off-line tidal analysis of time series, GETIJSYS for performing tidal analysis on time series of measured water levels or velocities and Delft-GPP for visualisation and animation of simulation results.

3.3.2 Governing equations

The numerical hydrodynamic modeling system Delft3D-FLOW solves the unsteady

shallow water equations in two (depth-averaged) or in three dimensions. These equations are derived from the three dimensional Navier Stokes equations for incompressible free surface flow. The system of equations consists of the horizontal equations of motion, the continuity equation and the transport equations for conservative constituents. The equations are formulated in orthogonal curvilinear co-ordinates or in spherical co-ordinates on the globe. However, some assumptions with respect to Delft3D-FLOW are applied, such as shallow water assumption (hydrostatic pressure assumption), Boussinesq approximation, slip boundary condition at the bed, anisotropic turbulence model (horizontal-vertical).

Continuity equation

The depth-averaged continuity equation is given by

$$\frac{\partial \zeta}{\partial t}+\frac{1}{\sqrt{G_{\xi\xi}}\sqrt{G_{\eta\eta}}}\frac{\partial[(d+\zeta)U\sqrt{G_{\eta\eta}}]}{\partial \xi}+\frac{1}{\sqrt{G_{\xi\xi}}\sqrt{G_{\eta\eta}}}\frac{\partial[(d+\zeta)V\sqrt{G_{\xi\xi}}]}{\partial \eta}=Q \qquad (3.1)$$

with Q representing the contributions per unit area due to the discharge or withdrawal of water, evaporation and precipitation.

Momentum equations

The momentum equations in ξ- and η-direction are given by

$$\frac{\partial u}{\partial t}+\frac{u}{\sqrt{G_{\xi\xi}}}\frac{\partial u}{\partial \xi}+\frac{v}{\sqrt{G_{\eta\eta}}}\frac{\partial u}{\partial \eta}+\frac{\omega}{d+\zeta}\frac{\partial u}{\partial \sigma}+\frac{uv}{\sqrt{G_{\xi\xi}}\sqrt{G_{\eta\eta}}}\frac{\partial\sqrt{G_{\xi\xi}}}{\partial \eta}-\frac{v^2}{\sqrt{G_{\xi\xi}}\sqrt{G_{\eta\eta}}}\frac{\partial\sqrt{G_{\eta\eta}}}{\partial \xi}-fv=$$
$$-\frac{1}{\rho_0\sqrt{G_{\xi\xi}}}P_\xi+F_\xi+\frac{1}{(d+\zeta)^2}\frac{\partial}{\partial \sigma}(\nu_v\frac{\partial u}{\partial \sigma})+M_\xi \qquad (3.2)$$

and

$$\frac{\partial v}{\partial t}+\frac{u}{\sqrt{G_{\xi\xi}}}\frac{\partial v}{\partial \xi}+\frac{v}{\sqrt{G_{\eta\eta}}}\frac{\partial v}{\partial \eta}+\frac{\omega}{d+\zeta}\frac{\partial v}{\partial \sigma}+\frac{uv}{\sqrt{G_{\xi\xi}}\sqrt{G_{\eta\eta}}}\frac{\partial\sqrt{G_{\xi\xi}}}{\partial \eta}-\frac{u^2}{\sqrt{G_{\xi\xi}}\sqrt{G_{\eta\eta}}}\frac{\partial\sqrt{G_{\eta\eta}}}{\partial \xi}+fu=$$
$$-\frac{1}{\rho_0\sqrt{G_{\eta\eta}}}P_\eta+F_\eta+\frac{1}{(d+\zeta)^2}\frac{\partial}{\partial \sigma}(\nu_v\frac{\partial v}{\partial \sigma})+M_\eta$$

(3.3)

The vertical velocity ω in the adapting σ-coordinate system is computed from the continuity equation

$$\frac{\partial \zeta}{\partial t}+\frac{1}{\sqrt{G_{\xi\xi}}\sqrt{G_{\eta\eta}}}\frac{\partial[(d+\zeta)u\sqrt{G_{\eta\eta}}]}{\partial \xi}+\frac{1}{\sqrt{G_{\xi\xi}}\sqrt{G_{\eta\eta}}}\frac{\partial[(d+\zeta)v\sqrt{G_{\xi\xi}}]}{\partial \eta}=H(q_{in}-q_{out})$$

(3.4)

ω is the vertical velocity relative to the moving σ-plane. The physical vertical velocity w in the Cartesian coordinate system can be expressed in the horizontal velocities, water depths, water levels and vertical ω-velocity according to

$$w=\omega+\frac{1}{\sqrt{G_{\xi\xi}}\sqrt{G_{\eta\eta}}}[u\sqrt{G_{\eta\eta}}(\sigma\frac{\partial H}{\partial \xi}+\frac{\partial \zeta}{\partial \xi})+v\sqrt{G_{\xi\xi}}(\sigma\frac{\partial H}{\partial \eta}+\frac{\partial \zeta}{\partial \eta})]+(\sigma\frac{\partial H}{\partial t}+\frac{\partial \zeta}{\partial t})$$

(3.5)

Under the shallow water assumption, the vertical momentum equation is reduced to a hydrostatic pressure equation.

Transport of conservative constituents

In Delft3D-FLOW the transport of matter and heat is modelled by an advection-diffusion equation in three co-ordinate directions. The transport equation is formulated in a conservative form (Finite Volume approximation) in orthogonal curvilinear co-ordinates in the horizontal direction and s-co-ordinates in the vertical:

$$\frac{\partial[(d+\zeta)c]}{\partial t}+\frac{1}{\sqrt{G_{\xi\xi}}\sqrt{G_{\eta\eta}}}\left\{\frac{\partial(d+\zeta)u\sqrt{G_{\eta\eta}}c}{\partial \xi}+\frac{\partial(d+\zeta)v\sqrt{G_{\eta\eta}}c}{\partial \eta}\right\}+\frac{\partial(\omega c)}{\partial \sigma}=$$

$$\frac{d+\zeta}{\sqrt{G_{\xi\xi}}\sqrt{G_{\eta\eta}}}\left\{\frac{\partial}{\partial \xi}\left[D_H\frac{\sqrt{G_{\eta\eta}}}{\sqrt{G_{\xi\xi}}}\frac{\partial c}{\partial \xi}\right]+\frac{\partial}{\partial \eta}\left[D_H\frac{\sqrt{G_{\xi\xi}}}{\sqrt{G_{\eta\eta}}}\frac{\partial c}{\partial \eta}\right]\right\}+\frac{1}{d+\zeta}\frac{\partial}{\partial \sigma}(D_v\frac{\partial c}{\partial \sigma})-\lambda_d(d+\zeta)c+S$$

(3.6)

with λ_d representing the first order decay process and S the source and sink terms per unit area due to the discharge q_{in} or withdrawal q_{out} of water.

3.3.3 Initial and boundary conditions

To get a well-posed mathematical problem, a set of initial and boundary conditions for water levels and horizontal velocities must be specified.

Initial condition

Usually it is assumed that initially the model is at rest. The initial conditions can be specified as a uniform value in whole area or taken from a pervious run.

Boundary conditions

Delft3D-FLOW includes several boundaries, such as open boundaries (inflow/ outflow), bed /free surface boundaries and fixed boundaries.

For inflow/outflow boundaries, the boundary conditions can be given as discharge or water level.

Open boundaries are always introduced to obtain a limited computational area. In nature, waves can cross these boundaries unhampered and without reflections. In a numerical model this property must be included in the boundary conditions. To reduce the reflections at the open boundary, the boundary condition based on the Riemann invariant is adapted which pass normal to the boundary and it reduces the reflection for waves which have an oblique incidence.

At the bed and the free surface, the boundary conditions for momentum equations can be specified as the relations between the velocity gradients and bed stress/wind stress. At the free surface and the bottom, ω is set to zero.

For the fixed boundaries, a slip boundary condition is assumed.

3.3.4 Numerical methods

In pervious section the mathematical formulations of the 3D shallow water flow and

transport model Delft3D-FLOW were presented. To solve the partial differential equations the equations should be transformed to the discrete space.

Delft3D-FLOW is a numerical model based on finite differences. To discretize the 3D shallow water equations in space, the model area is covered by a rectangular, curvilinear or spherical grid. It is assumed that the grid is orthogonal and well-structured.

In the vertical direction boundary-fitted σ-co-ordinates are used. The vertical grid consists of layers bounded by two sigma planes. This means that over the entire computational area, irrespective of the local water depth, the number of layers is constant. As a result a smooth representation of the topography is obtained. The relative layer thicknesses are usually non-uniformly distributed, which allows for more resolution in the zones of interest, such as the near surface area (important for e.g. wind-driven flows, heat exchange with the atmosphere and the near bed area (sediment transport).

The numerical algorithm is based on the staggered C-grid. The combined method of time integration ADI (*Alternating Direction Implicit*) or AOI (*Alternating Operator Implicit*) method in horizontal and fully implicit in vertical is adapted in Delft3D-FLOW.

The ADI method for the shallow water equations is developed by Leendertse. It splits one time step into two stages. Each stage consists of half a time step. In both stages the terms of the model equations are solved in a consistent way. In the first half time step, the ξ-derivatives are taken implicitly and in the second half time step the η-derivatives are taken implicitly. The advantage of the ADI-method is that the implicitly integrated water levels and velocities are coupled along grid lines. A disadvantage of the ADI method is the numerical inaccuracies for large time steps.

The AOI method is a two-stage time splitting method, which is similar to the ADI method. However, for the AOI method a splitting in so-called operators is applied, whereas the ADI method is based on a splitting in directions. In the first half time step, the advection and diffusion terms are taken implicitly and in the second half time step the terms describing the propagation of the surface waves are integrated implicitly. The advantages of an AOI time integration method in comparison to the ADI method are possibility to apply larger time steps while the accuracy hardly decreases and increased

ease of use. The choice of the time step does not depend on the model geometry, which is the case for the ADI method. So, less knowledge of the user is required. A disadvantage of the AOI method is the larger computational costs per time step.

The horizontal velocities of adjacent vertical layers are coupled by the vertical advection and the vertical viscosity term. The sigma co-ordinate system can lead to very thin layers in shallow areas. To prevent instabilities induced by the vertical viscosity term, a fully implicit time integration is used for the vertical exchange terms.

However, some special numerical technique are used, such as filter for negative concentrations and unstable vertical density profiles, correction for sigma-problem, drying and flooding points, special hydraulic structures and thin dams.

3.4 Determination of the computational conditions

3.4.1 Computational grid and bathymetry

As described in section 3.1, the reach for case study is the wanding section being about 100 km long. The computational domain is discretised by the grid. The computational grid and depth file can be generated by use of RGFGRID module, see as Fig 3.11 and Fig. 3.12. The features of the grid is shown in Table 3.2.

Table 3.2 the feature of grid

The Grid Main Features		
Grid	M-direction	335
	N-direction	33
Number of Grid cells		10688
Cell size	M-direction	78.68-1011.26m
	N-direction	52.85-711.84m
Orthogonality	max.	0. 18
Apect ratio		1.0-4.61
Curvature	M-direction	0-1.25
	N-direction	0-1.82
Smoothness	M-direction	1.0-2.35
	N-direction	1.0-1.84

3.4.2 Initial and boundary conditions

In case study for the lower Yellow River, the static field is specified as initial condition that the initial water levels for the whole computational domain are given a constant value and the initial flow velocities at each grid cell are set to zero. Also a trial result can be given as initial condition.

The open boundaries are defined in the case study, including inflow boundary at Huayuankou section and outflow boundary at Jiahetan section. These boundary conditions are specified as time-series according to the measured data in the period of 1996's flood. For the inflow boundary, the measured discharge process during 1996's flood at Huayuankou section is adapted as the boundary condition. For the outflow boundary, the measured water level process of the same period at Jiahetan station is adapted as the boundary condition, see Fig 3.13 and Fig 3.14.

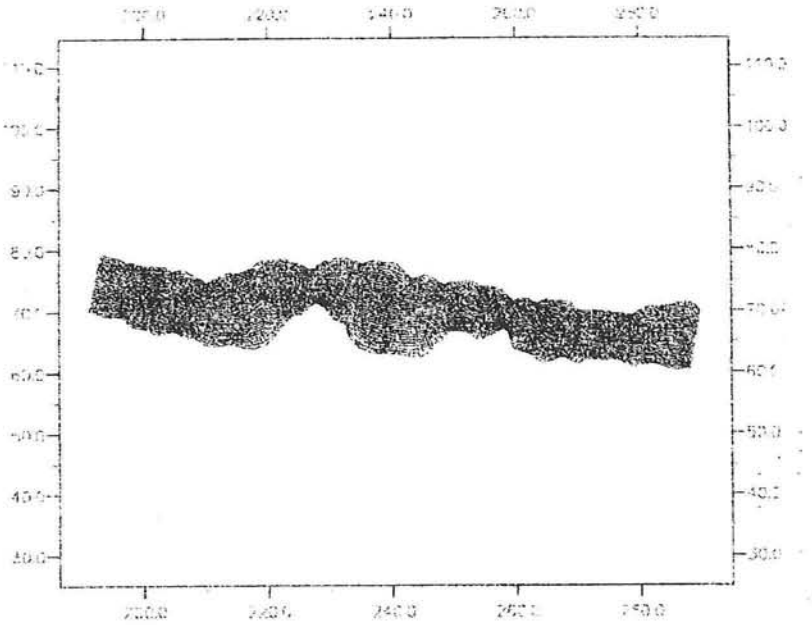

Fig 3.11 the computational grid

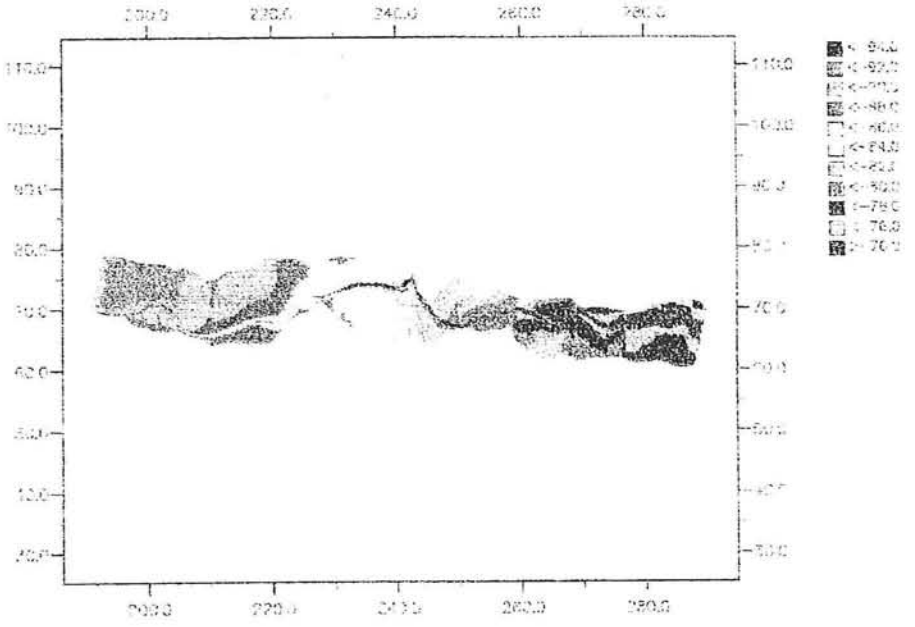

Fig 3.12 the bathymetry for case study

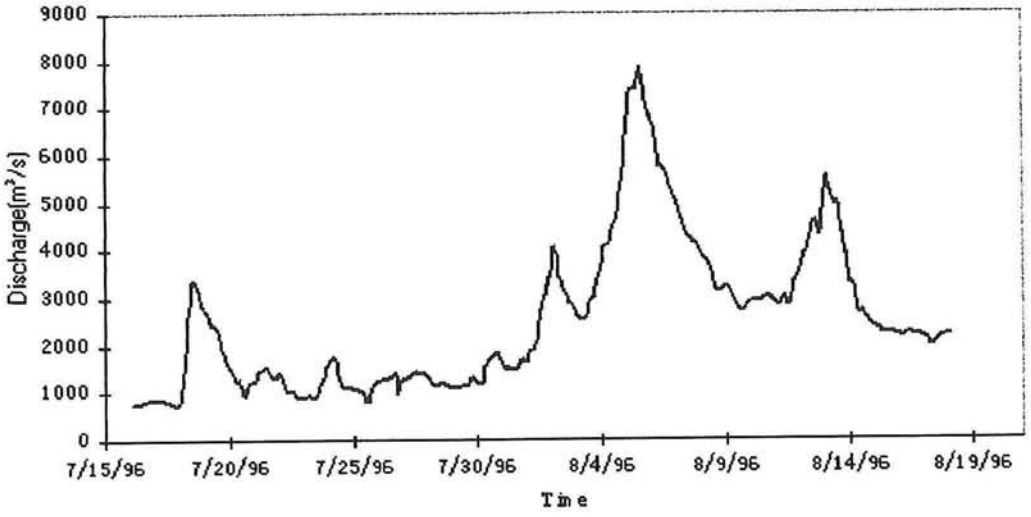

Fig 3.13 The discharge boundary condition at Huayuankou section

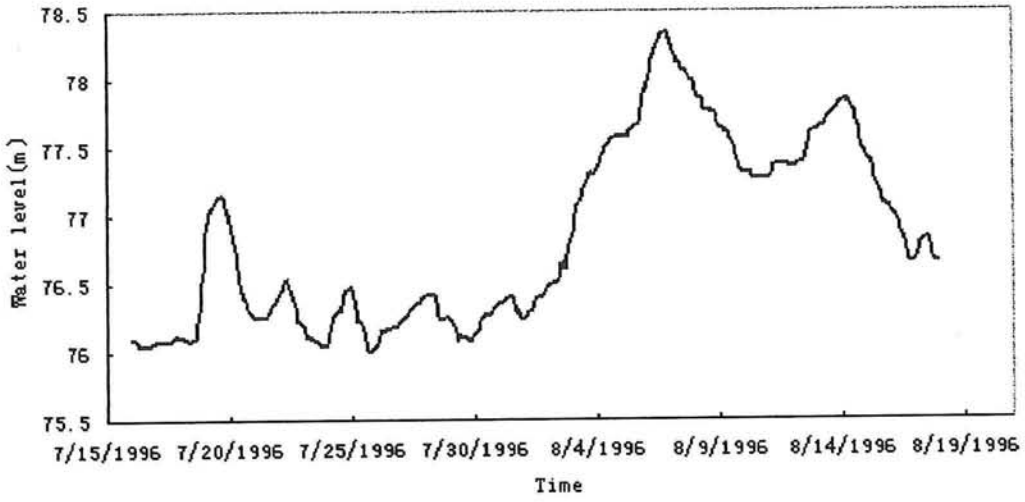

Fig 3.14 The water level boundary condition at Jiahetan station

3.4.3 Numerical and physical parameters

In the verified calculation, some physical and numerical parameters must be selected correctly according to the lower Yellow River. The main parameters are selected as the following:

- Secondary flow velocity=0.1 m/s
- Viscosity coefficient=0.01m^2/s
- Bottom Roughness:

For Manning formula: n=0.010~0.025 $m^{1/2}/s$;

For Chezy formula: C=65 and 100

- Threshold depth=0.05m
- Time step: 1 min and 5 min
- Boundary reflect parameter: alf=10

3.5 Flow verification of Delft3D model

3.5.1 comparison of the specified ways for discharge boundary

In Delft3D-FLOW, as the boundary condition, the discharge is prescribed at both of a boundary section and intermediate values are determined by linear interpolation. However, the discharge prescribed in an endpoint is the discharge through the grid cell related to that specific endpoint. If a certain discharge through the total cross-section is prescribed, This total discharge must be translated into discharge at the endpoints. This is a rather difficult task if the bathymetry changes appreciably over the cross-section. So at inflow boundary, three methods are adapted respectively to compare the impact of specified discharge on the result. Three methods are the following:

Method I : Averaging the discharge in inlet cross-section, while the discharge at each section is defined as the total discharge divided by the number of sections.

Method II Adding a transition reach upstream about 2.0km, which the domain is extended about 2 km along upstream. The open boundary section is the same bed elevation and the bathymetry change gradually between the new and original inflow section. The discharge at the upstream section is specified in the same ways as for Method I, this is more accurate than Method I.

Method III : Dividing the inlet discharge at cross-section by experimential methods. The method determines the boundary conditions per grid cell using the following approach:

$$Q_i = \frac{B_i H_i^{3/2}}{\sum_{j=1}^{N} B_i H_j^{3/2}} Q \tag{3.7}$$

where Q_j, H_j, Q and N are the discharge through section j, the average depth in section j, the total discharge through the cross-section and the total number of sections in the cross-section, respectively.

The comparisons of the water level process at Huayuankou station and the discharge process at Jiahetan with three specified methods are carried out, shown as Fig 3.15 and Fig 3.16.

As shown in Fig 3.15 and Fig 3.16, Method I fails to calculate the flood flow. The velocity is larger than 5 m/s at the floodplain area where become drying when the water level is lower. The Courant number is larger than 10. It is the main reason that results in the failure of computation. So Method I is not reasonable under case study. Comparison of the computational results of Method II and Method III on the observed data is shown that the water level of Method III at Huayuankou station is lower than that of Method II under the same computational parameters. The conclusion can be obtained that Method II and Method III is suitable for case study. Relatively the accuracy for Method II is better than Method III. The different specified methods for BC is influence on the flow field near inlet area.

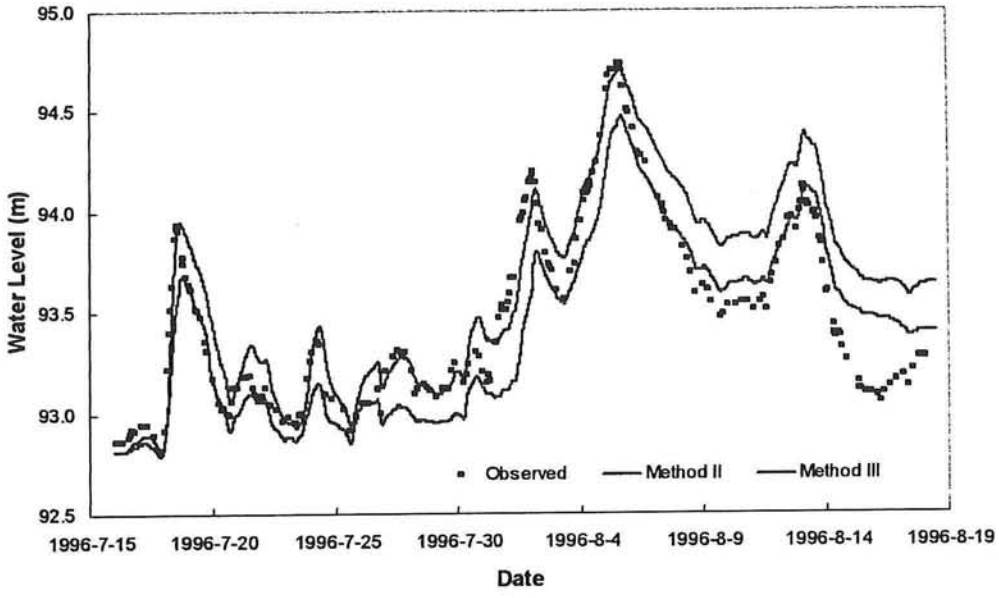

Fig 3.15 Comparison of water levels with difference specified ways of BC at Huayuankou station

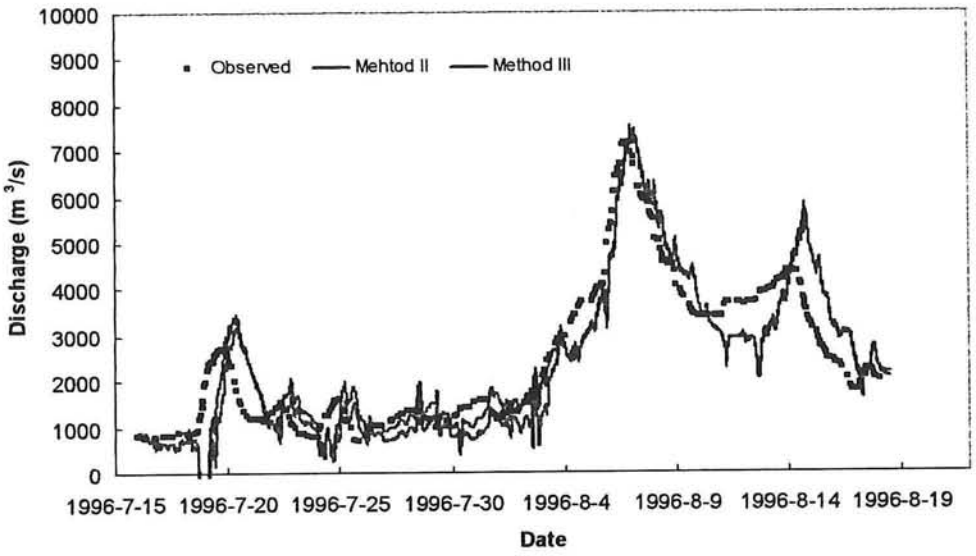

Fig 3.16 Comparison of Discharges with Difference Given ways of BC at Jiahetan Section

3.5.2 Flow verification for case study

This section shows the flow verified results for case study. The comparison of various bed roughness with different formulae is developed. In Delft3D-FLOW module, the bed roughness can be computed according to Manning, White-Colebrook and Chezy formula. It is assumed that the bed roughness is uniform at whole computational domain, regardless the difference of the main channel or floodplain.

Manning and Chezy formulae are selected in flow verified computation. As described in the previous section, the Chezy coefficient C is specified as 65 and 100 $m^{1/2}/s$ for Chazy formula and the bed roughness n is chosen from 0.010 to 0.025$m^{1/2}/s$. The calculated results are shown as Fig 3.17 and Fig 3.18. The statistical features for verified computation are given in Table 3.3.

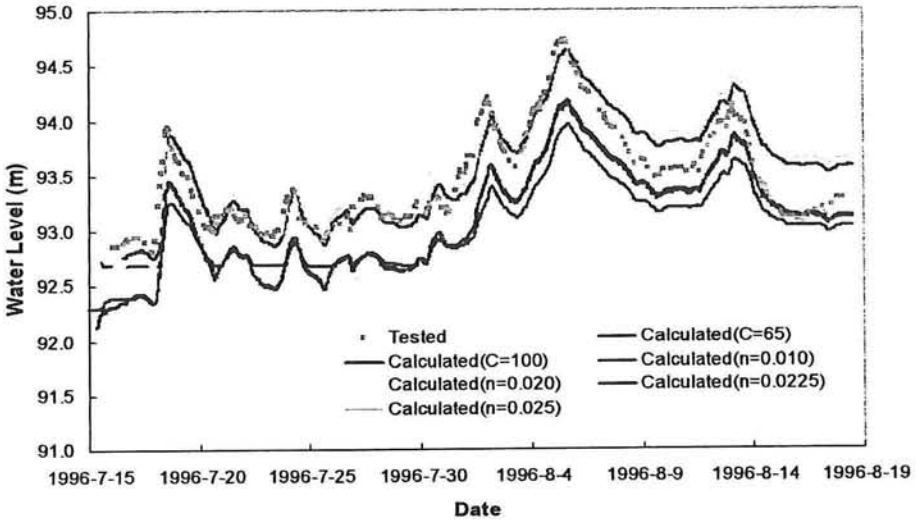

Fig 3.17 Comparison of water levels at Huayuankou station

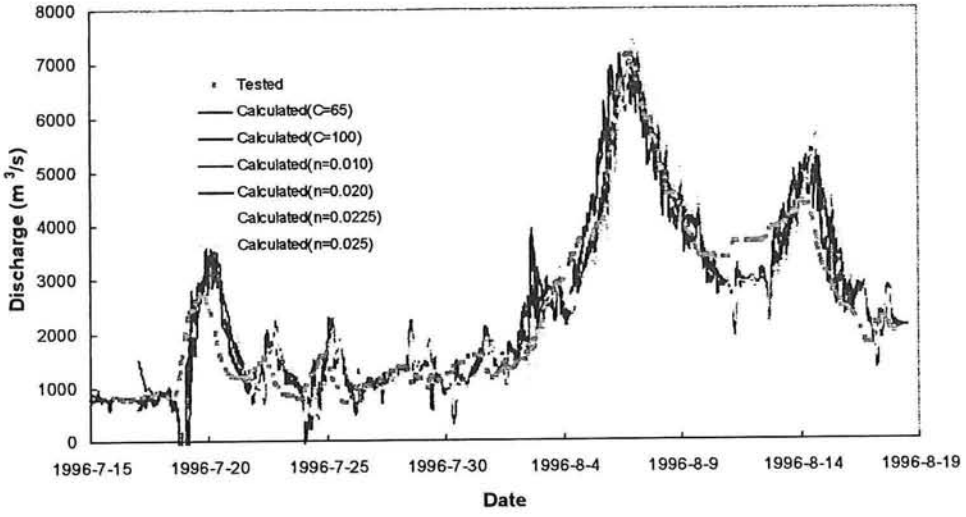

Fig 3.18 Comparison of discharges at Jiahetan section

Table 3.3 Comparison of the flood peak features with tested values

Variable	Cases		Peak Time	Error	Peak Value	Error
Highest Water Level	Tested		1996-8-5 3:00 PM	0:00	94.73	0.00
	Chezy	C=65	1996-8-5 4:10 PM	1:10	93.96	-0.77
		C=100	1996-8-5 3:20 PM	0:20	94.17	-0.56
	Manning	N=0.0100$m^{1/2}$/s	1996-8-5 3:00 PM	0:00	94.14	-0.59
		N=0.0200 $m^{1/2}$/s	1996-8-5 3:00 PM	0:00	94.55	-0.18
		N=0.0225 $m^{1/2}$/s	1996-8-5 3:00 PM	0:00	94.63	-0.10
		N=0.0250 $m^{1/2}$/s	1996-8-5 3:00 PM	0:00	94.72	-0.01
Peak	Tested		1996-8-6 5:30 PM	0:00	7150	0.00

Discharge	Chezy	C=65	1996-8-7 12:00 AM	6:30	7364.00	214.00
		C=100	1996-8-6 10:00 AM	-7:30	7151.00	1.00
	Manning	n=0.0100 $m^{1/2}/s$	1996-8-610:00 AM	-7:30	7152.00	2.00
		n=0.0200 $m^{1/2}/s$	1996-8-7 3:00 AM	9:30	7401.00	251.00
		n=0.0225 $m^{1/2}/s$	1996-8-7 12:00 AM	6:30	7426.00	276.00
		n=0.0250 $m^{1/2}/s$	1996-8-7 3:00 AM	9:30	7408.00	258.00

It is clear from figure 3.17 that the Manning parameter (n) has less influence on the water level at Huayuankou section, and in contrary the Chzy coefficient(C) has rather large influence on the water level at Huayuankou section. Relatively, the result with bed roughness according to Manning formula does agree better with the observed data than Chezy formula. However, It is notable that the water level becomes unfit with observed data after the main peak discharge of the flood. This difference is caused by the remarkable change of the river bed during the flood. The Yellow River is known all over the world for its high sediment concentration. In an ordinary sediment-laden flow, sediment is carried by the flow and has little effect on flow behavior. Therefore such effect can be neglected. In hyper-concentrated flow, however, the existence of large amounts of solid particles remarkably influences or changes the fluid properties and flow behavior. In such case the above mentioned influence or change must be considered.

The calculated discharge process has the same pattern as the water level, seen Fig 3.18. The good agreement between observed data and calculated result at Jiahetan section is obtained before the peak discharge of the flood. The unfitted tendency is occurred after that time. The same reason as water level is explained.

The analysis of the characteristics of the flood is carried out in Table 3.3. The peak water level and flood transported time at Huayuankou station can be well simulated by Delft3D with n=0.025. The peak water level with other bed roughness is larger than 0.10m at Huayuankou station. However, The peak discharge and corresponding time have some difference with observed data at Jiahetan section, the relative error is under 4% which is under allowance range. Therefore, it is concluded that the result with bed roughness 0.025 is relatively better than others. So in the following calculation, the bed roughness is selected as n=0.025.

3.5.3 Sensitivity test of time step

The Delft3D-FLOW system is discretized by finite difference method. The scheme is unconditionally stable. Theoretically, the time step can be selected without limited condition. In Delft3D-FLOW the Courant number is an indication for numerical stability and accuracy. The Courant number gives the relation between the propagation speed and time step. The magnitude of the time step determines the total computational time. To reduce the total computational time, it is necessary to choose the largest time step possible, without the loss of accuracy and stability. For many practical applications, the time step is related to the Courant number. If time step is selected as larger which lead to the Courant number lager than 10, it may lead to badly predicted flow patterns. So several runs were made with different time steps to study the influence of the time step on the results. Runs were made with time steps of 1 minute and 5 minutes.

As shown in Fig 19 and Fig 20, the flow accuracy with difference selected time step basically is the same. That is said that under case study time step can be selected as 5 minutes and 1 minute. However, it is only reasonable for FLOW and too large for MOR shown in the following section.

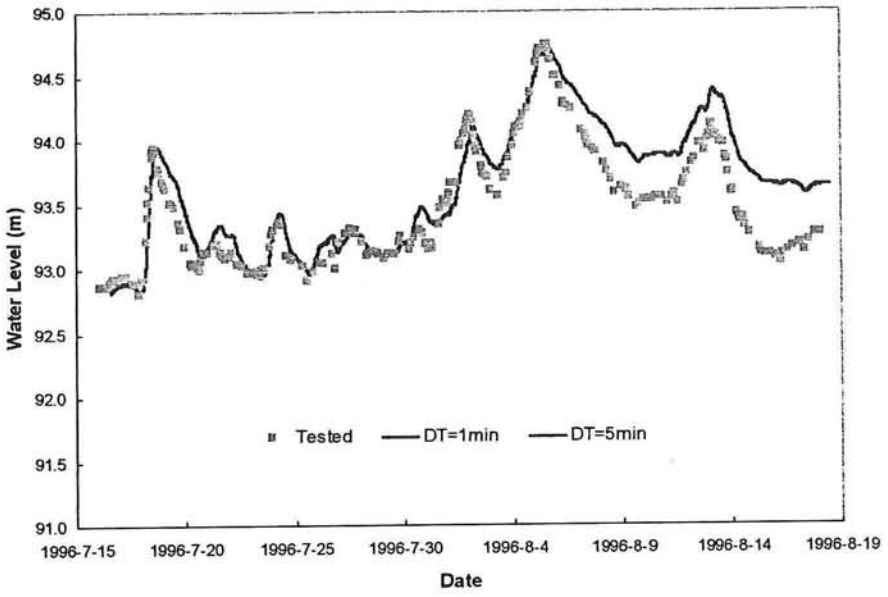

Fig 3.19 Comparison of water level under difference time steps at Huayuankou Station

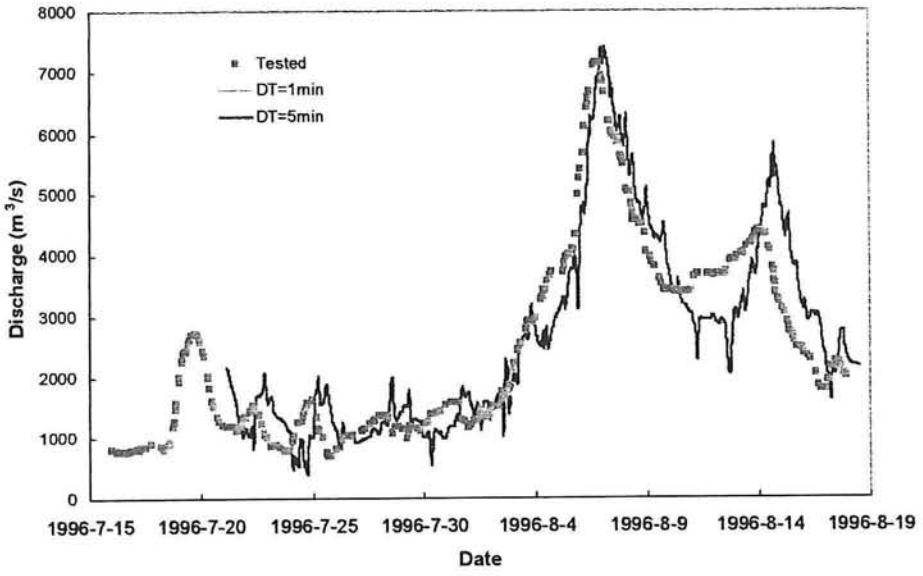

Fig 3.20 Comparison of discharge under difference time steps at Jiahetan Section

3.5.4 Result assessment

The flow velocity fields at the different instants are shown in Fig 3.21. It can be seen that the smaller the discharge is, the smaller the flow velocity is at the computational domain. In the initial period of the flood, it is signally shown that the flow only exists in main channel and the two-side floodplain are drying. Along with the increasing discharge, the water level rises and the floodplain is overflowing. At 6 o'clock, Aug 5, 1996, the peak discharge at Huayuankou section occurred and the flooding area reached largest. Then the discharge decreased with time, the flooding area also decreased.

The water level contour patterns at the same instants as the flow velocity is shown in Fig 3.22. The same regular can be reviewed.

The flow features with Method III near the regulation projects along the studied reach are compared with measured data (Fig 3.23). The comparison of the peak water levels at several stations along the studied reach is conducted in Table 3.4. In general, the predicted results are good agreement with the observed data. However, the flow field near the thin dams is very complicated due to re-circular flow around thin dams. At these area the flow need to be simulated with fine grids. In this case study the grid is

much too coarse to accurately simulate the flow pattern. This is the main reason leading to some error between calculated and measured data.

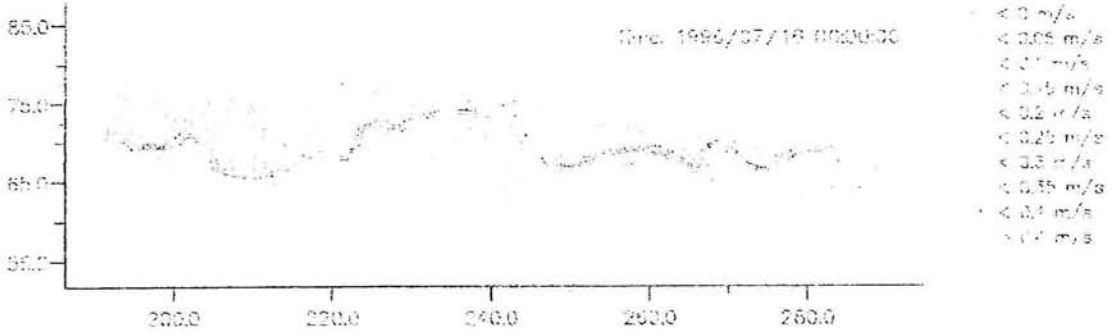

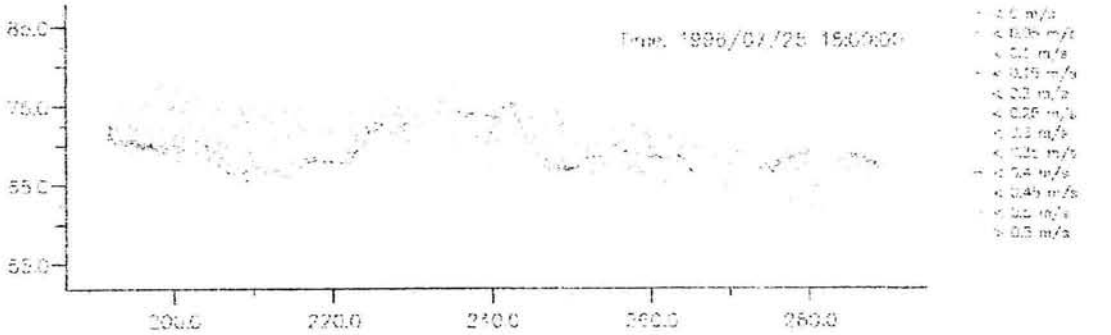

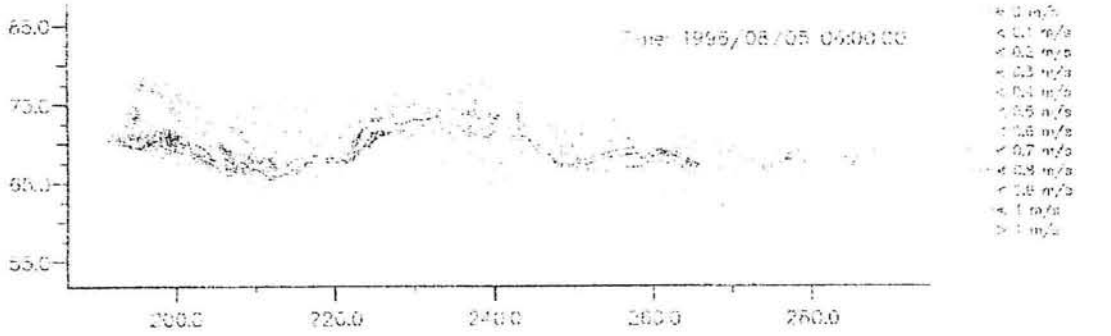

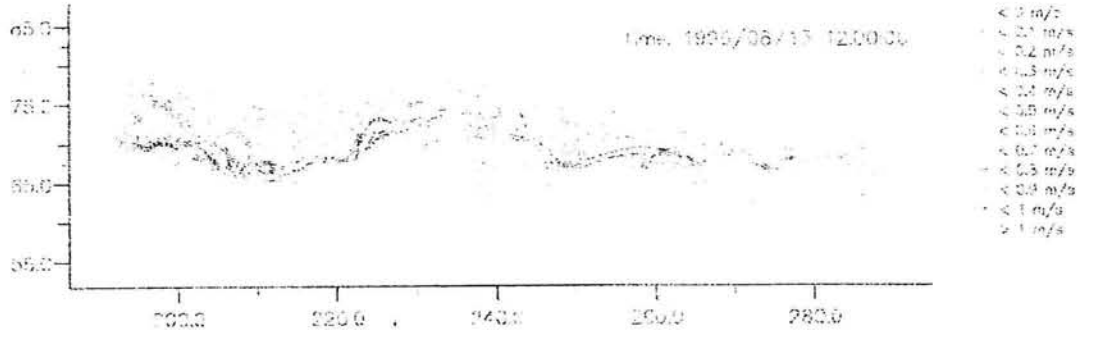

Fig 3.21 the velocity fields at several instants during the flood

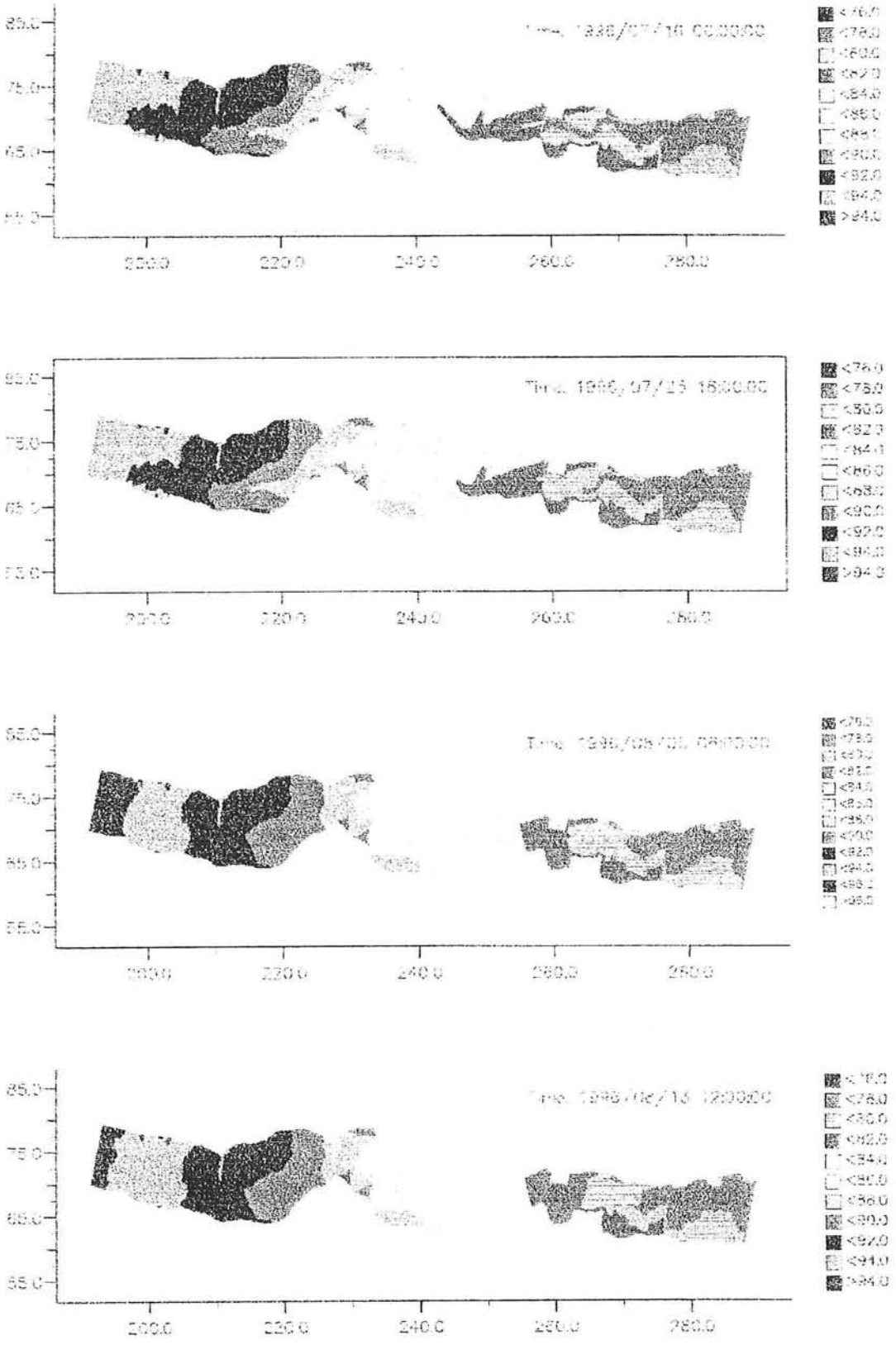

Fig 3.22 the water level distributions at several instants during the flood

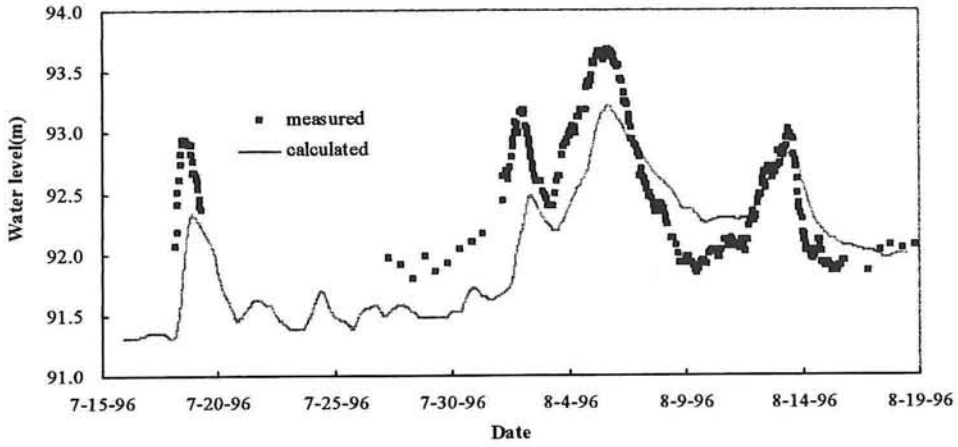

(a) Yuanyangshuangjin station

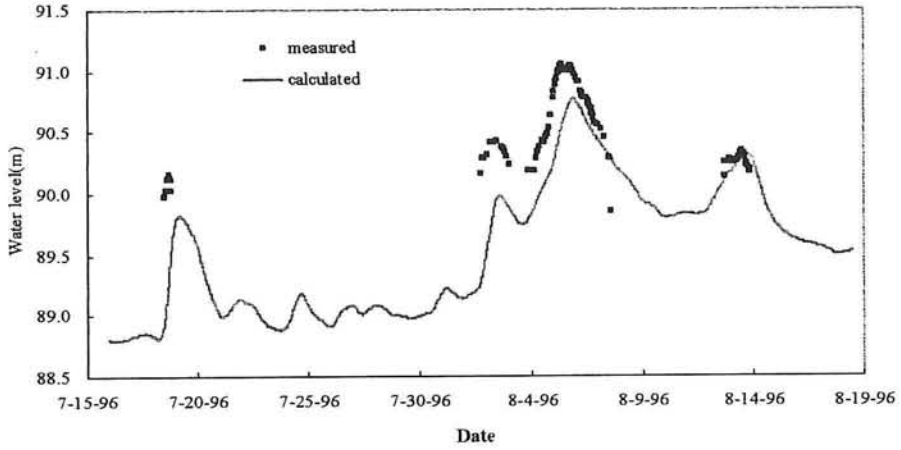

(b) yangqiao station

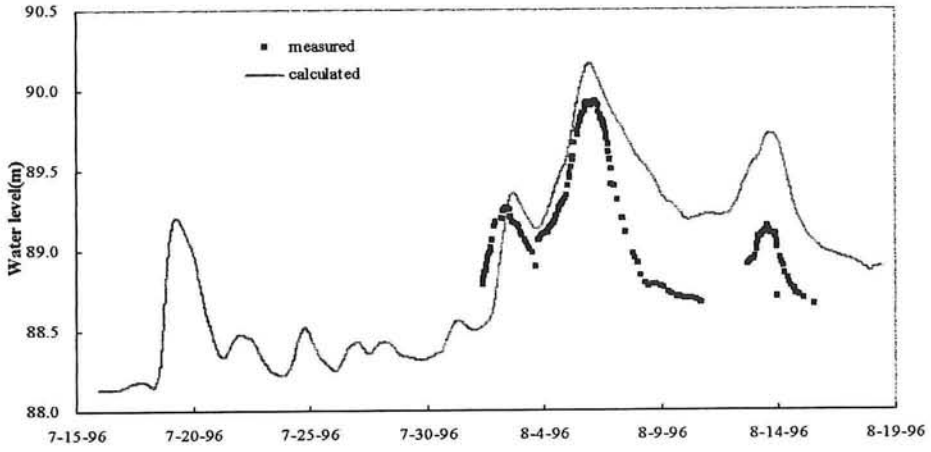

(c) Wantan station

Fig 3.23 The verified water levels at several stations along the studied reach

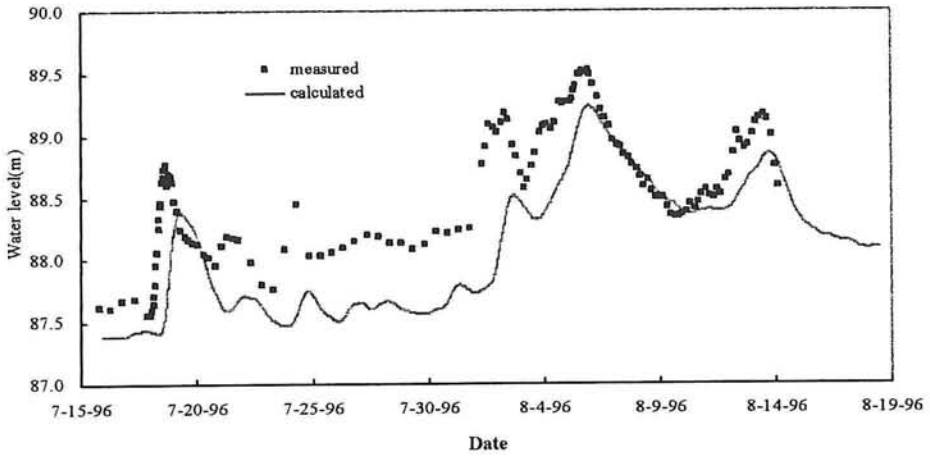

(d) Zhaokou station

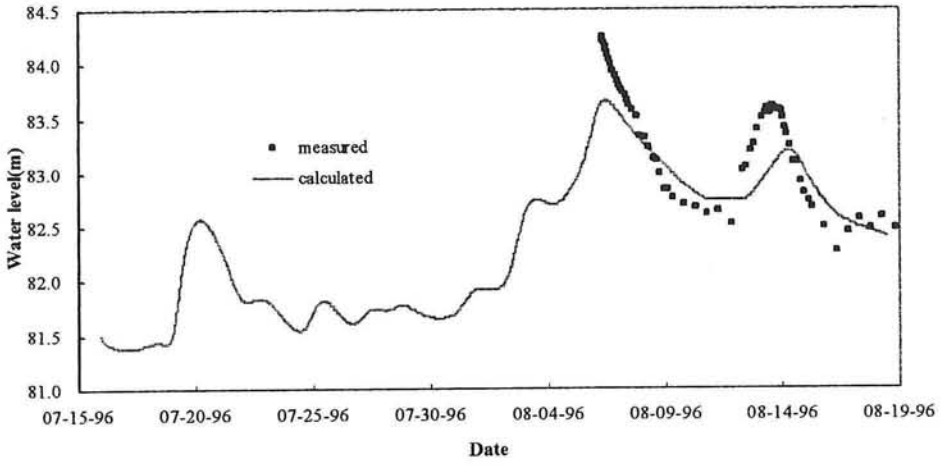

(e) Heigangkou station

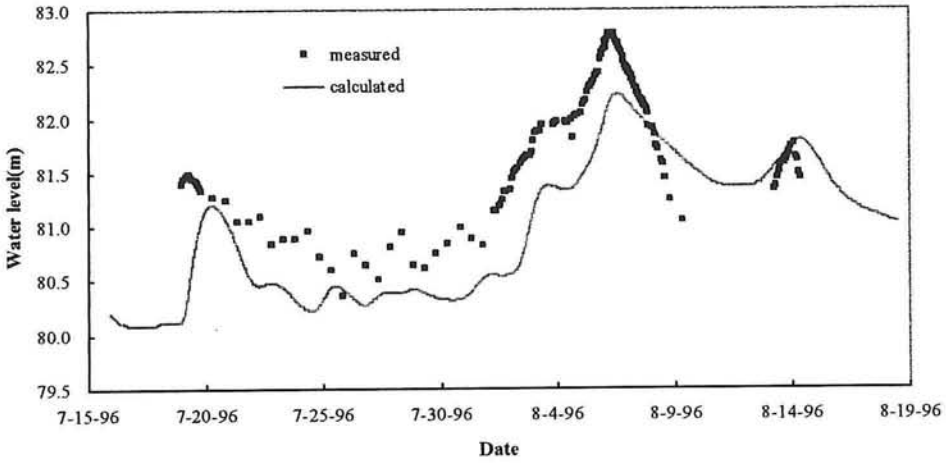

(f) Liuyuankou station

Fig 3.23 The verified water levels at several stations along the studied reach(Cont.)

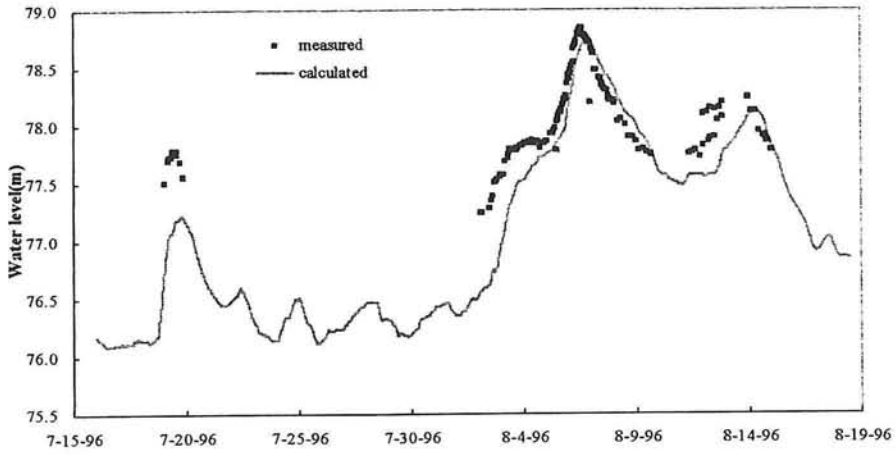

(g) Fujunsi station

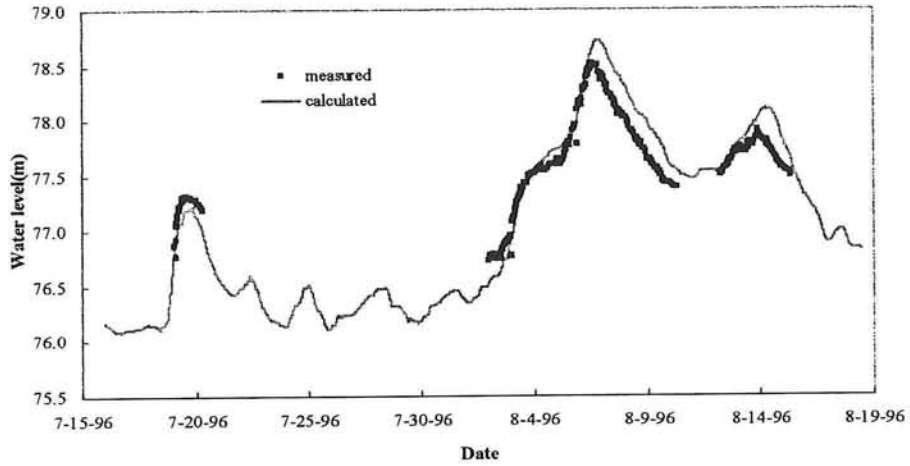

(h) Caogang station

Fig 3.23 The verified water levels at several stations along the studied reach(Cont.)

Table 3.4 comparison of the peak water levels at several stations along the studied reach

Station	Water Level (m)		
	Measured	Calculated	Error
Yuanyangshuangjin	93.67	93.22	0.45
Yangqiao	91.05	90.77	0.28
Wantan	89.92	90.16	-0.24
Zhaokou	89.52	89.24	0.28
Heigangkou	84.24	83.66	0.58
Liuyuankou	82.77	82.22	0.55
Fujunsi	78.84	78.76	0.08
Caogang	78.51	78.72	-0.21

3.6 Morphological model for Case Study

3.6.1 Introduction

The MOR-module of Delft3D fully integrates the effects of waves, currents and sediment transport on morphological developments. It has been designed to simulate the morph-dynamic behavior of rivers, estuaries and coasts on time scales of days to years due to the complex interactions between waves, currents, sediment transport and bathymetry. Each of these processes is dealt with in separate modules. The module simulates the processes on the curvilinear grid system as it is used in the FLOW-module, which allows a very efficient and accurate representation of complex areas.

A steering module allows you to link model inputs and outputs for the model components. The morphological process can be modeled as hierarchical tree structure of processes. You are free to build up processes with varying complexity; single calls to only one model and complex morphodynamic simulations spanning a number of years can be set up.

3.6.2 Sediment transport module

The sediment transport module, Delft3D-SED, can be applied to model the transport of cohesive and non-cohesive sediments, i.e. to study the spreading of dredged materials, to study sedimentation/erosion patterns, to carry out water quality and ecology studies where sediment is the dominant factor.

3.6.3 General description

The temporal resolution of the flow data on the communication file should be sufficient to enable a reliable sediment transport simulation as it determines the smallest possible time step which can be used by the Transport module. If the suspended transport mode is used, this is especially important as large time steps can induce numerical instabilities in the solution of the advection-diffusion equation that is used to determine the suspended sediment concentrations. When the Transport module is used in total mode, sediment transports are determined with algebraic formulation, the time interval imposed by Morsys may have zero length (i.e. only one flow field and one transport field).

As all modules communicate via the communication file it is possible to make an morphological simulation without having to include the Waves and FLOW models in the process tree. Copy or rename a communication file including consistent Wave and flow data from a previous computation to the new run-id.

3.6.4 Cohesive sediment

This section describes the implementation of the physical processes in some detail. For cohesive sediment transport sedimentation, erosion, burial and digging are taken into account.

For sedimentation the following assumptions apply:

- Sedimentation takes place when the bottom shear stress drops below a critical value.
- There is no correlation between the sediment components (i.e. each of the particulate fractions can settle independently).
- Sedimentation always results in an increase of sediment in the uppermost sediment layer.
- The total shear stress is the linear sum of the shear stresses caused by water velocity and wind effects. Effects of shipping and fisheries can also be included.

The effects of 'hindered settling' (i.e. decrease in sedimentation velocity at very high suspended solids concentration) can be included.

For resuspension the assumptions are:

- The bottom sediments are homogenous within a layer. Therefore, the composition of the resuspending sediment is the same as that of the bottom sediment.
- The resuspension flux is limited based on the available amount of sediment in a sediment layer for the variable layer option. The resuspension is unlimited if the fixed layer option is used.
- As long as mass is available in the upper sediment layer, resuspension takes place from that layer only.
- Resuspension flux is zero if the water depth becomes too small.

Burial is the process in which sediment is transferred downward to an underlying layer. The sediment layer is assumed to be homogeneous, therefore the composition of the sediment being buried is the same as that of the (overlying) sediment layer.

Digging is the process in which sediment is transferred upward from an underlying layer. The sediment layers are homogeneous, therefore the composition of the sediment being transported upwards is the same as that of the (underlying) sediment layer. A third and deeper layer allows for an unlimited 'digging' flux to the second layer. The quality of this third layer must be defined by the user and is not modeled by Delft3D-SED.

3.6.5 Non-cohesive sediment

For non-cohesive sediment (sand) the transport rate is calculated according to the transport formulae of Engelund-Hansen and Ackers-White. These (semi-)empirical relations describe the total transport (bed load and suspended load) in the situation of local equilibrium.

The implementation recognizes two options: unlimited supply of sand via the boundaries and the presence or absence of bedrock.

3.6.6 Continuity correction

The Transport module can be called a number of times (in combination with the Bottom module) without an intermediate flow computation. It will re-compute the flow velocities based on the discharges, water levels and the actual, most recent computed bed level. This so-called continuity correction is applied to reduce the number of calls to the FLOW module. In coastal, tide dominated, areas the continuity correction can usually be applied about 10 to 30 times before the FLOW module has to be called again.

3.6.7 Classification of sediment transport

The transport of sediment by a water flow can be in the form of bed load and suspended load, depending on the size of the bed material and the flow conditions. Although in natural conditions there is no sharp division between the bed load transport and suspended sediment transport, it is necessary to define a layer with bed load transport for model representation. The Sediment transport in a steady uniform flow is assumed to

be equal to the transport capacity defined as the quantities of sediment that can be carried by the flow without erosion or deposition, given sufficient of bed material.

When the value of the bed shear stress velocity just exceeds the critical value for initiation of motion, the particles will start rolling and sliding in continuous contact with the bed(defined as bed load). When the value of the bed shear stress velocity exceeds the particle fall velocity, the particles can be lifted to a higher level at which turbulent forces will be comparable to or higher than the submerged particle weight. The particle velocity in the longitudinal direction is approximately equal to the water velocity. Usually, the behaviour of the suspended sediment particles is described in terms of the sediment concentration.

In the transport module there are sediment transport formulas that predict a total sediment transport, but there are also more advanced formulas available that make a clear distinction between the bed load and the suspended sediment. From the suspended load an equilibrium sediment concentration can be derived which, in combination with an advection-diffusion equation, can be used to obtain local(depth averaged) concentration.

In principle these relations concern both bed load contribution and a equilibrium suspended sediment transport contribution. The transport module has three options available to determine the total sediment transport fields:

1. Total Model: in this mode the sediment transports resulting from the algebraic sediment transport formula are used to determine the total sediment transport contribution.
2. Suspended Mode: in this mode, the equilibrium suspended sediment transport is used to derive the(depth-averaged) equilibrium concentration. The actual concentration is computed from an advection-diffusion equation. The bed load transport is determined based on the algebraic sediment transport formula, according to the methodology used in total mode.
3. Silt Mode: similar to the suspended mode an advection-diffusion equation is used to calculate the silt concentration and the resulting silt transport component. In this mode no bed load is accounted for.

3.6.8 Suspended sediment transport

In suspended mode, the transport of suspended sediment is determined with an advection-diffusion equation. The concentration computed by the module is the depth-averaged concentration defined by:

$$C_s = \int_0^1 C(\zeta) d\zeta \tag{3.8}$$

where c(ζ) is the vertical distribution of the suspended sediment concentration and ζ is the dimensionless vertical coordinate.

In practice, using the numerically integrated expressions does not add much to the overall accuracy, in view of other uncertainties, algebraic expressions are used in general since they are much more robust and less time-consuming.

For the case of algebraic equations the depth-averaged advection diffusion equation to be solved for C_s reads:

$$\frac{\partial hC_s}{\partial t} + \frac{\partial huC_s}{\partial x} + \frac{\partial hvC_s}{\partial y} + \frac{\partial}{\partial x}\left(D_x h \frac{\partial C_s}{\partial x}\right) + \frac{\partial}{\partial y}\left(D_y h \frac{\partial C_s}{\partial y}\right) = \frac{h(C_{se} - C_s)}{T_s} \tag{3.9}$$

where:

$$T_s = \frac{h}{w_s} T_{sd} \tag{3.10}$$

in which:

W_s settling velocity of suspended sediment

C_{se} equilibrium concentration of suspended sediment.

T_s adaptation time for vertical sediment concentration profile.

3.6.9 Silt transport mode

The silt option is a special facility available in the suspended mode in the transport

module. If the silt option is selected, it is assumed that all deposition and erosion is due to suspended sediment(bed load is irrelevant and is not modelled).

The silt option uses the following advect-diffusion equation:

$$\frac{\partial hC_s}{\partial t}+\frac{\partial huC_s}{\partial x}+\frac{\partial hvC_s}{\partial y}-\frac{\partial}{\partial x}\left(D_x h\frac{\partial C_s}{\partial x}\right)-\frac{\partial}{\partial y}\left(D_y h\frac{\partial C_s}{\partial y}\right)=E-D \tag{3.11}$$

where:

$$E=\begin{cases}0, \tau_{bs}\le\tau_e\\ M\left(\frac{\tau_{bs}}{\tau_e}-1\right), \tau_{bs}\ge\tau_e\end{cases}$$

$$D=\begin{cases}0, \tau_{bs}\ge\tau_e\\ w_s C_s\left(1-\frac{\tau_{bs}}{\tau_e}\right), \tau_{bs}\le\tau_e\end{cases}$$

τ_{bs} is the effective shear stress.

3.6.10 Limitations

To apply the sediment transport module the following limitations must be observed:

- In the sedimentation process, there is no correlation between the cohesive and non-cohesive components, i.e. between sand and silt; each is treated independently.
- The effect of short waves must be taken into account through the hydrodynamic module or through a localized wave effect estimation (that is, the waves are considered to be in equilibrium with local circumstances).
- Delft3D-SED should only be used for short- or medium-term (days, weeks, months) modelling of erosion and sedimentation process as the changes on bottom topography and its effects on the flow are neglected. For long-term processes (years), whereby the flow changes induced by changing bottom topography is significant, the separate morphological and sediment module (Delft3D-MOR) should be used. This module has advanced on-line coupling capabilities with the hydrodynamic flow and wave modules.

3.6.11 Bottom module

3.6.11.1 Description of Bottom module

In the bottom module the bed level variation are determined based on the sediment transport fields as calculated by the transport module. The module will execute one time step, being the time interval imposed by steering module Morsys or the time step calculated by the transport module. The effect of a non-erodible layer can be included. Samilar to the transport module, it operates on the flow grid. As a consequence, it has the same open boundary as the flow module.

3.6.11.2 Physics and mathematical model

The bottom module is a sediment conservation model that solves the bed level continuity equation:

$$(1-\varepsilon_{por})\frac{\partial z_a}{\partial t}+\frac{\partial S_x}{\partial x}+\frac{\partial S_y}{\partial y}=T_d \tag{3.12}$$

where:

(S_x, S_y) the sediment transport components

Z_x, the bed level

ε_{por} the bed porosity

T_d the deposition or erosion rate(of suspended sediment/silt)

The sediment transport components(S_x, S_y)are computed by use of the initial and averaged transport components that are available on the transport data group on the communication file:

$$S_x=\begin{cases}\dfrac{TIXI+(Dt_{mor}-Dt_i)ITXA}{Dt_{mor}}\\ ITXA\end{cases} \tag{3.13}$$

where:

TIXI the time integrated sediment transport over the initial interval Dt_i

TIXA the averaged sediment transport

Dt_{mor} the time increment used by the bottom module

Dt_i the initial time interval

The interpretation of the above described transport quantities depends on the mode in which the transport module is applied:

- Total Model

  S,TTXI and TTXA concern total sediment transport properties(bed load and suspended sediment transport. The deposition/erosion rate in EQ (1) is zero(T_d=0).

- Suspended Mode

  S,TTXI and TTXA concern bed load transport. T_d is the deposition/erosion rate of the suspended sediment.

- Silt Mode

  There is no bed load transport(i.e. S=TTXI=TTXA=0). T_d is the deposition/erosion rate by(suspended) silt.

In suspended mode, the deposition/erosion rate(T_d) i s computed as:

$$T_d = -\frac{\partial S_{sx}}{\partial x} - \frac{\partial S_{sy}}{\partial y} \tag{3.14}$$

where (S_{sx}, S_{sy}) represents the suspended sediment.

These quantities will be computed as:

$$S_{sx} = \begin{cases} \dfrac{TIXSI + (Dt_{mor} - Dt_i)TTXSA}{Dt_{mor}} \\ TTXSA \end{cases} \tag{3.15}$$

where:

TTXSI the time integrated suspended sediment transport over the initial interval Dt_i

TTXSA the averaged suspended sediment transport

Dt_i the initial time interval(if Dt_i=0 then all initial transports are zero: TTXSI=TTYSI=TTXI=TTYI=0)

In silt mode, the deposition/erosion rate(T_d) is determined directly from the right hand side of EQ.(4):

$$T_d = E - D \tag{3.16}$$

3.6.12 Boundary conditions

The required boundary conditions at the open boundaries may be either sediment transport conditions or bed level conditions. The sediment boundary conditions will be specified in the input file of the transport module, the prescribed bed level conditions will be specified in the input file of the bottom module.

A prescribed bed level may be a function of place and time. These conditions are only imposed when there is an inflow state at the model boundaries. At outflow boundaries equilibrium sediment transport will be imposed. As the bottom module operates on the computational grid of the flow module. The bottom module uses the same numbering as the flow module. Boundary conditions have to be specified for all open(flow) boundaries.

3.6.13 Morphodynamic module

The morphological module, Delft3D-MOR, integrates the effects of waves, currents, sediment transport on morphological development, related to sediment sizes ranging from silt to gravel. It is designed to simulate the morphodynamic behaviour of rivers, estuaries and coasts on time-scales of days to years.

The typical problems to be studied using this system involve complex interactions between waves, currents, sediment transport and bathymetry. To allow such interactions, the individual modules within Delft3D all interact through a well-defined common interface; a flexible steering module controls the calling sequence of the individual modules.

The computational modules within Delft3D are identical to their stand-alone counterparts and each offer the full range of physical processes. In this way, WL | Delft Hydraulics combined experience of over thirty years in computer modeling is built into this system.

A morphological simulation in Delft3D is defined as a tree structure of processes and sub-processes down to elementary processes which contain calls to the computational

modules. The user is free to build up processes of increasing complexity, from a single call to the flow model to morph-dynamic simulations spanning years, with varying boundary conditions.

This module simulates the processes on a curvilinear grid system used in the hydrodynamic module, which allows a very efficient and accurate representation of complex areas.

3.6.13.1 Module description

Delft3D-MOR contains or is able to utilize the following components:

Steering module

Allows the user to link model inputs for the module components. The morphological process can be specified as a hierarchical tree structure of processes. Time intervals for the elementary processes are defined. Processes may be executed a fixed number of times, for a given time span or as long as a certain condition is not satisfied. A variety of options are available to specify the time progress.

Waves

The wave module (Delft3D-WAVE) is built around the stationary short-crested wave model HISWA (Holthuijsen et al., 1989). This model computes the effects of refraction, shoaling, wave dissipation by bottom friction and breaking and wave blocking for a discrete directional wave spectrum, over a two-dimensional bathymetry. Within the module the user can specify several HISWA computations in one run, with varying boundary conditions, and for each boundary condition various nested runs can be executed. Flow and water level information can be used from a flow run, and the results can be passed on to the flow module.

At present also the SWAN model is available in the wave module of Delft3D. The SWAN model is fully spectral (in all directions and frequencies) and computes the evolution of random, short-crested waves in coastal regions with shallow water and ambient currents. The SWAN model accounts for (refractive) propagation - as the HISWA model - and represents the processes of wave generation by wind, dissipation due to white-capping, bottom friction and depth-induced wave breaking and non-linear wave-wave interactions (both quadruplets and triads) explicitly with state-of-the-art

formulations. It is noted that the SWAN model (as the HISWA model) does not account for diffraction effects.

Hydrodynamics

The hydrodynamic module (Delft3D-FLOW) used by Delft3D-MOR is based on the shallow water equations, including effects of tides, wind, density currents, waves, and turbulence models up to k-eps. The module includes a transport solver for salinity, temperature and conservative substances. The effects of salinity and temperature on the density and on the momentum balance are taken into account automatically.

The module uses a curvilinear grid in the horizontal plane. The vertical grid sizes are proportional to the local water depth.

For efficient morphological computations a one-layer, depth-averaged approach is used. The effects of spiral flow, i.e. in river bends, are computed by a secondary flow module which takes into account the advection of spiral flow intensity and the effect of the secondary flow on the primary current.

Wave effects in the model include radiation stress gradients associated with wave dissipation, wave-induced mass flux and enhanced bed shear stress, computed by a choice of formulations.

Sediment transport

The sediment transport module computes the bed-load and suspended-load sediment transport field over the curvilinear model grid, for a given period of time.

The bed-load transport is computed as a local function of wave and flow properties and the bed characteristics. The equilibrium suspended load is also computed as a local function of these parameters. The module then recognizes two modes of transport: total transport (equilibrium) mode, or suspended load mode. In the first, the total transport is simply the addition of bed-load and equilibrium suspended-load transport. In the second mode, the entrainment, deposition, advection and diffusion of the suspended sediment is computed by a transport solver. Here, a quasi-3D approach is followed, where the vertical profiles of sediment concentration and velocity are given by shape functions.

The bed-load and equilibrium suspended-load transport can be modeled by a range of formulations, among which are Engelund-Hansen, Meyer-Peter-Muller, Bijker, Bailard and Van Rijn for sand, and a separate formulation for silt transport.

Effects of the bed slope on magnitude and direction of transport, and effects of un-erodible layers can be taken into account for all formulations.

Bottom change

The bottom update module contains several explicit schemes of Lax-Wendroff type for updating the bathymetry based on the sediment transport field. Options are available for fixed or automatic time-stepping, fixed (non-erodible) layers, various boundary conditions, and dredging.

3.6.13.2 Numerical aspects

All modules except the wave module operate on the same rectangular or curvilinear, orthogonal grid. Fully implicit ADI or AOI schemes are applied in the hydrodynamic module for the momentum and continuity equations. The solver has robust drying and flooding procedures for both 2D and 3D cases. In the transport solver a Forrester filter can be applied which guarantees positive concentrations throughout.

The same transport solver is applied for suspended sediment computations.

The wave model HISWA operates on rectangular grids, and uses an implicit scheme in propagation direction, combined with a forward marching technique. The wave module takes care of all transformations and interpolations between these rectangular grids and the curvilinear flow and transport grid. The wave model SWAN can perform computations directly on a curvilinear grid.

The bottom update model uses an explicit scheme of Lax-Wendroff type. This leads to a Courant type stability criterion. However, cheap intermediate "continuity correction" steps keep the computational effort at a reasonable level.

3.6.14 Application areas

Delft3D-MOR is designed to simulate wave propagation, currents, sediment transport and morphological developments in coastal, river and estuarine areas.

Coastal areas including beaches, channels, sand bars, harbor moles, offshore breakwaters, groynes and other structures. The coastal areas may be intersected by tidal inlets or rivers; parts of it may be drying and flooding.

Rivers including bars, river bends (spiral flow effect), bifurcations, non-erodible layers, dredging operations and having arbitrary cross-sections (with over-bank flow). Various structures may be represented. Special features for 2D river applications are presently being developed and validated, such as a bottom-vanes and graded-sediment.

Estuarine areas including estuaries, tidal inlets and river deltas influenced by tidal currents, river discharges and density currents. Sediment can be sandy or silts. The areas may include tidal flats, channels and man-made structures, e.g. docks, jetties and land reclamations.

3.6.15 result assessment

The application of Delft3D-MOR module fails to calculate the sedimental transport and morphology in lower Yellow River. It is probably caused by the sediment concentration of the Yellow River. Some parameters including the module are not suitable to be set. The improvement of Delft3D-MOR module is needed to apply in lower Yellow River.

3.7 Conclusions and recommendations

The ability of Delft3D-FLOW model to simulate the flooding wave propagation in lower Yellow River is illustrated by comparison of the calculated flood features at several stations with measured data. The results from the numerical model show a fair agreement with the observed data. Deviation from the data is found at the stations near regulation projects and after the instant when peak discharge occurred. The errors observed are explained to the coarse grids near regulation projects (thin dams) and the bed remarkable changed in the period of this flood. However, some conclusions and recommendations can be summarized as the following.

3.7.1 Conclusions

- Delft3D model is a powerful software package with flexible framework which simulates two and three-dimensional flow, waves, water quality, ecology, sediment transport and bottom morphology and is capable of handling the interactions between these processes.
- Delft3D-FLOW module can reasonably simulate the flood process in the lower Yellow River through the flow verification of 1996 flood.
- GPP provides a comprehensive post-processor that can notably improve work efficiency and figure quality.
- Manning formula is much better one than Chezy to deal with bed roughness under the circumstances of the case study. Flow verified results are agreeable with the measured values, specially flood peak and processes of water level and discharge.
- By performing several sensitivity studies, experience and knowledge on the effects of different parameters are acquired. The knowledge is used to adjust the existing detailed model
- The results also show that the flood features are not good with measured data after peak flood due to the remarkable morphological change caused by peak discharge.
- In order to improve the simulated accuracy, the bottom morphology must be simulated with MOR module.

3.7.2 Recommendations

The solution of the discretized equations is just an approximation of the exact solution. The accuracy of the solution depends not only the numerical scheme, but also on the way in which the bottom topography, the geographical area and the physical processes are modeled.

In Delft3D-FLOW, the open boundary is divided into segments (sections). The boundary conditions are specified for these segments, two values per segment are required, one for each segment end. However, it is difficult to exactly specified the boundary condition for each segment in many practical cases. The errors are not avoidable near the open boundary. Application of the specified Method I which adopted in the case study results in break-down of the calculation.

Also time step is limited by the Courant number due to adapting time integration method to solve governing equations. In the calculation with Method III, time step must be shorter than 1 minute, unless the computation is halted. So time step is selected relative to the specified way of boundary condition.

In general, the application of Delft3D-FLOW model in lower Yellow River is carried out with less information of case study. Some problems may be caused by it. Further verifications are required, including flow and morphology simulations. And the improvement of Delft3D model is required to well fit the special case of lower Yellow River.

Chapter 4 1D case study on Dredging and recovery in the Lower Yellow River

4.1 Introduction

The Yellow River carries 1.6 billion tons of sediment load annually, and ranked the first in the world. Sedimentation in the lower reaches resulted in frequently shift of the river courses. Throughout the history of China, the Yellow River has been associated with floods and famine, earning the river name "China's sorrow". Instability of the river channel, especially the delta channel, restrains the economic development of the area. The Dongying municipal government, the Shenli Oil Corporation and the Yellow River Mouth Management Bureau of YRCC (Yellow River Conservancy Commission) launched a project to train the river mouth. It was the first effort of humankind to control the Yellow River mouth. The project achieved great success to end the 10 years period of channel migration and prospect a long term of stability of the channel. The experience of "making full use of the sea current to transport sediment for stabilizing the river mouth" is of not only practical but also theoretical significance.

From 602 BC to 1998 AD the river mouth migration has been recorded for 2600 year. In the period the river has been pouring into the Bohai's sea for more than 1800 year except a period during which the river flowed into the Huanghai's Sea due to artificial dike breaches. In 1127 and 1938 the river dike was artificially broken for resisting invasion of Mongolian and Japanese army, the river was then flowed into the Huanghai's sea for 766 years. During the 1800 years when the river flowed into the Bohai's sea, the mouth moved from north near Tianjin to south near Lijin. Lijin seems the best mouth location for the river to pour into sea in more than 62.6% of time near Lijin.

Since the river dike at Tongwaxiang (about 600 km from the present river mouth) was broken and the floodwater captured the Daqing River channel to flow into the Bohai Sea in 1855 the river shifted its channel ten times with apex at Ninghai (about 100 km from the present river mouth). The mouth moved in the fan area from Taoerhe in the north to Zimaihe in the south. The river has been flowing within the area between the

present Qingshuigou channel to Diaokouhe mouth for 75% of the period, exhibiting the sea current around the present river mouth the most capable to transport sediment and the area being the most stable river mouth.

The river delta is flat with ground slope 0.01% inclined to the sea. The coast is also very flat showing no coastward sediment transport by wave and storm current. The sea current carries sediment to the mid sea and therefore the river mouth stayed here for so long time.

Historically the river mouth migrated once per ten years. The river shifted from the Diaokouhe's channel to the present Qingshuigou's channel in 1976. In 1986 the river mouth had been seriously silted and many small branch channels and sand bars to separate the channels emerged. Ice jam flood occurred when 230 m^3/s discharge arrived at the delta in the 1987 spring and the delta was flooded again in summer when a 2750 m^3/s flood occurred. The oil production in the delta was stopped two times because of the floods. The river mouth training was urgently needed. The traditional solution was to artificially shift the channel again but at great loss because the Gudong oil field would be flooded. The decision makers adopted a new strategy-to stabilize the Qingshuigou channel through engineering efforts.

It was conducted in 1988. People blocked many branches to concentrate the flow in the main channel, directed the flow in a given direction by building guiding dikes, dredged the channel and dug the mouth sand bar with various dredgers, utilizing tidal currents to transport sediment into the mid sea, built bank revetment to stabilize the channel. Before the flood season in the year 44 km long guiding dikes had been built, 3.4 km^2 of sand bars in the river mouth dredged, 2060 m long levee reinforced and 1250 m long channel dredged. The guiding dikes were built in accordance to accommodate 4000 m3/s flood and may be overflowed but not destroyed by floods at higher discharges.

Now, dredging has become an important auxiliary measure to handle the Yellow River. Through dredging the river channel shrinkage at individual places can be alleviated or stopped and a smooth, high capacity, sediment, ice and water-conveying channel can be preserved. If the sediment load and water continue to reduce, dredging will possibly become a main measure to maintain the lower Yellow River channel. The functions of dredging are: (a) to widen and deepen the shrinking river channel at special sections; (b)

to remove coarser sediment of diameter larger than 0.025-0.05 mm from main channel to floodplain so avoiding accumulative siltation of the main channel; (c) to raise the elevation of surrounding ground, reinforce dikes and improve soil quality. Nevertheless, problems have to be solved before employment of dredging becomes the main strategy for river training: (1) effects of dredging on flow and sediment carrying capacity; (2) how to avoid or reduce resiltation in the dredged channel; (3) efficiency of dredging at different places; (4) disposal of dredged silt to prevent it from becoming a source of pollution.

4.2 Available data

In this study case, the available data include two parts: the prototype data and the data of the physical scale model.

4.2.1 Prototype data

In 1998, a prototype experiment of dredging was carried out at the delta area of the Yellow River. The length of the concerned reach is about 80 km with sixteen measured cross-sections, including three hydraulic stations at LJ, ZJ and QS cross-sections respectively and three water level stations at YH, YW and XH cross-sections respectively. The reach of dredging channel is between ZJ section and SI section with a distance of 11 km, shown in figure 4.1.

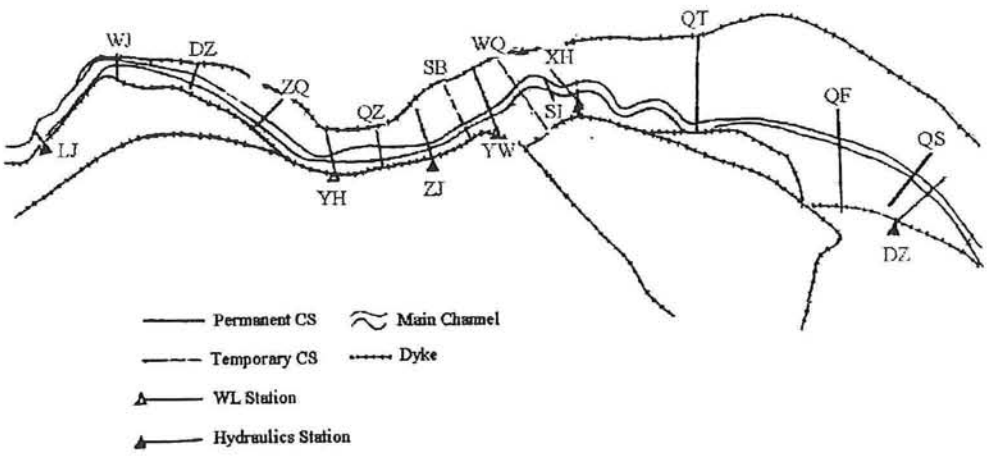

Figure 4.1 Sketch of the simulated reach in the Lower Yellow River

(1) Primary data

The duration of prototype experiment lasted about five months, from June to October in 1998. The measured data included mainly the altitude of cross-sections, discharge, sediment concentrations, water levels, and bed material distributions and suspend loads.

(a) Cross-sections

The topography at sixteen cross-sections is measured six times during this period. Some typical sections are shown in figure 4.2.

(b) Discharge and sediment concentration

LJ station is an entrance of experiment reach. There are some relations of discharge, sediment concentration with time, as shown in figure 4.3.

(c) Water level

LJ station and other five stations in YH, ZJ, YW, XH and DZ sections have the relation of water level with time (shown in figure 4.4).

(d) Sediment gradation

There are some sediment gradations of bed material in all sixteen sections. But, some sediment gradations of suspended sediment only include three stations in LJ, ZJ and DZ sections. The sediment gradations have been seen in figures 4.5, 4.6 and 4.7.

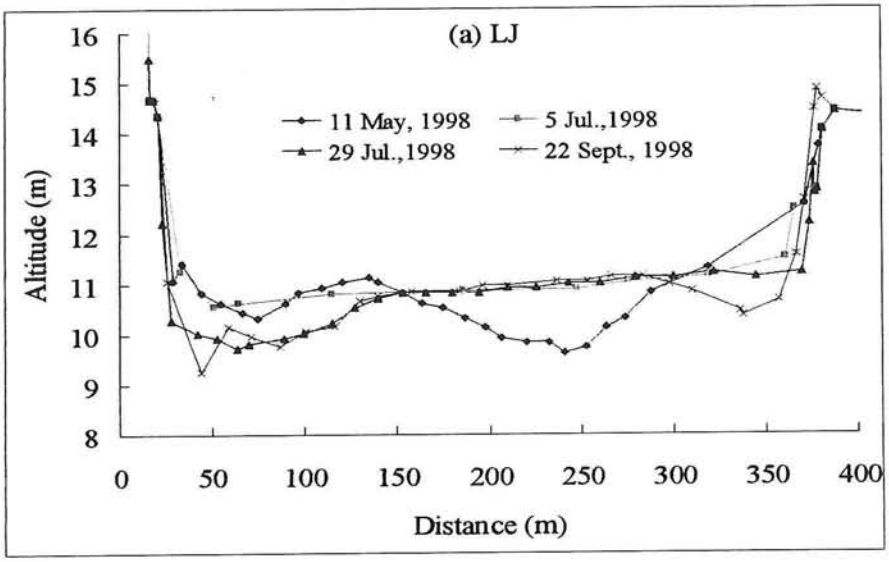

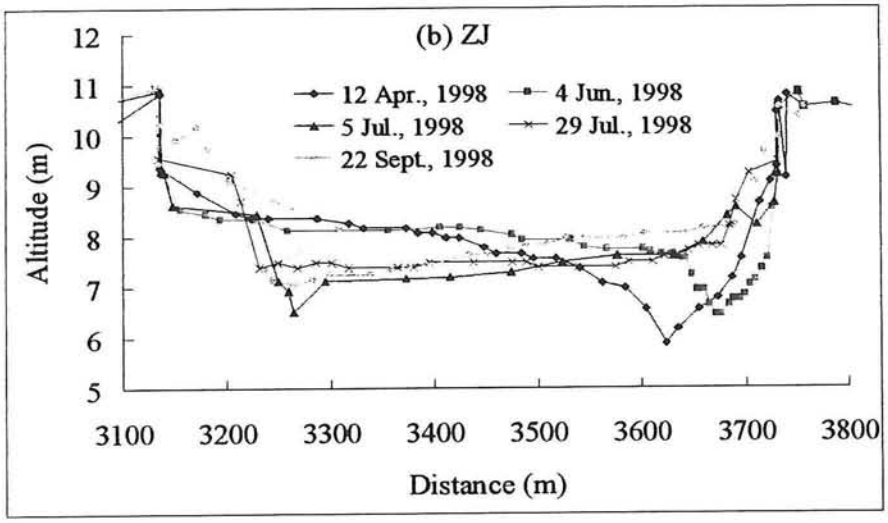
(b) ZJ
12 Apr., 1998
4 Jun., 1998
5 Jul., 1998
29 Jul., 1998
22 Sept., 1998
Altitude (m)
Distance (m)
12
11
10
9
8
7
6
5
3100
3200
3300
3400
3500
3600
3700
3800

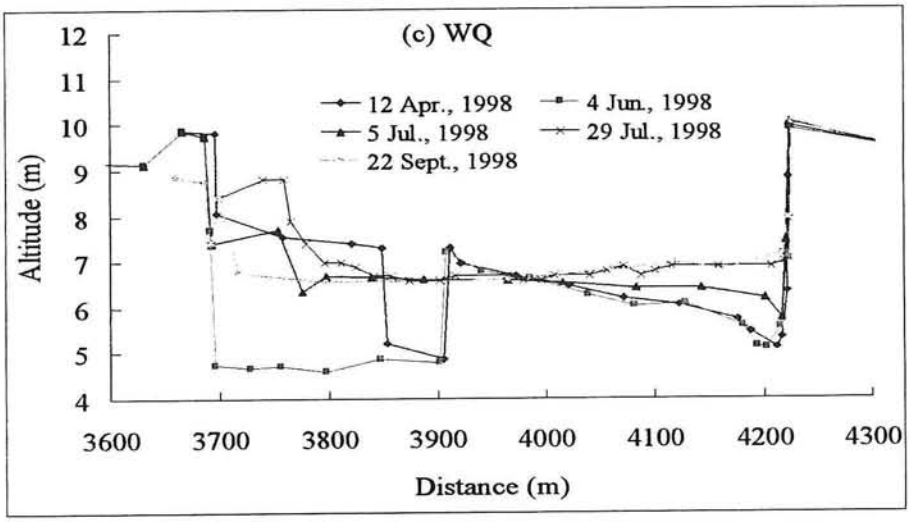
(c) WQ
12 Apr., 1998
4 Jun., 1998
5 Jul., 1998
29 Jul., 1998
22 Sept., 1998
Altitude (m)
Distance (m)
12
11
10
9
8
7
6
5
4
3600
3700
3800
3900
4000
4100
4200
4300

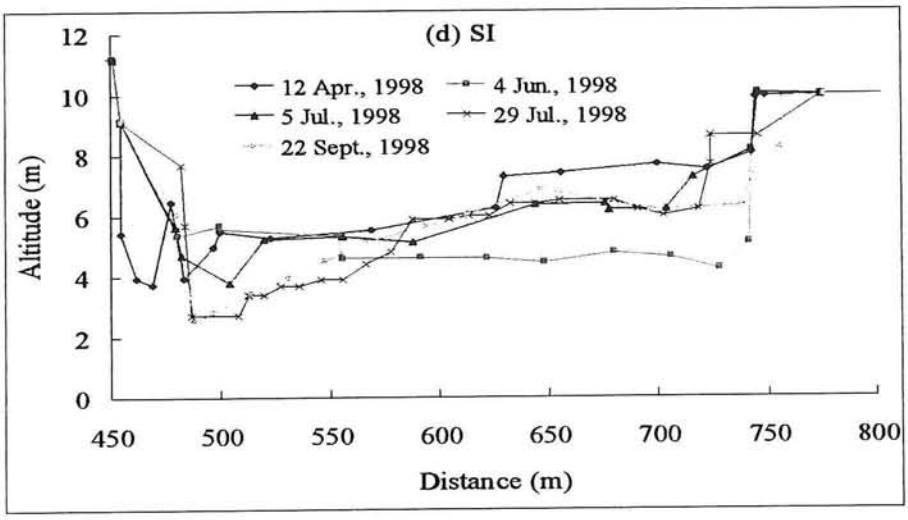
(d) SI
12 Apr., 1998
4 Jun., 1998
5 Jul., 1998
29 Jul., 1998
22 Sept., 1998
Altitude (m)
Distance (m)
12
10
8
6
4
2
0
450
500
550
600
650
700
750
800

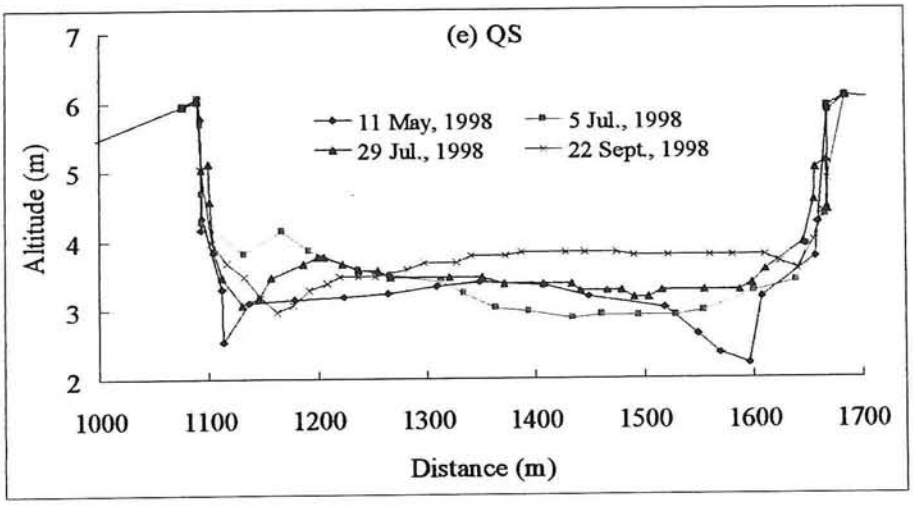

Figure 4.2 Typical cross-sections at different measured times

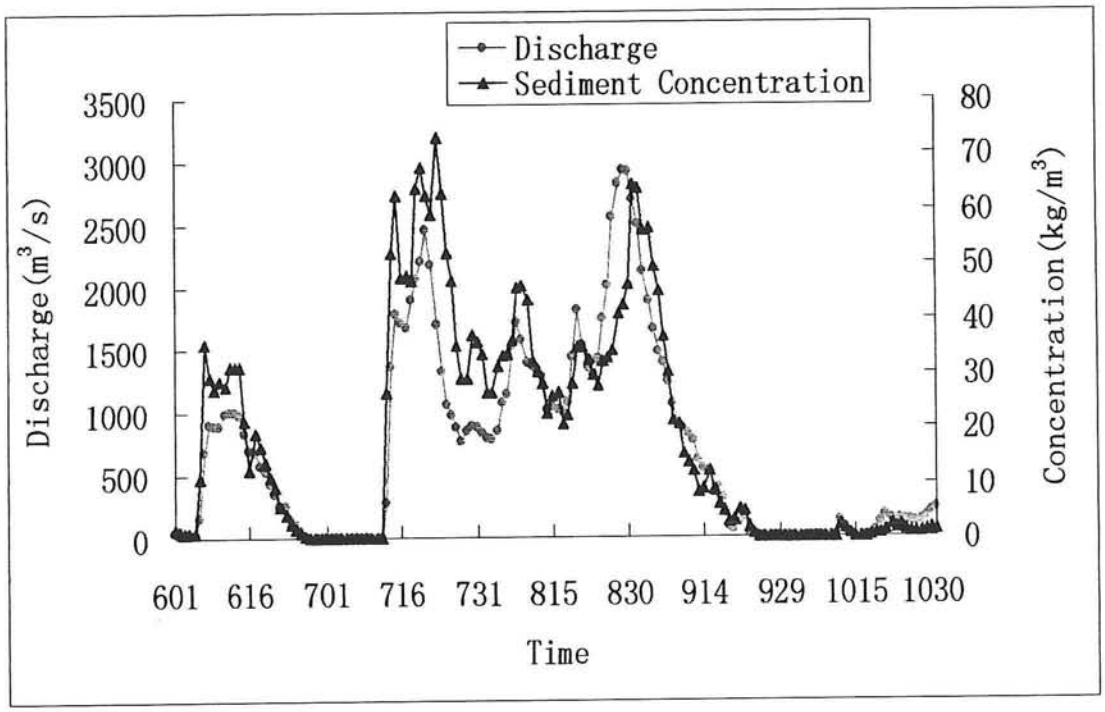

Figure 4.3 Relations of discharge and sediment concentration with time at LJ station

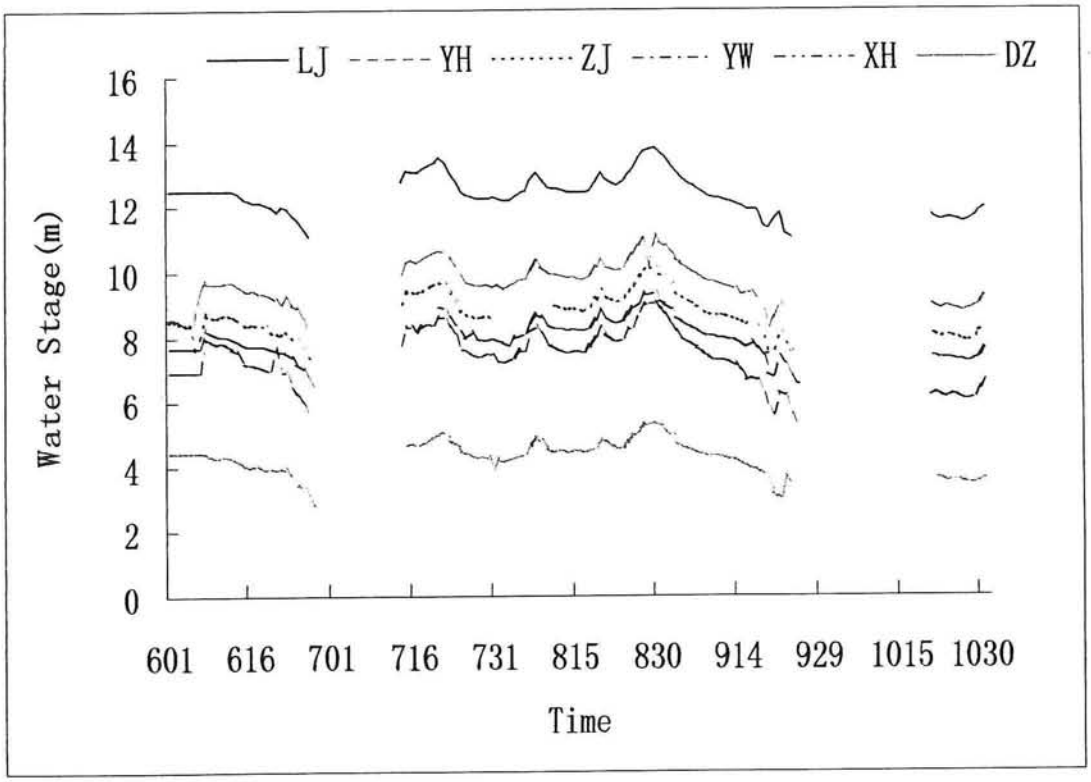

Fig. 4.4 Relations of water level with time at different stations

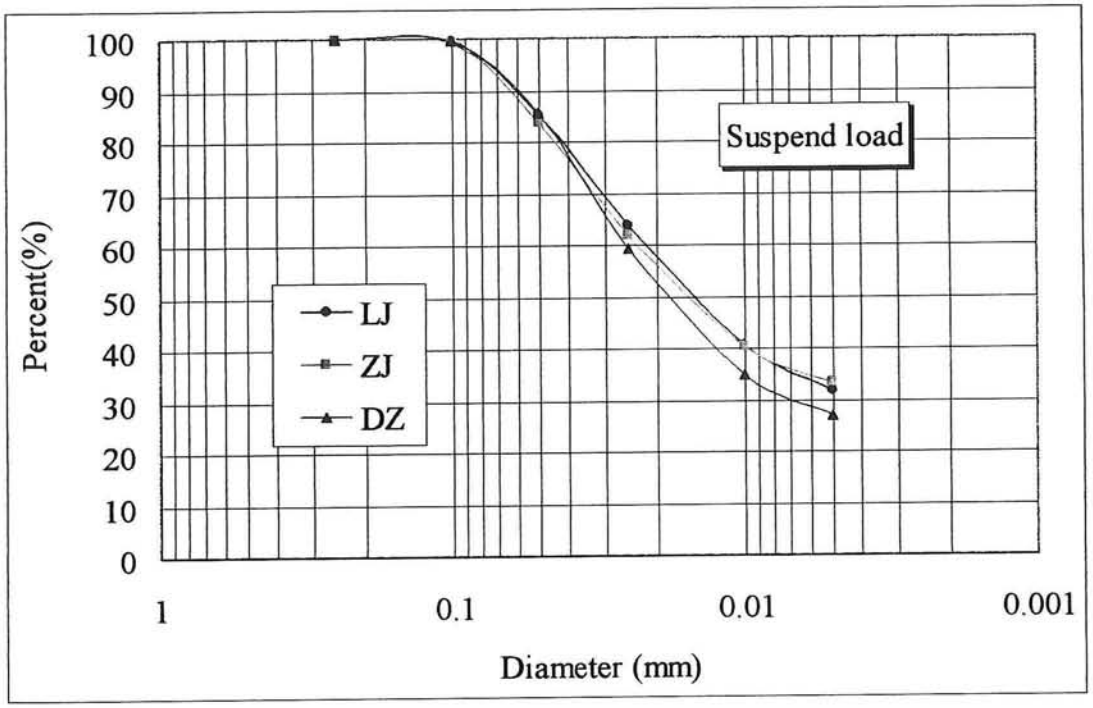

Fig. 4.5 Grain sizes of suspended load at three stations

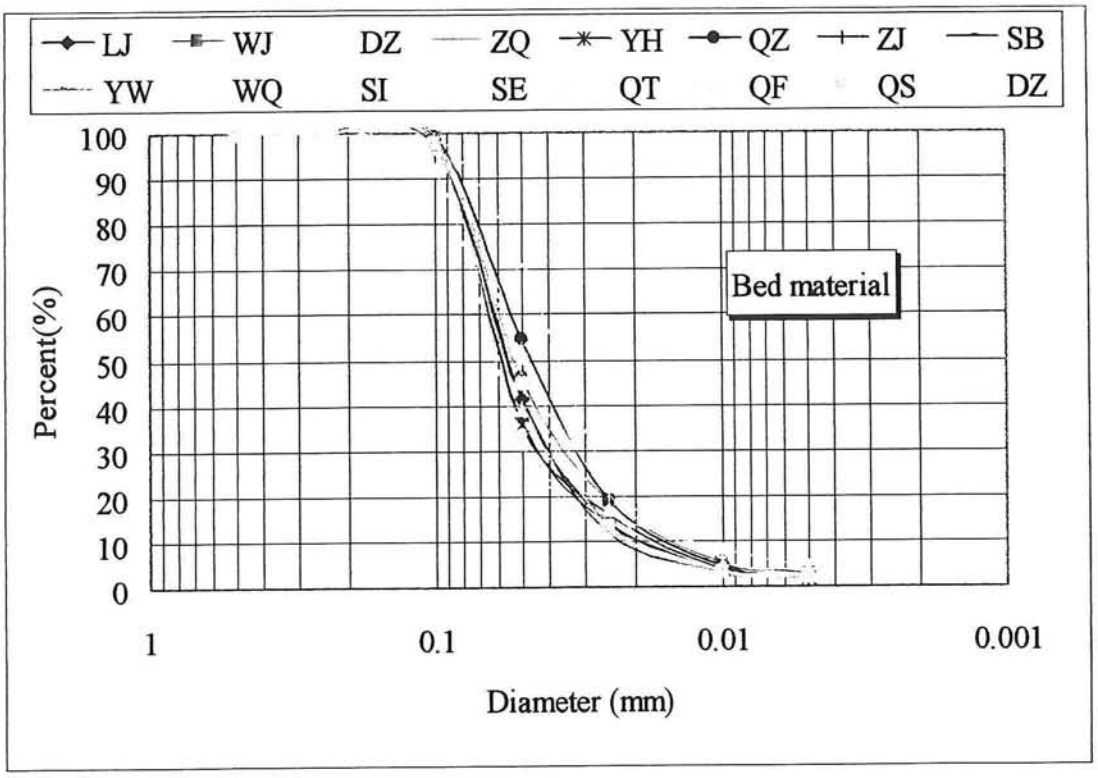

Fig. 4.6 Grain sizes of bed material at sixteen sections

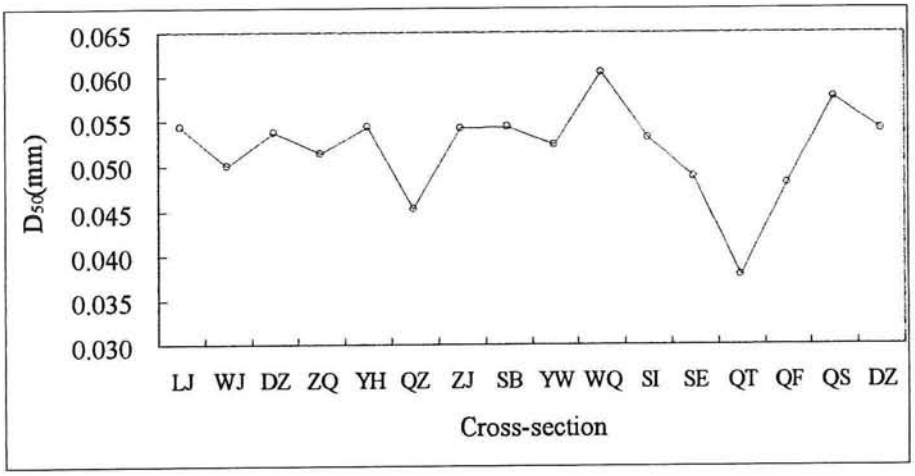

Fig. 4.7 Distribution of middle diameters D_{50} along cross-sections

(2) Characteristics of oncoming runoff and sediment load

The total oncoming runoff and sediment load are about 9.32 billions m^3 and 0.37 billions tons respectively from 6 June to 9 October in 1998. The time on 6 June is the first day to run flow after dredging. It is indicated in Figure 4.3 that there are three flood peaks during the flood season. The first peak is formed by Sanmenxia reservoir. The maximum discharge is 1,030 m^3/s. The averaged discharge is about 413 m^3/s and the averaged sediment concentration is about 23.9 kg/m^3 (as shown in table 4.1). The

second and third peaks come from the middle reach of the Yellow River. During the second peak, the maximum discharge is 2,480 m^3/s, and the averaged discharge is about 1,028 m^3/s and the averaged sediment concentration is about 55.4 kg/m^3. The third peak is bigger than the second one. A maximum discharge is 3,060 m^3/s, and the averaged discharge and the averaged sediment concentration are about 1,292 m^3/s and 37.1 kg/m^3 respectively. During the flood season, flow cut-offs have occurred from 29 June to 13 July and from 26 September to 9 October.

Fig. 4.4 indicates the diameter scopes of suspended load and bed material are from 0.001 mm to 0.5 mm, but the diameter of suspended load is smaller than that of bed material. The middle diameter of suspended load is about 0.016 mm, and that of bed material is about 0.052 mm averaged along the experimental reach.

In table 4.2, the particle diameter with smaller than 0.025 mm is named as the fine one, and the particle diameter with bigger than 0.05 mm is named as the coarse one. The sediment between them will be named as the middle one. It can be shown in table 4.2 that sediment load of fine sand is about 207 millions tons, and that of coarse sand is about 72 millions tons, and their rates are 55.7 % and 19.3 % in total load.

Table 4.1 Oncoming runoff and sediment load at difference periods in LJ station

Season	Duration	Runoff (billion m^3)	Discharge (m^3/s)	Sediment load (million tons)	Sediment concentration (kg/m^3)
Flood	6 Jun., 98 – 5 Jul., 98	1.07	413	25.60	23.9
	6 Jul., 98 – 30 Jul., 98	2.22	1028	122.89	55.4
	31 Jul., 98 – 9 Oct., 98	6.03	1292	223.42	37.1
	6 Jun., 98 – 9 Oct., 98	9.32	989	371.91	39.9
Non-flood	10 Oct., 98 – 13 May, 99	2.22	119	572	2.6
Whole year	6 Jun., 98 - 13 May, 99	11.54	391	377.64	32.7
Non-flood	14 May, 99 – 9 Oct., 99	3.46	269	154.00	44.5

Table 4.2 Consist of sediment load at flood season in LJ station

Duration	Sediment load (million tons)			Percent in total (%)		
	Fine	Middle	Coarse	Fine	Middle	Coarse
6 Jun., 98 – 5 Jul., 98	13.21	6.07	6.32	51.6	23.7	24.7
6 Jul., 98 – 30 Jul., 98	65.98	28.50	28.41	53.7	23.2	23.1
31 Jul., 98 – 9 Oct., 98	127.93	58.29	37.20	57.3	26.1	16.6

6 Jun., 98 – 9 Oct., 98	207.12	92.86	71.93	55.7	25.0	19.3

4.2.2 Data of physical scale model

The simulated reach of physical scale model is from WJ to YW cross-sections, and its length is about 38 km (see figure 4.1). The physical model has been built according to the reduced scale of 1200 in plane direction and 50 in vertical direction. The dimension of the model is about 35m long and 3m wide. There are twenty-six experimental plans in all, and their boundary conditions are shown in table 4.3. During the experiment, these data of water level, velocity, sediment concentration and cross-section have been collected.

4.3 Approaches

At present, dredging is a possibility and it has some measures in the Lower Yellow River. Nevertheless, problems have to be solved before employment of dredging becomes the main strategy for river training, including recovery in the dredged channel and efficiency of dredging.

In order to study these problems, a generalized physical model has been built according to the reduced scale of 1200 in plane direction and 50 in vertical direction. The simulated reach is under LJ station in the Lower Yellow River, about 38 km long. The physical model will be used to study the dredging effects under different conditions, including the dimension of dredging channel and the oncoming runoff and sediment load.

In 1998, a prototype experiment of dredging has been executed in the Lower Yellow River. According to the measured data, the dredging effects will be analyzed and compare with the results of the generalized physical model.

A 1-D numerical model of SOBEK in the reach mentioned above will be applied as well and validated separately against the prototype dataset.

In principle, each of these three sources of information is uncertain: the physical scale model may involve scale effects and/or model effects, the prototype data are inaccurate

Table 4.3 Dimensions and boundary conditions at different experimental plans

Number of experimental plan	Dimension of dredged channel				Boundary conditions		
	breadth (m)	depth (m)	Length (km)	Bed slope ($^0/_{000}$)	discharge (m^3/s)	Water level (m)	Concentration (kg/m^3)
S1	100	2	10	1	3000	10.39	75
S2	100	3	10	1	3000	10.39	75
S3	100	4	10	1	3000	10.39	75
S4	100	3	5	1	3000	10.39	75
S5	100	3	15	1	3000	10.39	75
S6	200	1	10	1	3000	10.39	75
S7	200	2	10	1	3000	10.39	75
S8	200	3	10	1	3000	10.39	75
S9	200	2	10	1	1500	9.09	75
S10	200	2	10	1	500	8.07	15
S11	200	2	10	2	3000	10.39	75
S12	200	4	10	1	3000	10.39	75
S13	200	2	5	1	3000	10.39	75
S14	200	2	15	1	3000	10.39	75
S15	300	1	10	1	3000	10.39	75
S16	300	2	10	1	3000	10.39	75
S17	300	4	10	1	3000	10.39	75
S18	200	2	10	1	3000	10.39	38
S19	200	2	10	1	3000	10.39	125
S20	200	2	10	1	3000	10.39	200
S21	200	2	10	1	3000	10.39	75
S22	200	2	10	1	3000	10.39	75
S23	200	2	10	1	3000+75+finersand of bed material		
S24	200	2	10	1	3000+75+coarserand of suspend load		
S25	200	2	10	1	Unsteady process of flow and sediment		
S26	200	3	10	1	Unsteady process of flow and sediment		

and probably sparse in space and/or time, the numerical model is at best a schematic representation of reality, but this need a support that the numerical model must be suit for some characteristics of the Yellow River. Therefore, if possible, the three sources will be compared with each other.

4.4 Verification of the SOBEK model

SOBEK is the name of a highly sophisticated software package, which in concise technical terms is a one-dimensional open-channel dynamic numerical modelling system, equipped with the user shell and which is capable of solving the equations that describe

unsteady water flow, salt intrusion, sediment transport, morphology and water quality. It can be simulated and solved these problems in river management, flood protection, design of canals, irrigation systems, water quality, navigation and dredging. A very user-friendly interface helps the user schematise the problem and organise the required data into such a form that they can be handled by SOBEK computational core. The interface also helps you in effective analysing and reporting of simulation results.

4.4.1 Basic theory

The flow in one dimension is described by two equations: the momentum equation and the continuity equation. The sediment includes the continuity equation of sediment and the formula of sediment load, and so on.

(1) Continuity equation

$$\frac{\partial A_t}{\partial t} + \frac{\partial Q}{\partial x} = q_{lat}$$

in which

A_t = total cross-section area

Q_{lat} = lateral discharge per unit length

Q = discharge

(2) Momentum equation

$$\frac{\partial Q}{\partial t} + \frac{\partial}{\partial x}\left(\alpha_B \frac{Q^2}{A_f}\right) + g A_f \frac{\partial h}{\partial x} + \frac{gQ|Q|}{C^2 R A_f} - W_f \frac{\tau_{wi}}{\rho_w} +$$

$$g A_f(\eta + \xi Q|Q|) + \frac{g}{\rho_w}\frac{\partial \rho}{\partial x} A_{1m} = 0$$

in which

t = time,

x = distance,

B = Boussinesq constant,

Af = cross-section flow area,

g = gravity acceleration,

h = water level (with respect to the reference level),

C = Chézy coefficient,

R = hydraulic radius,

W_f = flow width,

w_i =wind shear stress

w = water density,

A_{1m} = first order moment cross-section.

(3) Continuity equation for bed material

$$\frac{\partial A_s}{\partial t} - \frac{\partial S}{\partial x} = -s_{lat}$$

in which:

A_S = sediment-transporting cross-sectional area [m²]

S = sediment transport through the cross-section including pore volume [m³/s]

S_{lat} = lateral sediment supply including pore volume

(positive value means supply!) [m²/s]

(4) Formula of sediment transport

In SOBEK model, many formula can be described the sediment load, such as these formulas of Engelund & Hansen, Meyer-Peter & Muller, Ackers & White, Van Rijn and Parker & Klingeman. These formulae have been developed to compute bed load, suspended load or total load. Total load is computed by the formula of Engelund & Hansen. Bed load is computed by the formula of Meyer-Peter & Müller. Depending on the grain size of the bed, bed load or suspended load is computed by the formula of Ackers & White. The formula of Van Rijn computes bed load, suspended load and total load (bed load + suspended load). Bed load in a paved river can be computed by the formula of Parker & Klingeman. However, because the sediment problem is very complex, and the sediment load is very high and the diameter of sediment is very fine in the Yellow River. These formulas cannot be used directly. In this case, we decided to elect the user-defined formula.

This is a generally shaped sediment transport formula available for the user to adjust according to his wishes.

$$\phi = \frac{1}{1-\varepsilon}\beta_u(\mu\theta_s)^{\gamma_u}(\mu\theta_s - \theta_c)^{\alpha_u}$$

$$\theta_s = \frac{\overline{u}^2}{C^2\Delta_d D_r}$$

$$C = \frac{R^{\frac{1}{6}}}{n_m}$$

in which:

ϕ = the transport parameter

μ = the ripple factor

θ_S = Shields parameter (-)

$\bar{u}$ = average flow velocity

C = Chézy coefficient

Δ_d = relative density of the sediment

D_r = representative grain size

n_m = Manning coefficient

In this formula, the value of the coefficients α_u, β_u, γ_u, θ_c are supplied by the user. The ripple factor μ can be computed by the program in the same way as for the Meyer-Peter & Müller formula, but can also be supplied by the user as a constant value.

4.4.2 Prepared data

For open channel, some initial and boundary conditions must be given in order to assure a numerical model can be run normally. In SOBEK model, the following input data are reguired.

(1) Cross section

A cross-section is defined as an input element of SOBEK in which the shape and size of the river profiles perpendicular to the flow is described. The field data of cross section are the relations between the vertical, Z and the lateral, Y. In SOBEK model, these cross sections must be given as the relations between the vertical, Z and the width of cross-section, W. In a cross-section the sediment transport rate is computed and morphological changes are distributed over the sediment transporting width Ws. This width is always smaller or equal to the width of the main channel, and is prescribed by the user. In this case, I assumed these two widths are equal.

(2) Initial condition

(a) Friction

The friction is very important for numerical calculation. In the Yellow River, the cross section can be divided in a main channel and a flood plain. The same division was made for the friction. But, because the maximum discharge in this simulation wasn't over flood plain, the friction can only be considered in the main channel. The Manning

coefficient was used for the compensative friction. In the main channel the Manning coefficient is low and varies between 0.007 and 0.025, and decreases with the increment of flow discharge. In general, when the discharge is larger than 1000 m3/s, the Manning coefficient would be taken a small value, 0.007. Figure 4.8 is some effects of Manning coefficient to water level.

(b) Diameter of bed material

The grain size is the characteristic dimension of bed material and suspend load. The bed material is the granular material forming river bed. It is characterized by a relative density of sediment and a characteristic grain size. The sediment density has one value for the entire model. The characteristic grain size may be a function of place in a SOBEK model. In SOBEK the following characteristic grain sizes should be entered, such as D35, D50, D90 and Dm. In this case, their average diameters are 0.041mm, 0.054mm, 0.086mm and 0.053mm. The grain size of suspend load can not be considered in SOBEK model. Figure 4.9 is some effects of bed material to sediment load.

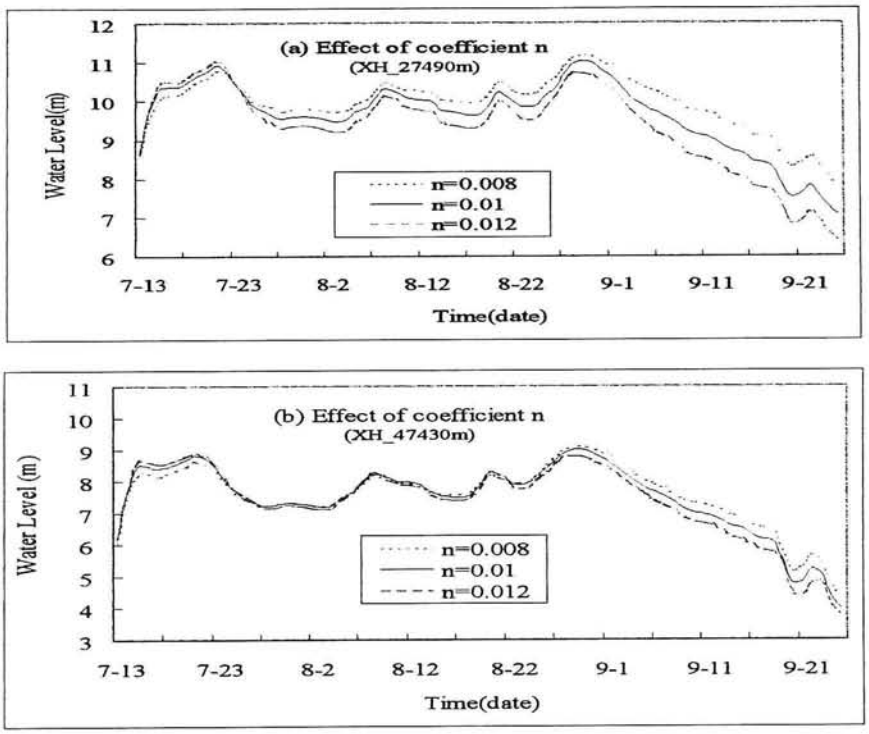

Fig. 4.8 Effects of Minning coefficient to water level.

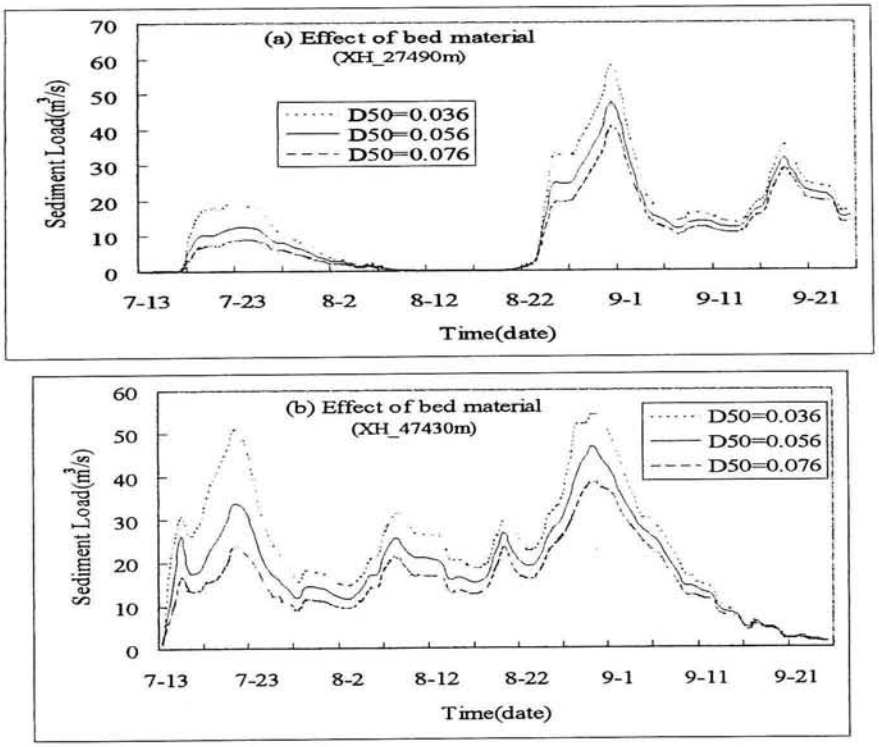

Figure 4.9 Effects of bed material to sediment load

(3) Boundary condition

The continuity equation of flow requires a discharge at the entrance of a simulated reach, and a water level at the outlet. The continuity equation of sediment requires a sediment load at the entrance. These conditions may be a function of time, and sediment transport is imposed in [m^3/s] including the pore volume

(a) Discharge

The discharge is the amount of water passing a grid point per unit of time. It is by default given in [m^3/s]. In this case, the simulated period is from June 3, 1998 to Sept. 25, 1998, and includes three flood peaks. The maximum discharge is about 3060 m^3/s. This kind of discharge runs generally in the main channel, not over flood plain.

(b) Sediment transport

The collected data about sediment transport are some sediment concentrations. In SOBEK model, sediment transport must be offered as the sediment load including pore volume [m^3/s]. The sediment load can be divided into wash load, suspend load and bed load. The wash load can't be included in the user-defined formula. This part of sediment must be deleted. According to our experiences to handle the Yellow River, the sediment

to be smaller than five percent in grain size of bed material will be known as wash load. By this rule, the percent of wash load in suspend load is about forty-five, and the critical diameter is about 0.015mm (see in figure 4.10). In figure 4.11, the green line is a process of the total sediment load. The red line indicates the wash load has been deleted.

(c) Water level

The relation of water level with time has been given at the outlet of simulated reach. Its location is at the QS cross-section.

(4) Time step and space scale

The time step used in this case is five minutes. The flow and the morphological calculation are same step. The grid size was varied from 200 to 500 meters.

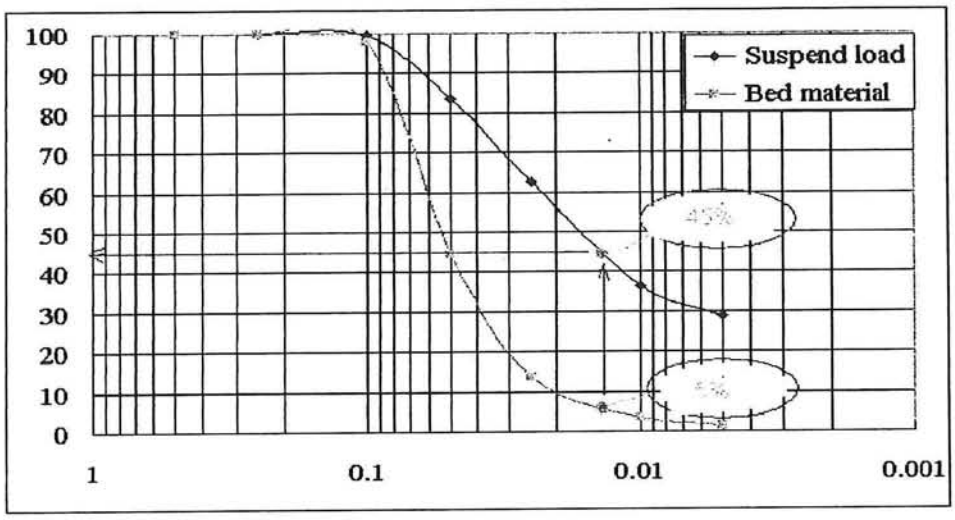

Figure 4.10 Criterion to divide out wash load in sediment load

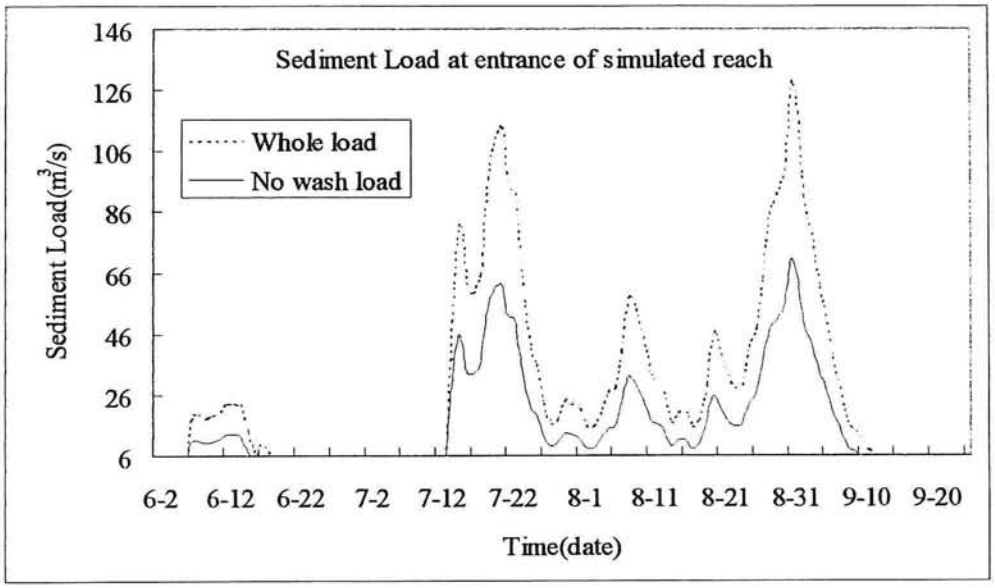

Figure 4.11 Compared with two kinds of sediment load

(5) Parameters of the transport formula Parameters of the transport formula

Some coefficients of the α_u, β_u and γ_u must be supplied in the user-defined formula. In order to master the effects of these coefficients, we have compared with their differences of sediment load. It can be seen from figure 4.12. The sediment load would be increased with the increment of the α_u, the γ_u, the multiplication and the ripple factor. But the change of the β_u is smaller than that of the γ_u, the multiplication and the ripple factor. These alterations indicate that the coefficient γ_u is very important factor in the user-defined formula, and it is convenient to adjust the coefficient for verified calculation of sedimentation. Furthermore, the sediment load would be decreased with the increment of diameter of bed material, and the change is larger.

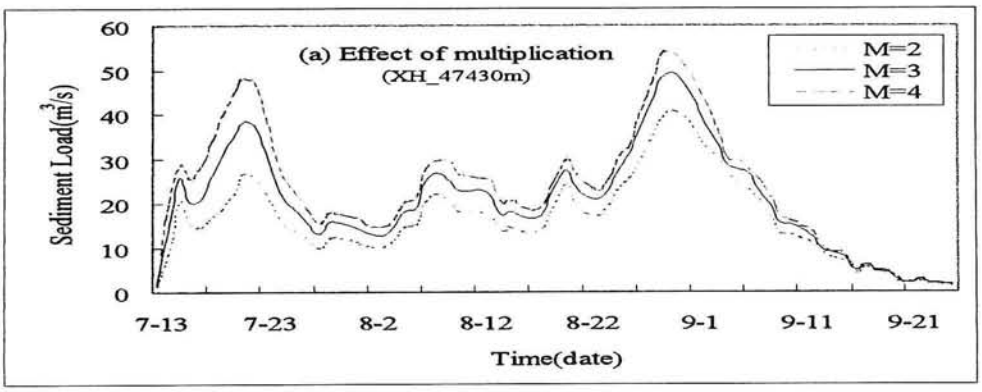

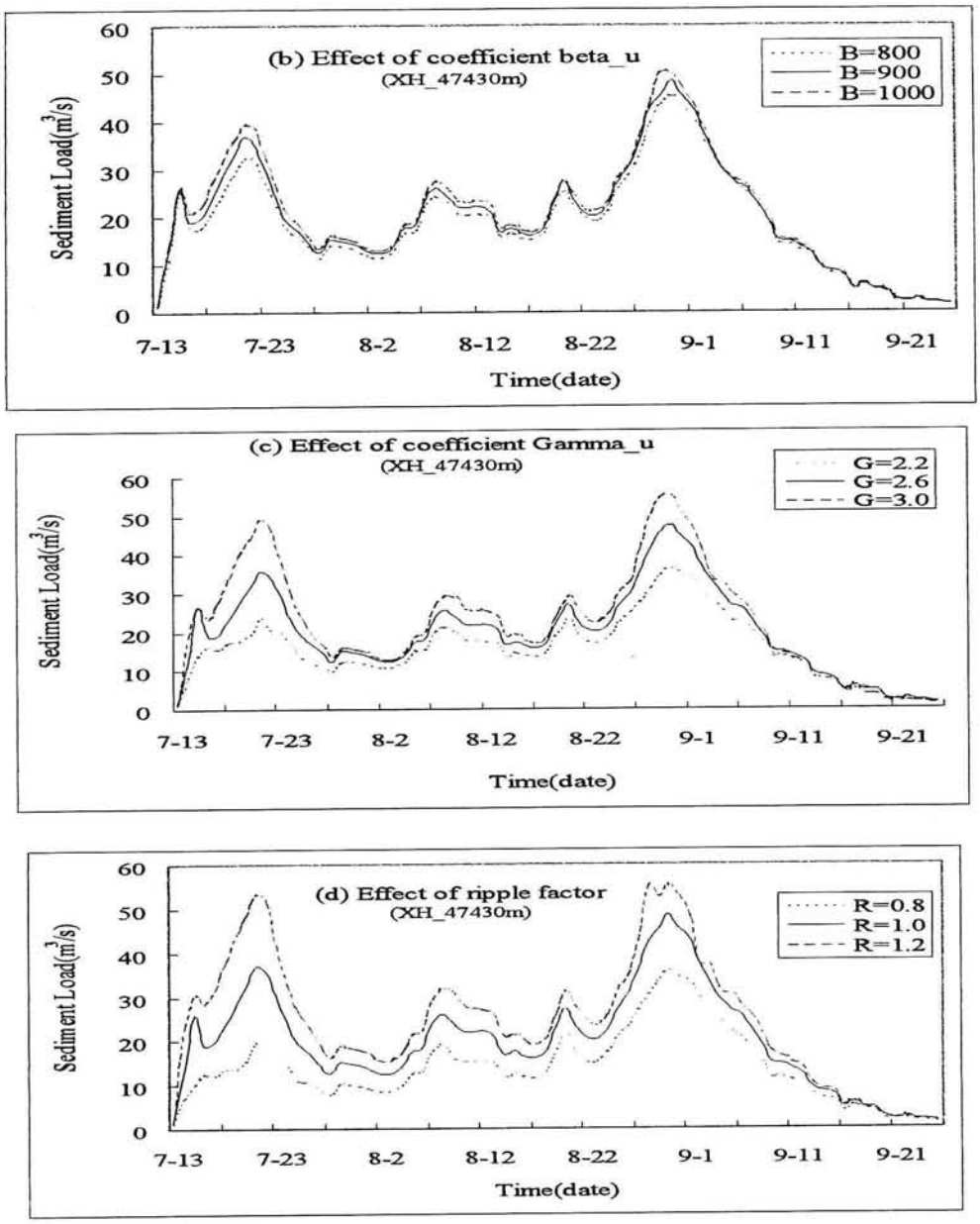

Figure 4.12 Effects of different coefficients to sediment load

It is very difficult to assure these coefficients exactly. In this case, these coefficients have been found by trial and error to conform the calculated and the measured distributions of sediment deposition. These values used in this case are shown in figure 4.13.

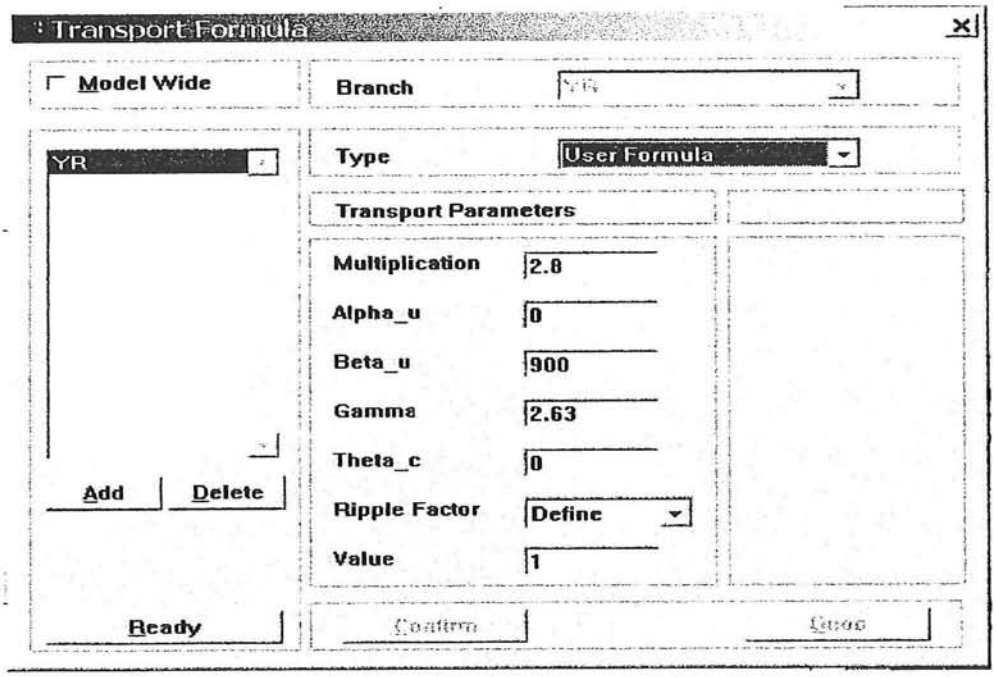

Figure 4.13 Coefficients used in the user-defined formula

4.4.3 Verified results

The verification of the model was carried out in two steps. First the flow part was verified, and next, the morphological part was verified. The verified period is over two months, from July 13, 1998 to September 25, 1998. In the simulated period, four peaks of flood occurred, including two bigger peaks and two smaller peaks. The sediment concentration was relatively low during this flood and the maximum only arrived at 72.9 kg/m^3.

(1) Water level

There are one hydraulic station at LJ cross-section and five stations of water level at YH, ZJ, YW, XH and DZ cross-sections. As only the discharge at the inlet is known, the process of discharge cannot be verified at simulated reach. But the water level can be verified at difference locations. It can be seen from figure 4.14 that the measured and the calculated water levels can be calibrated well by adjusting the manning coefficient. The difference of the calculated water level at LJ station is worst than others. The maximum error will be near to 0.7 meter at some place, but is still acceptable. The errors of flood peak are smaller. The table 4.4 indicates that the scope of error is from 0.07m to 0.49m. In the Yellow River, if considering the change of bed level, there exist apparently some differences in water level. The water level would be improved at LJ,

ZJ and YW stations, and would be decreased at YH and XH stations if the change of bed level had been considered. The alteration is between 0.01m and 0.48 m.

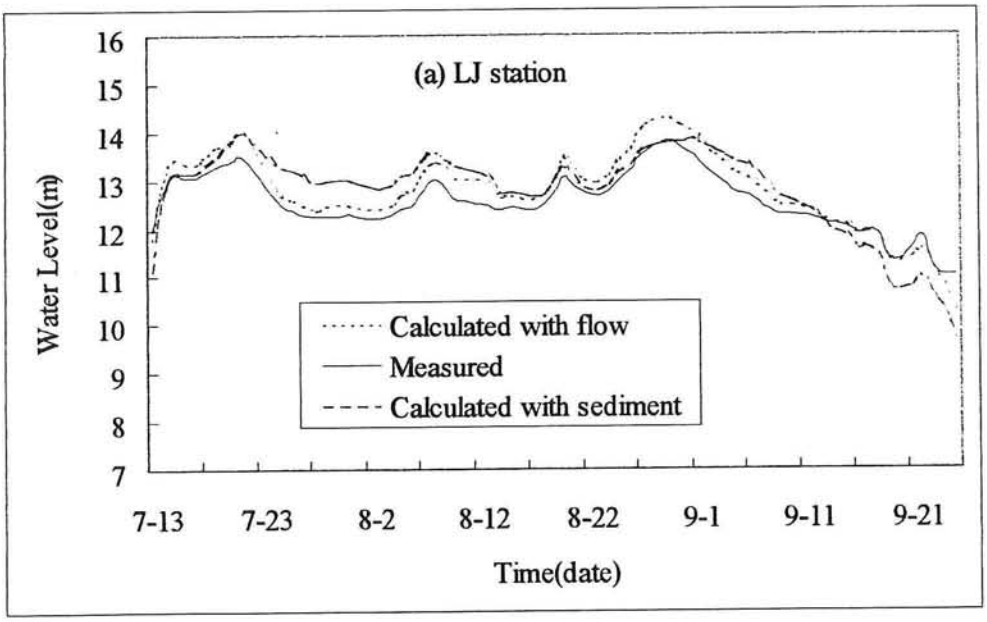

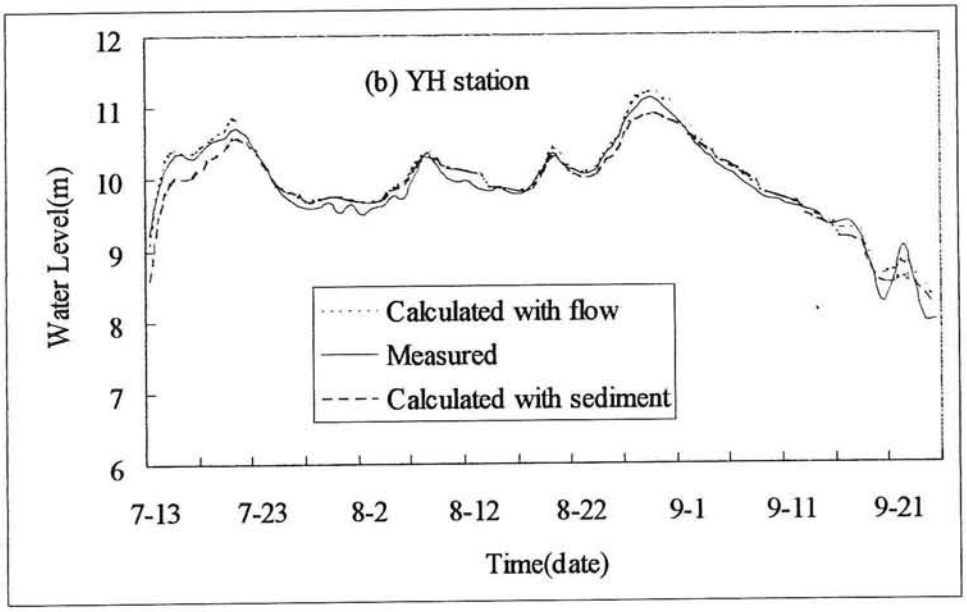

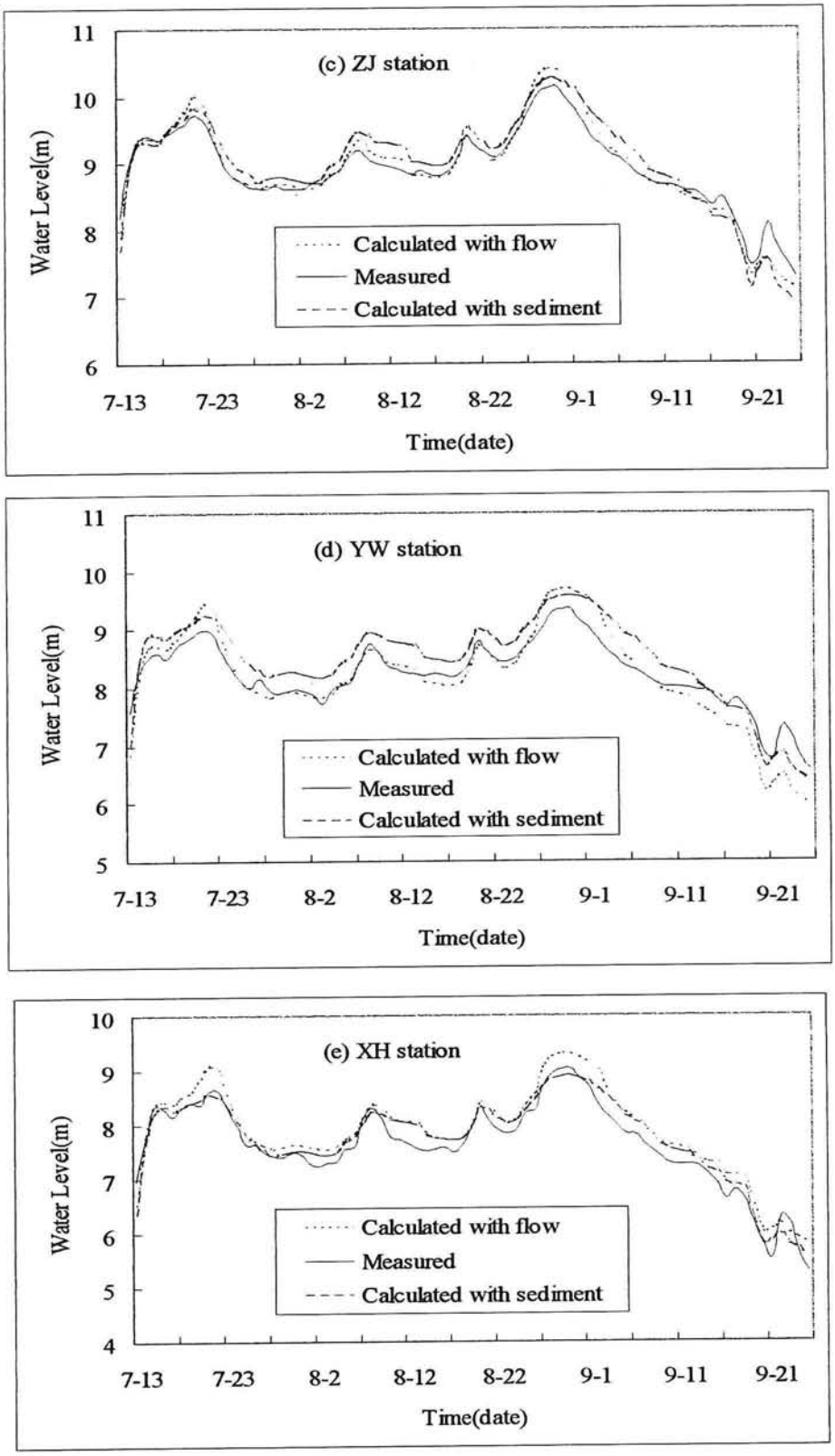

Figure 4.14 Verification of water level at different stations

Table 4.4 Comparison of calculated water level of flood peak with the measured data (m)

Station	No.	Time	Measured	No considering bed change		Considering bed change		
				Calculated	Error	Calculated	Error	Error
LJ	1	Jul. 21, 1998	13.50	13.99	-0.49	14.00	-0.50	0.01
	2	Aug. 8, 1998	13.03	13.38	-0.35	13.56	-0.53	0.18
	3	Aug. 20, 1998	13.05	13.47	-0.42	13.29	-0.24	-0.18
	4	Aug. 30, 1998	13.81	14.28	-0.47	13.80	0.01	-0.48
YH	1	Jul. 21, 1998	10.70	10.85	-0.15	10.57	0.13	-0.28
	2	Aug. 8, 1998	10.35	10.36	-0.01	10.30	0.05	-0.06
	3	Aug. 20, 1998	10.34	10.41	-0.07	10.30	0.04	-0.11
	4	Aug. 30, 1998	11.10	11.19	-0.09	10.88	0.22	-0.31
ZJ	1	Jul. 21, 1998	9.73	10.00	-0.27	9.83	-0.10	-0.17
	2	Aug. 8, 1998	9.20	9.34	-0.14	9.47	-0.27	0.13
	3	Aug. 20, 1998	9.40	9.39	0.01	9.53	-0.13	0.14
	4	Aug. 30, 1998	10.13	10.41	-0.28	10.27	-0.14	-0.14
YW	1	Jul. 21, 1998	8.98	9.46	-0.48	9.25	-0.27	-0.21
	2	Aug. 8, 1998	8.74	8.67	0.07	8.94	-0.20	0.27
	3	Aug. 20, 1998	8.79	8.72	0.07	9.01	-0.22	0.29
	4	Aug. 30, 1998	9.34	9.70	-0.36	9.60	-0.26	-0.10
XH	1	Jul. 21, 1998	8.61	9.09	-0.48	8.57	0.04	-0.52
	2	Aug. 8, 1998	8.30	8.37	-0.07	8.24	0.06	-0.13
	3	Aug. 20, 1998	8.32	8.42	-0.10	8.31	0.01	-0.11
	4	Aug. 30, 1998	9.03	9.32	-0.29	8.92	0.11	-0.40

(2) Volume of sedimentation

The verification of the morphology included two parts. The one is a distribution of sedimentation along the simulated reach. The other is amount of sedimentation at different reaches.

(a) Distribution of sedimentation.

The bed level change creates a decrease in cross sectional area. With the use of the available data the cross sectional change between June and September 1998 was calculated. The figure 4.15 is the verified distribution of sediment deposition. The x – axis indicates the distance along the simulated reach. The Y- axis indicates the decrease area at various cross-sections. It can be seen from the figure that their distributional tendencies of the measured and the calculated areas of cross-section are near. But the cross sectional area of the model computations does not meet the measured data at all in the reach from LJ to SI, see table 4.5. In order to decrease these calculated errors, we have done our best to adjust these coefficients in the user-defined formula. But these efforts cannot acquire some better outcomes. We think the structure of the formula must be modified. Because their mechanisms of sediment transport for the bed load and the suspend load are different, and most of sediment transport in the Yellow River are the

suspend load. We think the different formula should be applied for the bed load and the suspend load in SOBEK model.

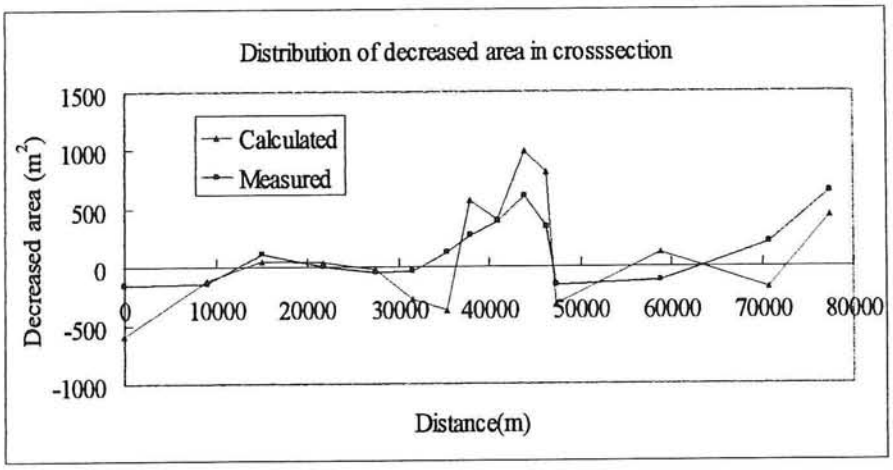

Figure 4.15 Verified distribution of decreased area in cross-section

(b) Amounts of sedimentation at different reaches

Figure 4.16 is some amounts of sedimentation at LJ to ZJ, ZJ to SI and SI to QS. They are the upper reach, the reach and the lower reach of dredged channel, respectively. The error in amount of sedimentation is smallest at the lower reach than at the other two reaches, and the percent of error is about 15% (see the figure 4.16). The measured amount of sedimentation in the total simulated reach is about 4.88 millions m^3, and the calculated amount is about 4.54 millions m^3. They are very close.

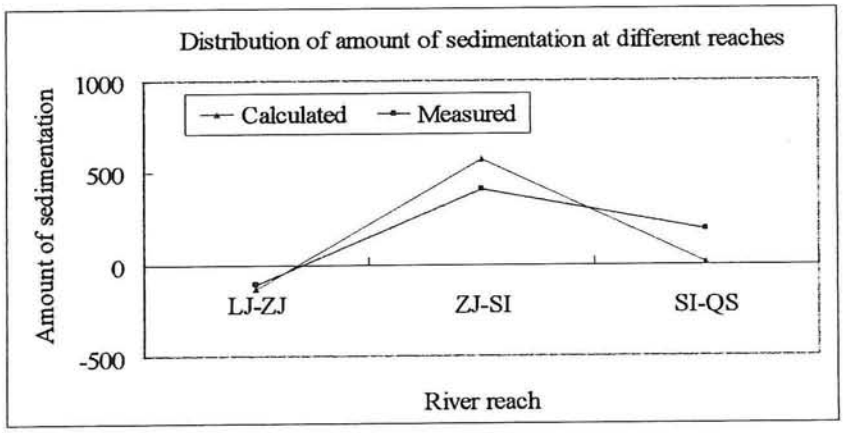

Figure 4.16 Verified amount of sedimentation at different reaches

Table 4.5 Decreased area at difference cross-section

C. S.	Distance (m)	Calculated (m^2)	Measured (m^2)	Error (m^2)
LJ	0	-593	-149	444
WJ	9140	-116	-137	-21
DZ	15120	55	116	61
ZQ	21760	44	-2	-46
YH	27490	-22	-51	-30
QZ	31590	-274	-29	244
ZJ	35350	-375	127	502
SB	37930	567	270	-296
YW	40930	398	388	-10
WQ	43860	992	601	-391
SI	46240	809	339	-470
XH	47430	-324	-159	165
QT	58850	119	-121	-240
QF	70770	-173	211	384
QS	77530	438	640	202

4.5 Fill-in rate and dredging efficiency

Dredging will adjust some boundaries of river, such as water level, bed level, flow velocity, sediment concentration, and so on. At dredging reach, the flow velocity will decrease, and sedimentation will increase. At the upper reach, the velocity will be increase, and the scouring bed will be formed. A large scale of dredging can bring an obvious fall of water level, and induce more sedimentation in dredged channel and consequently will cost more money. Therefore, the fill-in rate and dredging efficient must be studied, and many approaches can be used. Because the SOBEK model cannot be modified further and we have no more time. Its precision in sedimentation isn't suitable. The numerical model doesn't be applied to the research of dredging in the Yellow River. Here, we study the fill-in rate and the dredging efficient depending on a physical model.

4.5.1 Defines of fill-in rate and dredging efficient

In this case, the dredged efficiency can be defined as the pure decreasing volume of sedimentation to be aroused by dredging for one unit of dredging volume at a research reach. Its content include these aspects: the dredging volume, W_d, the fill-in volume, W_b,

the scouring and depositing volume in the upper and the lower reaches of dredged channel, W_u, W_l. A formula to calculate the dredging efficiency can be expressed as

$$\eta = \frac{W_d + W_u + W_b + W_l}{W_d}$$

If $\eta_u = W_u / W_d$, $\eta_b = W_b / W_d$ and $\eta_l = W_l / W_d$ then

$$\eta = 1 + \eta_u + \eta_b + \eta_l$$

where η_u is known as a scouring and depositing rate (SDR) in the upper reach of dredged channel. η_b is known as a fill-in rate of dredged channel. η_l is known as a SDR in the lower reach of dredged channel. When η is smaller than 1, the decreasing volume is not over the dredging volume. This indicates the dredging efficient is lower. When η is bigger than 1. The dredging efficient is higher.

4.5.2 Factors to affect fill-in rate and dredging efficiency

The factors to affect the dredging efficiency include the dimension of dredging channel and the conditions of flow and sediment. The former is consists of the width, the depth, the length and the bed slope. The latter is mainly the discharge, the sediment concentration and the sediment diameter.

(a) Dimension of dredged channel

In general, the scouring volume in the upper reach and the fill-in volume would rise gradually, when the width or the depth of dredged channel increased. But the alterations of their SDR are different. Figure 4.17 is some relations of the SDR and the rate of width and depth (RWD) in dredged channel. We can see from the figure. In the upper reach of dredged channel, the SDR will first rise up, then down with the increment of the RWD. The variation scope of the SDR is from –0.2 to –0.5, and bigger. When the RWD is about between 6 and 8, the SDR will reach a maximum, -0.5. In the lower reach of dredged channel, the SDR will increase with the increment of the RWD, and the variation scope is under 0.1. Therefore, the effort is bigger in the upper reach than in the lower reach. In dredged channel, the change of the SDR is similar with that of the upper reach. When the RWD is smaller, the fill-in rate will rise with the decrement of the RWD, and the increasing velocity is slow. When the RWD is bigger, the fill-in rate will rise with the increment of the RWD, and the increasing velocity is rapid. When the

RWD is about between 5 and 8, the fill-in rate will reach a maximum, 0.5. For the whole simulated reach, the dredging efficiency will first rise up, and then down with the increment of the RWD. When the RWD is between 5 and 8, the dredging efficiency will arrive at a maximum, 0.95.

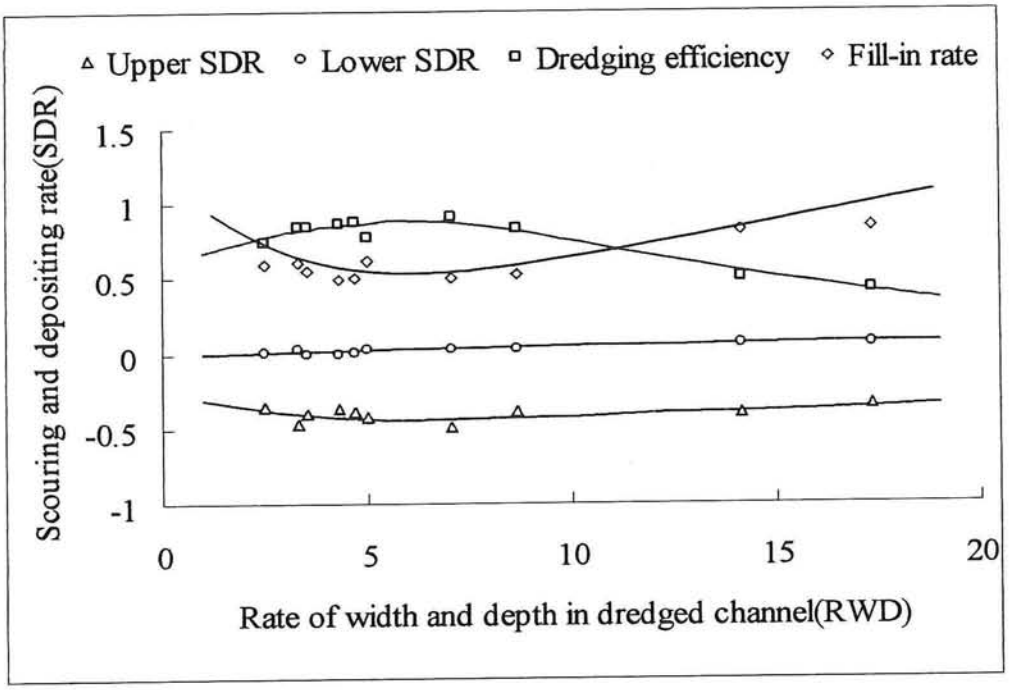

Figure 4.17 Relations of the RWD and the difference SDR

At same dimension of dredged channel, the scouring volume in the upper reach will increase gradually with the increment of the length of dredged channel. In initial stages, the increasing tendency is rapid. In latter stages, the increasing tendency is slow. The tendency of the upper SDR is similar, and its inflexion is about 10 km. This tendency indicates that it will increase the dredging efficiency to add the length when the length of dredged channel is shorter, and increasing velocity is rapid. When the length of dredged channel is longer, it will decrease the dredging efficiency to add the length, but decreasing velocity is slow.

(b) Flow and sediment

Figure 4.18 is some relations of the SDR and the rate of the sediment concentration and the discharge (RSCD). The SDR in upper reach and the fill-in rate will decrease with the increment of the RSCD, and the increasing velocity is near basically. When the RSCD is smaller than 0.025, the increasing velocity of them is slow. When the RSCD is

bigger than 0.025, the increasing velocity of them is fast. These characteristics of the SDR are suitable to the sediment carrying capacity. When the RSCD locates between 0.01 and 0.07, the variable scope of the fill-in rate is from 0.3 to 1.5, and that of the upper SDR is from –0.7 to –0.5. The fill-in rate is always larger than zero, and this indicates the dredged channel is always in silting. The SDR in upper reach alter from negative value to positive value, and this indicates the upper reach locates from scouring status to depositing status with the increment of the RSCD. Because the lower SDR is only 0.05, and is a constant basically. The dredging efficiency will be decided by the fill-in rate and the upper SDR. It can be seen from figure 8 that the dredging efficiency decreases rapidly with the increment of the RSCD. When the RSCD is smaller than 0.025, the dredging efficiency is high. When the RSCD is larger than 0.05, the dredging efficiency is almost disappear.

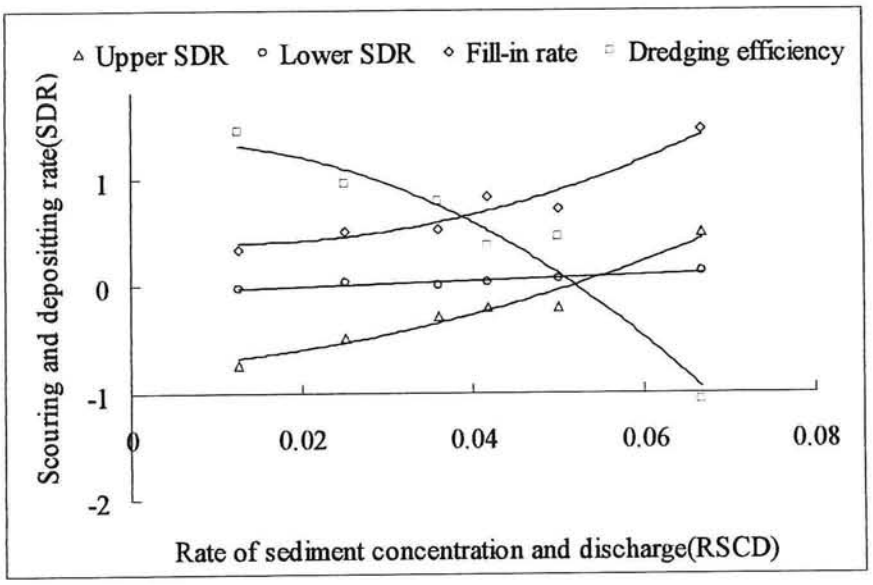

Figure 4.18 Relations of the RSCD and the SDR

(c) Diameter of sediment

At the same diameter of suspend load, the fill-in rate and the SDR in upper and lower reaches will decrease, when the diameter of bed material turns fine. If the diameter of bed material alters from 0.065mm to 0.042mm, the upper SDR is from –0.49 to –0.68, and the fill-in rate is from 0.51 to 0.46, and the dredging efficiency rises from 0.96 to 1.30.

At the same diameter of bed material, the fill-in rate and the upper SDR will increase, and the lower SDR will decrease, when the diameter of suspend load turns coarse. If the

diameter of suspend load alters from 0.016mm to 0.025mm, the upper SDR is from –0.49 to –0.28, and the fill-in rate is from 0.51 to 0.84, and the dredging efficiency falls from 0.96 to 0.42.

4.5.3 Main factors to affect fill-in rate and dredging efficiency

Figure 4.19 is some fill-in rates and some dredging efficiencies of all experimental plans. Effect of dredging is larger in the upper reach than in the lower reach of dredged channel. The scouring volume in the upper reach will affect directly the dredging efficiency. When the scouring volume is very large, the dredging efficiency is high. When the scouring volume is small or no, the dredging efficiency is very low. Although it can increase the scouring volume to add the dimension of dredged channel, the fill-in and the dredging volumes will also increase, and these will decrease the dredging efficiency. For the dimension of dredged channel and the conditions of flow and sediment, the conditions of flow and sediment are main factors to affect the fill-in rate and the dredging efficiency.

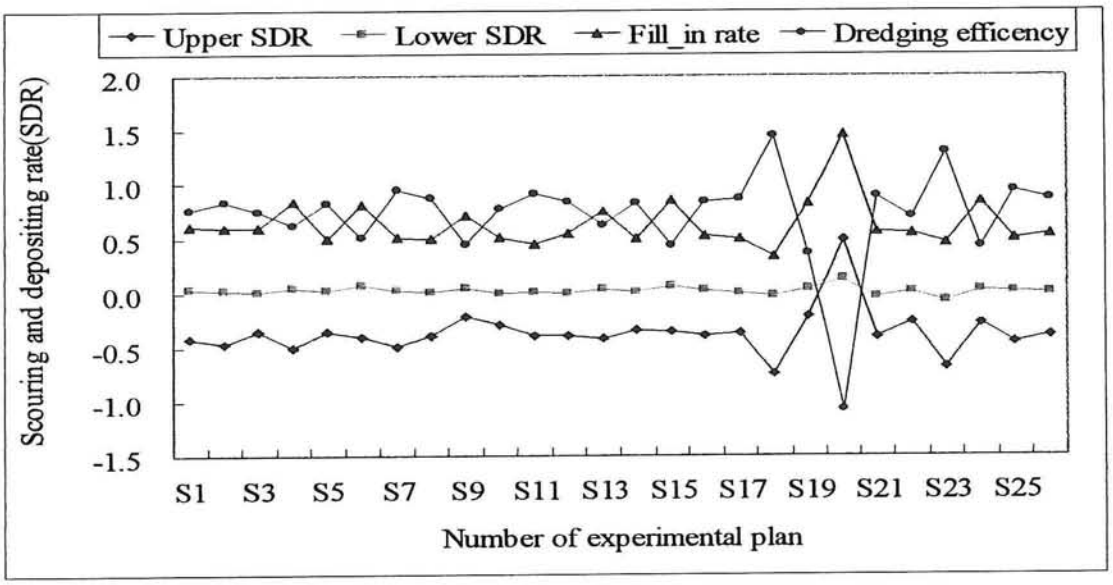

Figure 4.19 Fill-in rate and dredging efficiency of all experimental plans

4.5.4 A suitable dimension of dredged channel

We can know from these relations of the upper SDR, the fill-in rate, the dredging efficiency and the RWD (see figure 4.18). In order to acquire a good dredging effect, the RWD of dredged channel must be fixed between 5 and 8, and the length of the channel

is about 10 km.

4.5.5 Compared with fill-in rate and dredging efficiency at different methods

In table 4.6, some outcomes are compared with the upper SDR, the lower SDR, the fill-in

Table 4.6 Compared with recovery and dredging efficiency at different plans

Type	Calculated	Measured	Physical_1	Physical_2
Width (m)	200	200	200	200
Depth (m)	2.5	2.5	2	3
Length (m)	10000	10000	10000	10000
Dredging volume (10^4m^3)	547.00	547.00	335.00	590.00
Fill-in volume (10^4m^3)	870.00	350.82	171.00	255.00
Upper scouring volume (10^4m^3)	174.00	294.38	165.00	201.00
Lower depositing volume (10^4m^3)	-618.00	31.57	9.00	6.00
Upper scouring rate	0.32	0.54	0.49	0.34
Lower depositing rate	-1.13	0.06	0.03	0.01
Fill-in rate	1.59	0.64	0.51	0.43
Dredging efficiency	0.86	0.84	0.96	0.90

rate and the dredging efficiency at the numerical model, the physical model and the field measure. No dredging influence has been considered when the fill-in, the upper scouring and the depositing volumes are calculated. In the table, the dredging efficiency and the upper SDR of three methods are near. The fill-in rate and the lower SDR of the calculated and the measured methods have some clear differences. The reason is the distribution of sedimentation is not close well at the verification of the SOBEK model. The fill-in rate and the lower SDR of the physical and the measured methods are still near, but these are smaller in the physical model than in the measured method. The reason is too many generalizations at making physical model.

4.6 Recommendations and conclusions

1. In this dredging case, the water level and the total amount of sedimentation in the simulated reach have been be verified well, but the distribution of sedimentation at different reaches has been fitted closely, and its precision still cannot be applied to the dredging prediction in the Lower Yellow River. It can improve the precision of

sedimentation in some degree to adjust some parameters in the user-defined formula, but these clear differences cannot still be solved in the end.

2. The dredging efficiency is composed of three parts: the scouring and depositing rate (SDR) in the upper dredged channel, the fill-in rate in the dredged channel and the scouring and depositing in the lower dredged channel. In these rates, the upper SDR and the fill-in rate are main factors to decide the dredging efficiency.

3. The factors to affect dredging efficiency include the dimension of dredged channel and the flow and sediment conditions, and the effects of the latter are larger than that of the former. If the rate of width and depth of dredged channel was about from 5 to 8, and the length of dredging channel was about 10 km, the dredging efficiency would be the highest in the Lower Yellow River.

4. For the same dimension of dredging channel, the dredging efficiency would decrease rapidly with the increment of the rate of sediment concentration and discharge. When the rate is about 0.025, the dredging efficiency is better. When the rate is over 0.05, the dredging efficiency is almost lost.

5. The numerical mode, the physical scale model and the analysis of field data have been used and compared with each other in this case. Compared with the physical model and the field data, the fill-in rate and the dredging efficiency are near, but all of these are smaller in the physical model than in the field data. Compared with the numerical model and the field data, the dredging efficiency is similar, but for the fill-in rate a large difference exists.

Chapter 5 Summary and Conclusions

In this study, two case studies on lower Yellow River are carried out by use of Delft3D and SOBEK models developed by Delft Hydraulics. A number of conclusions and recommendations for further improvement are given in the sequence.

5.1 Conclusions

1. Some advanced technical measures and strategies of flood management in the Netherlands can be applied in lower Yellow River and other rivers of China combining with the relative conditions.

2. Through the case study of Delft3D-FLOW and MOR models in lower Yellow River, the following achievements can be obtained:

- Delft3D model is a powerful software package with flexible framework which simulates two and three-dimensional flow, waves, water quality, ecology, sediment transport and bottom morphology and is capable of handling the interactions between these processes.
- Delft3D-FLOW module can reasonably simulate the flood process in the lower Yellow River through the flow verification of 1996 flood.
- GPP provides a comprehensive post-processor that can notably improve work efficiency and figure quality.

  Manning formula is much fitter than Chezy one to deal with bed roughness under the circumstance of case study. Flow verified results are agreeable with the measured values, specially flood peak and processes of water level and discharge.
- By performing several sensitivity studies, experience and knowledge on the effects of different parameters are acquired. The knowledge is used to adjust the existing detailed model
- The results also show that the flood features are not good with measured data after peak flood due to the remarkable morphological change caused by peak discharge.
- In order to improve the simulated accuracy, the bottom morphology must be simulated with MOR module.

3. In the dredging case, the calculation is made by SOBEK model. Main achievements are drawn as the following:

- The water level and total amount of sedimentation in the simulated reach have been be verified well, but the distribution of sedimentation at different reaches has been fitted closely, and its precision can not still be applied to the dredging prediction in the Lower Yellow River. It can improve the precision of sedimentation in some degree to adjust some parameters in the user-defined formula, but these clear differences cannot still be solved in the end.
- The dredging efficiency is composed of three parts: the scouring and depositing rate (SDR) in the upper dredged channel, the fill-in rate in the dredged channel and the scouring and depositing in the lower dredged channel. In these rates, the upper SDR and the fill-in rate are main factors to decide the dredging efficiency.
- The factors to affect dredging efficiency include the dimension of dredged channel and the flow and sediment conditions, and the effects of the latter are larger than that of the former. If the rate of width and depth of dredged channel was about from 5 to 8, and the length of dredging channel was about 10 km, the dredging efficiency would be the highest in the Lower Yellow River.
- For the same dimension of dredging channel, the dredging efficiency would decrease rapidly with the increment of the rate of sediment concentration and discharge. When the rate is about 0.025, the dredging efficiency is better. When the rate is over 0.05, the dredging efficiency is almost lost.
- Three kinds of models, involving numerical mode, physical scale model and analysis of field data have been compared each other in this case. Compared with physical model and the field data, the fill-in rate and the dredging efficiency are close, but all of these are smaller in the physical model than in the field data. Compared with the numerical model and the field data, the dredging efficiency is similar, but the fill-in rate exist a large difference.

5.2 Recommendations

With the respect of Delft3D-FLOW model, some recommendations for further development are as the follows.

In Delft3D-FLOW, the open boundary is divided into segments (sections). The boundary conditions are specified for these segments, two values per segment are required, one for each segment end. However, it is difficult to exactly specified the

boundary condition for each segment in many practical cases. The errors are not avoidable near the open boundary and lead to the calculation failed, such as the specified Method I adapted in case study.

Also time step is limited by the Courant number due to adapting time integration method to solve governing equations. In the calculation with Method III, time step must be shorter than 1 minute, unless the computation is halted. So time step is selected relative to the specified way of boundary condition.

In general, the application of Delft3D-FLOW model in lower Yellow ```River is carried out with less information of case study. Some problems may be caused by it. Further verifications are required, including flow and morphology simulations. The reliable and accurate information is need for the application of Delft3D model in lower Yellow River.

5.3 Future activities

The Yellow River is much complicate with boundaries and flow features, specially high sediment concentration. Hence, much detail research work is required to be made as follows.

- The improvement of Delft3D model is needed to be made for application for lower Yellow River, special for morphological module.
- More verifications of Delft3D model are required to be carried out in future
- Some detail information is ugent to be collected for Delft3D model.

Acknowledgements

After 3 months study, March 12 – June 7 2002, we finally fulfilled the research work of project phase II on Yellow River under the cooperation project between P.R. China and the Netherlands entitled: *Strengthening of education and applied research in water resources engineering and water management at a selected number of institutes in the P.R.China* (China-DC/WRE) . At this moment, we want to thank all of the people that helped us during our staying Delft, the Netherlands.

We want to express our great respect and gratitude to our supervisors Prof. Dr. Huib de Vriend (TUD), Dr. Zheng Bing Wang (TUD), Dr. Paul J.Visser (TUD), Dr.J.C,H. Winterwerp (WLD) and Dr. C.J.Sloff (WLD) for their advices and suggestions. In the period of this research, they gave us much support and help for our work. Dr Paul J. Visser arranged our research plan at the initial stage of this study. Dr. C. J. Sloff still advised us to apply Delft3D and SOBEK models on case studies. It is his technical support that we can finish the research works. Dr Wang also gave us much help to solve the problems that we encountered in studies. We are also grateful to Mr. Cees Timmers, Mr. Erik Kemink and Mr. Hemon Móndeel.

Thank Prof van Duivendijk, Prof. Van Beek, Prof Vrijling, Dr Visser W., Prof Stelling G.S. (TUD) and Mr de Vries (Technical Advisory Committee for Water Retaining Structures, Ministry of Transport, Public Work and Water Management) to give us special lectures on flood control, water management, risk design of civil engineering morphology and flood control in the Netherlands during our staying at TU.

Great appreciation is also contributed to Mrs Theda Olsder who's unselfish and patient help to our work and life let us spend a happy time and make our life colorful in the Netherlands.

We want to thank CICAT of TUDelft for their support and help concerning both of our studying and living in the past few months.

Fellows of Cluster 3

May 2002

Delft University of Technology, the Netherlands

References

[1] H.E.J. Berger, Flow forecasting for the River Meuse

[2] Twice A River, Rhine and Meuse in the Netherlands, RIZA Report 99.003

[3] Uriel Rosenthal, Paul't Hart (eds.)(1998),Flood response and crisis management in western Europe—a comparative analysis, Springer-Verlag Berlin Heidelberg New York.

[4] Delft3D-FLOW User Manual, Version 3.05, September 1999.

[5] Delft-GPP User Manual, version 2.00, September 1999.

[6] Ge Beaufort, 1992, Environment impact assessment (EIA) and policy analysis as tools on for combatting flooding in the Netherlands, Fluid mechanics and its applications, Floods and flood management edited by A.J. Saul

[7] Hao-Ming Zhou, 1995, Towards an operational risk assessment in flood alleviation - theory, operationalization and application, Delft University Press.

[8] Jos Dijkman, Rob Klomp and Monique Villars, 1997, Flood management strategies for the rivers Rhine and Meuse in the Netherlands, in: Destructive water: water-caused Natural disasters, their abatement and control (Proceedings of the conference held at Anaheim, California, June 1996), IAHS Publ. No. 239.

[9] Paul't, Hart(eds.), 1998.Flood response and crisis management in western Europe, Springer, Berlin, Heidelberg.

[10] Kees Sloff, SOBEK One-dimensional Morphological Modeling, Delft Hydraulics.

[11] Kees Sloff, SOBEK Morphology - Introduction, Delft Hydraulics.

[12] SOBEK River/Estuary User Manual, Delft Hydraulics, March 20, 2002.

[13] SOBEK River/Estuary Technical Reference Manual, Delft Hydraulics, March 20, 2002.

[14] Erik Kemink, Model Setup, Delft Hydraulics, May 16, 2002.